Department of Physics and Astronomy

Heidelberg University

Master thesis

in Physics

submitted by

Martin Rabel

born in Ulm

2017

Dynamics of a One-Dimensional Two-Component Bose Gas Quenched to Criticality

This Master thesis has been carried out by Martin Rabel

at the

Kirchhoff-Institut für Physik

under the supervision of

Prof. Thomas Gasenzer

Dynamic eines eindimensionalen zweikomponentigen Bose-Gases nach plötzlicher Parameteränderung in die Nähe von kritischen Verhaltens:

Wir untersuchen die Echtzeitdynamik eines zwei-komponentigen Bose-Gases nach einer plötzlichen Änderung der Kopplungsparameter in die Nähe eines quantenkritischen Punktes unter Verwendung analytischer Techniken basierend auf Effektiven Wirkungen. Die relativen Freiheitsgrade des Systems bilden ein Quasispin-$1/2$ Modell. Dieses zeigt im Zentralfeld-Limit einen Quanten-Phasenübergang zwischen einer paramagnetischen und einer ferromagnetischen Phase. Für das Ausgangsmodell entspricht dies einem Übergang von einem Zustand in welchem beide Teilchensorten gemischt vorliegen in einen entmischten, phasenseparierten Zustand. Betrachtet wird dieser Übergang in einem dynamischen Kontext: Zunächst im Grundzustand für Parameter weit entfernt vom kritischen Punkt, werden diese plötzlich auf Werte Nahe am kritischen Punkt verändert. Die Zeitentwicklung hieraus resultierender Spinfluktuationen wird untersucht. In dem hier betrachteten eindimensionalen System sollte die durch die Parameterveränderung zugeführte Energie zu einer nicht-verschwindenden Energie-Lücke und im Zuge dessen zu einer endlichen Korrelationslänge führen. Dies wird hier in einer $1/\mathcal{N}$-Näherung in führender Ordnung sichtbar. Die analytischen Resultate werden mit bestehenden numerischen Simulationen verglichen und zeigen große Ähnlichkeit bei Anpassung von nur einem weiteren Parameter neben einer Amplituden-Skalierung.

Dynamics of a One-Dimensional Two-Component Bose Gas Quenched to Criticality:

We study the dynamics of a two-component Bose gas after a parameter quench into the proximity of a quantum critical point using analytical, real-time effective-action techniques. The relative degrees of freedom within the system can be described by a quasi-spin $1/2$ model. This model is subject to a mean-field paramagnetic to ferromagnetic quantum phase transition. For the full model this corresponds to a transition from a miscible to an immiscible phase. The transition is investigated in a dynamical setup: The initial state is the ground-state configuration far away from criticality. Following a sudden quench to criticality the time evolution of the emerging spin fluctuations is analysed. In the one-dimensional system under investigation, the non-vanishing energy introduced by the quench leads to a finite correlation length during the induced time evolution. The finite critical correlation length is determined within a leading-order $1/\mathcal{N}$ approximation. The obtained analytical results are compared with Truncated-Wigner numerical simulations and show good agreement with only one fit-parameter besides an overall amplitude.

Contents

1 Introduction

Understanding many body dynamics means understanding few effective quantities describing the *macroscopic* i. e. collectively emergent properties. The huge number of microscopic degrees of freedom as e. g. individual particle positions is in general neither treatable nor measurable. This raises the question how an emergent theory, effectively describing a system on large scales, can be classified. And how this classification relates to the underlying microscopic theory.

It is well-understood how this can be done close to continuous (or second order) phase transitions, in thermal equilibrium. Physical systems close to criticality, that is, close to the critical point where the transition occurs, can be described by a small number of parameters: As observed experimentally at first, the systems become scale invariant [Fisher, 1967; Kadanoff et al., 1967; Polyakov, 1970]. This mean zooming in or out, i. e. changing the spatial scale, does not alter the picture seen. This additional symmetry heavily constraints the system.

A classification can then be achieved using universality-classes [Hohenberg and Halperin, 1977], depending on the symmetries and dimensionality of the microscopic theory only. Each of these classes universally describes many different physical systems near criticality (e. g. magnetic systems of different materials [Stanley, 1999]).

Classifying thermal systems near criticality seems like a very special choice. One might wonder what happens in a more general context. Actually there is well-known example where universality plays a role also out of thermal equilibrium, namely thermalization itself: For very different initial conditions, systems approach, on large timescales, the same equilibrium state, see e. g. [Berges and Cox, 2001].

An important concept to understand this approach to thermal equilibrium is prethermalization [Berges, Borsányi, and Wetterich, 2004][Langen et al., 2016]. It is motivated by the experimental observation that bulk-quantities (like energy-density) and equations of state reach their equilibrium values surprisingly fast for example in heavy ion-collisions [Serreau, 2003]. This is attributed to the system-state approaching a universal trajectory after an initial dephasing of quasi-particles.

Closely related to prethermalization is the idea of non-thermal fixed-points (NTFP)

[Berges et al., 2008; Berges and Mesterházy, 2012]. It assumes that ensemble-states in their real-time flow are attracted to fixed-points similar to RG-flows being attracted by RG-fixed-points [Wilson and Fisher, 1972; Fisher, 1974]. This implies for example self-similarity, as close to second order phase transitions, when simultaneously rescaled in absolute time [neiro Orioli et al., 2015]. As for the question of classifications, remarkably, this opens up the possibility to generalize of the concept of universality classes to such, non-thermal, systems [e. g. Berges and Mesterházy, 2012].

The predicted phenomenon of temporal scaling is actually known to occur in coarsening dynamics [Bray, 2002]. These are observed after dynamically crossing a phase-transition. This, and the known scaling behavior near criticality in thermal-equilibrium makes quenches across or into the proximity phase-transitions an interesting candidate for eventually studying non-thermal fixed-points.

Among the available experimental systems, cold atomic gases offer an unprecedented degree of control over parameters and initial conditions while realizing almost perfectly isolated quantum systems [Bloch et al., 2008; Kinoshita et al., 2006]. The progress in experimental techniques on this field also requires theoretical investigation to understand experimental results and proceed in interesting directions.

Analytic treatments of such setups are difficult. Quantum effective actions, in combination with non-perturbative $1/\mathcal{N}$-expansions, where $\mathcal{N}$ is the number of field components have proven especially successful in this context. For a review see e. g. [Berges and Serreau, 2003, 2004]. These techniques will also be explained in more detail in chapter 2 of the main text.

The system under investigation in this thesis is a two-component Bose-gas, a non-relativistic system of two different bosonic particle species. It is considered in a quasi one-dimensional setup. If the interactions included are not $O(\mathcal{N})$-symmetric and a mixing-term, inter-converting particle-species, is added, a miscible and an immiscible phase can be observed (see also chapter 3). The parameters considered here have been realized experimentally by Nicklas et al. [2015] and were studied numerically by Karl [2016], finding scaling behavior after a parameter-quench close to criticality.

An important peculiarity of one-dimensional systems is the absence of long-range order at finite temperature. Far-from-equilibrium dynamics however, happen far from the ground-state, which would be the zero-temperature configuration. Therefore a crossover rather than a phase-transition is expected. The behavior observed in the numerical treatment by Karl [2016] indicates such crossover dynamics close to

the critical point. This deviation from critical behavior is not encompassed by a usual Bogoliubov-treatment as performed for example by Nicklas et al. [2015], whose experimental results range to just about where the different behavior seems to set in.

The major goal of this thesis is to provide a better understanding of these deviations and their origins. To this end, an effective action approach, namely a two-particle-irreducible (2 PI) action, is used in a $1/\mathcal{N}$-leading order approximation (chapter 4). From the set of equations obtained thereby, energy-gaps of excitations are studied. The results reveal both a shift of the critical point away from its mean-field value and an "effective mass", preventing divergencies as they would occur in a phase-transition other than at a cross-over (chapter 5).

Finally the numerical results [Karl, 2016] can be well reproduced by adjusting only one parameter, related to the "effective mass", and an overall amplitude (chapter 6). An interpretation of the results for the non-trivial fit-parameter is given, based on a slight difference in the initial conditions of numeric and analytic treatments. The overall amplitude is expected to require a fit by the choice of the observables that are compared.

2 Theoretical Background

The purpose of this chapter is, to give an overview of important challenges – and known resolution – in the theoretical description of many-body systems far from equilibrium, especially close to second order phase transitions. The focus is put on the two-particle-irreducible (2 PI) effective action method, which will be used in the following chapters. Reviews on these topics can be found e. g. by Berges [2005]; Berges and Serreau [2003, 2004].

2.1 Notation

Throughout this work, complex bosonic fields with multiple components ϕ_i ($i = 1, \ldots, N$) are used. We use multi-indices also including $\phi^\dagger$,

$$\phi^\alpha = \begin{pmatrix} \phi_1 \\ \phi_1^\dagger \\ \vdots \\ \phi_N \\ \phi_N^\dagger \end{pmatrix} \qquad \text{and} \qquad \phi_\alpha^\dagger = \begin{pmatrix} \phi_1^\dagger & \phi_1 & \ldots & \phi_N^\dagger & \phi_N \end{pmatrix} . \tag{2.1}$$

This notation is also used for other variables and matrices. In a non-relativistic theory time-derivatives of complex fields typically have different signs for their conjugate fields[1], $i\partial_t \phi = \omega\phi$ corresponds to $i\partial_t \phi^* = -\omega\phi^*$ (schematically). In the matrix-notation just introduced, it will hence be useful to define

$$V_t := \mathrm{diag}(1, -1, \ldots, 1, -1) , \tag{2.2}$$

which will typically appear together with partial time-derivatives ∂_t. Further, as notation also including the convolutions, define (with sums over repeated indices

[1] This can be demonstrated at the Schrödinger-equation $i\partial_t \psi = E\psi$ for an eigen-state ψ of energy E. This leads, by $E \in \mathbb{R}$, for complex wave-functions to a relative minus sign in the corresponding equation for the conjugate field $i\partial_t \psi^* = -(i\partial_t \psi)^* = -(E\psi)^* = -E\psi^*$.

implicit, also throughout the remainder of this thesis)

$$J^\dagger \cdot \phi := \int \mathrm{d}x \int_\zeta \mathrm{d}t\, J^\dagger_\alpha(x,t)\phi^\alpha(x,t) \tag{2.3}$$

$$\phi^\dagger \cdot R \cdot \phi := \iint \mathrm{d}x\, \mathrm{d}y \iint_\zeta \mathrm{d}t\, \mathrm{d}t'\, \phi^\dagger_\alpha(x,t) R^\alpha_\beta(x,t;y,t')\phi^\beta(y,t') \tag{2.4}$$

for a time-contour ζ (to be defined later). For better readability also space- and time-coordinates are sometimes combined in the form

$$\vec{x} := (x, t_x)\,. \tag{2.5}$$

2.2 Non-Equilibrium Quantum Field Theory

Essential for out-of-equilibrium problems is the treatment of an *initial state*, usually specified as a density-operator ρ_D at time $t = 0$. In such a setup, the expectation value of an arbitrary operator $\mathcal{O}$ is given by $\langle\mathcal{O}\rangle := \mathrm{Tr}(\rho_\mathrm{D}\mathcal{O})$. In this section, it is explained how Gaussian initial conditions can be included in a generating functional with modified external fields / sources.

2.2.1 Generating Functional

We begin by defining a generating functional as

$$Z[J, R; \rho_\mathrm{D}] = \mathrm{Tr}_\phi \left(\rho_\mathrm{D}(t=0) \mathcal{T}_\zeta e^{i(S[\phi] + J^\dagger\cdot\phi + \phi^\dagger\cdot R\cdot\phi)} \right)\,. \tag{2.6}$$

The symbol $\mathcal{T}_\zeta$ denotes time-ordering along a time-contour ζ. The products $J^\dagger \cdot \phi$ etc. are to be understood in the sense of (2.3, 2.4). This is a generating functional, in the sense that acting with functional derivatives with respect to J or R generates correlators in the presence of the initial density operator. Inserting an identity-operator twice in an eigen-basis of the field operator ϕ at $t = 0$ yields[2]

$$Z[J, R; \rho_\mathrm{D}] = \mathrm{Tr}_\phi \left(\iint d\phi_1 d\phi_2 \, \langle\phi_1|\rho_\mathrm{D}(0)|\phi_2\rangle \, \langle\phi_2|\mathcal{T}_\zeta e^{i(S[\phi] + J^\dagger\cdot\phi + \phi^\dagger\cdot R\cdot\phi)}|\phi_1\rangle \right)\,. \tag{2.7}$$

Since $|\phi_1\rangle$ and $|\phi_2\rangle$ are chosen at initial time $t = 0$, the expression $\langle\phi_1|\rho_\mathrm{D}(0)|\phi_2\rangle$ can be directly evaluated to the *known* initial matrix-elements of ρ_D. The second

[2]This is still a basis at later times, although in general not an eigen-basis anymore.

correlator can be evaluated as a path integral, but along a time-contour ζ. This contour has to start at $t = 0$ ($|\phi_1\rangle$), run through all operator insertions (at finite times), e. g. from functional derivatives $\frac{\delta}{\delta J^\dagger}$, and finally return to $t = 0$ (and $\langle\phi_2|$) again. This form is known as the Keldysh-contour [Keldysh, 1965]. Then

$$Z[J, R; \rho_{\mathrm{D}}] = \iint d\phi_1 d\phi_2 \, \langle\phi_1|\rho_D(0)|\phi_2\rangle \int_{\phi(t_{\mathrm{i}})=\phi_1}^{\phi(t_{\mathrm{f}})=\phi_2} \mathcal{D}\phi \, e^{i(S[\phi]+J^\dagger\cdot\phi+\phi^\dagger\cdot R\cdot\phi)} \,, \tag{2.8}$$

with t_{i} and t_{f} being the start- and endpoint of ζ respectively. Both are zero, but ϕ is a function defined on ζ, not on the "normal" time-axis, and thus $\phi(t_{\mathrm{i}}) \neq \phi(t_{\mathrm{f}})$ in general. The initial term $\langle\phi_1|\rho_D(0)|\phi_2\rangle$ can be pulled into the path-integral (it is independent of ϕ) and can be replaced with a function $\rho_{\mathrm{D}}\big(\phi(t_{\mathrm{i}}), \phi(t_{\mathrm{f}})\big)$ by the constraints of the path-integral. The first integral over $\phi_{1\,/\,2}$ then simply integrates all possible constraints for the path-integral, thus

$$Z[J, R; \rho_{\mathrm{D}}] = \int \mathcal{D}\phi \, \rho_{\mathrm{D}}\big(\phi(t_{\mathrm{i}}), \phi(t_{\mathrm{f}})\big) e^{i(S[\phi]+J^\dagger\cdot\phi+\phi^\dagger\cdot R\cdot\phi)} \,. \tag{2.9}$$

2.2.2 Gaussian Initial Conditions

For many applications, the initial density-matrix can be assumed to be Gaussian,

$$\rho_{\mathrm{D}}\big(\phi(t_{\mathrm{i}}), \phi(t_{\mathrm{f}})\big) = \mathcal{N} e^{i(\alpha_0+\alpha_1^\dagger\cdot\phi+\frac{1}{2}\phi^\dagger\cdot\alpha_2\cdot\phi)} \,, \tag{2.10}$$

where $\mathcal{N}$ and α_0 are only – for correlation-functions irrelevant – normalization constants, and ϕ is an arbitrary field interpolating $|\phi_2\rangle$ at $t \to t_{\mathrm{f}}$ and $|\phi_1\rangle$ at $t \to t_{\mathrm{i}}$. The α have support only at $t = t_{\mathrm{i}\,/\,\mathrm{f}}$. Then, the generating functional becomes

$$Z[J, R; \rho_{\mathrm{D}}] = \int \mathcal{D}\phi \, e^{i(S[\phi]+(J+\alpha_1)^\dagger\cdot\phi+\phi^\dagger\cdot(R+\alpha_2)\cdot\phi)} \,, \tag{2.11}$$

for suitably redefined measure to absorb the new normalization-constants. Now a redefinition of $J|_{t=0} \to J|_{t=0} + \alpha_1$ and $R|_{t=0} \to R|_{t=0} + \alpha_2$ restores a form of $Z[J, R]$ that does not explicitly depend on initial condiations, only implicitly through J and R at $t = 0$. This form can be used to establish the 2 PI formalism (section 2.5).

2.3 Continuous Phase-Transitions

We want to treat phase-transitions, out of equilibrium, in a field-theoretic context. This section briefly discusses problems related to such treatments. A solution will be provided by the 2 PI formalism (section 2.5) together with the $1/\mathcal{N}$-expansion scheme.

From a theoretical perspective the scale-invariance at continuous phase-transitions can be understood from Landau theory [Landau, 2008, (reprint)]. Expand the free energy F, symmetric in the order-parameter Q, to fourth order $F = a(T)Q^2 + b(T)Q^4$ where a and possibly b are dependent on some parameter T, for example the temperature. The prototypical second order critical point is found at the value of T where a changes sign. For $a > 0$ the order-parameter vanishes, while for $a < 0$ spontaneous symmetry-breaking is expected. In field-theoretic language a would be called a mass, and indeed it fixes a mass-scale. At the critical point this mass-scale vanishes, leaving the system without a typical scale and thus scale-invariant.

This vanishing mass also leads to instabilities in the respective modes, inducing non-perturbatively large fluctuations invalidating "standard" loop-expansions. A proper treatment requires a new expansion parameter replacing the small coupling. Additionally, loops of massless particles tend to create IR-divergences. Those divergences can be canceled by higher loop-orders. But to any finite order, there would be diagrams with a maximum number of divergent loops, not canceled to that order. A treatment which resums the "right" contributions to infinite order is required.

2.4 Secular Terms

For the far-from-equilibrium treatment we need to do, it must also be accounted for "secular terms", as briefly discussed in this section. Unresummed treatments of far-from-equilibrium dynamics suffer from secular terms, that is, from terms growing polynomially (and thus indefinitely) in time. An intuitive (but somewhat oversimplified) picture is, that expanding the time-evolution operator e^{-iHt} in some term of H to finite order results in a polynomial in t. To go beyond very short times it is thus necessary to avoid such unphysical divergences through resummations of the "right" contributions to infinite order in the coupling constant to get an analytic function in t rather a finite order polynomial [Berges and Serreau, 2004].

2.5 The 2 PI Effective Action

This section introduces the 2 PI effective action, and thereby the key concept, which the remainder of this thesis is based on. It logically follows the treatment in [Berges, 2005]. The n PI-Effective-Action generalizes the concept of the usual 1 PI one ([e. g. Weinberg, 1996], appendix A). It turns out that 2 PI is exactly what is needed to deal with Gaussian i. e. quadratic initial conditions / density-operators, and thus this case of $n = 2$ is studied here and used later for calculations. A generalization to higher n is straight-forward, but tedious. Effective actions in general are well-suited to study far-from-equilibrium systems, since they avoid "secular terms" growing in time. Also the problem of IR-divergences near second-order phase-transitions can be cured by this ansatz. Thereby it will resolve three main problems (initial state, secular terms, IR-divergences) recognized before. It remains the need for a good expansion-parameter which will be given by $1/\mathcal{N}$, see section 2.7.

2.5.1 Definition of the Effective Action Functional

The definition of the 2 PI effective-action mostly proceeds as in the 1 PI case (appendix A.1). Only the source-field J is supplemented by a tensorial / matrix term R:

$$Z[J,R] := \int \mathcal{D}\phi \, e^{i(S[\phi]+J^\dagger\cdot\phi+\phi^\dagger\cdot R\cdot\phi)}. \tag{2.12}$$

This is also the very same form as was obtained in 2.2.2 for Gaussian initial conditions in a non-equilibrium setting. The notation of products is defined in section 2.1. Connected diagrams (cumulants) are generated by $W[J]$ where

$$e^{iW[J,R]} = Z[J,R]\,. \tag{2.13}$$

This is, because functional derivatives of $W = -i \ln Z$ are derivatives of Z divided by Z. Dividing by the vacuum partition function (dividing out "vacuum bubbles") is the same as eliminating all disconnected contributions (which *are* the "vacuum

bubbles"). Further define the expectation values

$$\begin{aligned} \varphi^{\alpha}_{J,R}(x,t) &:= \frac{\delta W[J,R]}{\delta(iJ^{\dagger}_{\alpha}(x,t))}\,, \\ \frac{1}{2}\big(\varphi^{\dagger}_{\alpha;J,R}(x,t)\varphi^{\beta}_{J,R}(y,t') + G^{\beta}_{\alpha;J,R}(x,t;y,t')\big) &:= \frac{\delta W[J,R]}{\delta R^{\alpha}_{\beta}(x,t;y,t')}\,. \end{aligned} \tag{2.14}$$

Then assuming that $\varphi_{J,R}$ and $G_{J,R}$ are invertible with inverse $J_{\varphi,G}$ and $R_{\varphi,G}$, the quantum effective action $\Gamma[\varphi, G]$ is the Legendre-transform of W,

$$\Gamma[\varphi,G] := W[J_{\varphi,G}, R_{\varphi,G}] - \Big(J^{\dagger}_{\varphi,G}\cdot\varphi + \varphi^{\dagger}\cdot R_{\varphi,G}\cdot\varphi\Big) - \frac{1}{2}\,\mathrm{Tr}(G\cdot R_{\varphi,G})\,. \tag{2.15}$$

The functional above fulfills – as a property of the Legendre-transform – the equations

$$\frac{\delta\Gamma[\varphi,G]}{\delta\varphi} = -J_{\varphi,G} - \frac{1}{2}R_{\varphi,G}\cdot\varphi \qquad \text{and} \qquad \frac{\delta\Gamma[\varphi,G]}{\delta G} = -\frac{1}{2}R_{\varphi,G}\,. \tag{2.16}$$

These resemble the classical condition of a stationary action $\frac{\delta S}{\delta\phi} = 0$, and are hence often referred to as stationarity conditions. This analogy is also the reason for the name "effective action" [Weinberg, 1996]. Those stationarity conditions will be essential for actual calculations.

2.5.2 Derivation of the Form of $\Gamma[\varphi, G]$

Especially for the 1-loop parts many properties can be reduced to the 1 PI case. To this end it is useful to re-define the theory for fixed source R as an inherent part of the action

$$S^{(R)}[\phi] := S[\phi] + \phi^{\dagger}\cdot R\cdot\phi\,, \tag{2.17}$$

because then, the generating functional with one source-term only satisfies

$$Z^{(R)}[J] := \int \mathcal{D}\phi\, e^{i(S^{(R)}[\phi] + J^{\dagger}\cdot\phi)} = Z[J,R]. \tag{2.18}$$

Using the general form of the 1 PI-effective action $\Gamma^{(R)}[\phi]$ at 1-loop order (see appendix, equation (A.17)) this leads to

$$\Gamma^{(R)}[\varphi] = S^{(R)}[\varphi] + \frac{i}{2}\operatorname{Tr}\ln\left[\left(G_0^{(R)}\right)^{-1}\right] + \Gamma_2^{(R)}[\varphi]\,. \tag{2.19}$$

The term $\Gamma_2^{(R)}$ comprises all contributions from higher loop orders. $G_0^{(R)}$ can be replaced by

$$i\left(G_0^{(R)}\right)^{-1} = \frac{\delta^2 S^{(R)}[\phi]}{\delta\phi^2} = \frac{\delta^2 S[\phi]}{\delta\phi^2} + R = iG_0^{-1} + R\,. \tag{2.20}$$

As is apparent from the very definition of $\Gamma[\varphi, G]$ (2.15), it holds that

$$\begin{aligned}\Gamma[\varphi, G] &= \Gamma^{(R)}[\varphi] - \varphi^\dagger \cdot R_{\varphi,G} \cdot \varphi - \frac{1}{2}\operatorname{Tr}(R\cdot G) &(2.21)\\ &= S[\varphi] + \frac{i}{2}\operatorname{Tr}\ln\left(G_0^{-1} - iR\right) - \frac{1}{2}\operatorname{Tr}(R\cdot G) + \mathcal{O}(\text{2-loop}) &(2.22)\end{aligned}$$

Phrased differently doing one Legendre-transform in J to get $\Gamma^{(R)}[\varphi]$, then an other one in R is equivalent to doing a Legendre-transform in both "simultaneously" to get $\Gamma[\varphi, G]$ (first line). In the second line the form found in equation (2.19) was inserted. Further, using $G = G^{-1}_{(\text{1-loop})} = G_0^{-1} - iR$, at 1-loop, yields

$$\begin{aligned}\Gamma_{(\text{1-loop})}[\varphi, G_{(\text{1-loop})}] = S[\varphi] &+ \frac{i}{2}\operatorname{Tr}\ln\left(G^{-1}_{(\text{1-loop})}\right) + \frac{i}{2}\operatorname{Tr}(G_0^{-1}G_{(\text{1-loop})})\\ &- \frac{i}{2}\operatorname{Tr}(G^{-1}_{(\text{1-loop})}G_{(\text{1-loop})})\,,\end{aligned} \tag{2.23}$$

which is consistent with $G = G_{(\text{1-loop})}$ at 1-loop order to equation (2.16), i. e.

$$\frac{\delta\Gamma_{(\text{1-loop})}[\varphi, G_{(\text{1-loop})}]}{\delta G_{(\text{1-loop})}} = -\frac{1}{2}R\,. \tag{2.24}$$

Introducing a term $\Gamma_2[\varphi, G]$ to capture higher loop contributions,

$$\Gamma[\varphi, G] = \Gamma_{(\text{1-loop})}[\varphi, G] + \Gamma_2[\varphi, G]\,, \tag{2.25}$$

also adds higher order corrections to G, which can be derived from the stationarity condition (2.16),

$$\begin{aligned} -\frac{1}{2}R &= \frac{\delta\Gamma_{\text{(1-loop)}}[\varphi,G]}{\delta G} + \frac{\delta\Gamma_2[\varphi,G]}{\delta G} \overset{2.23}{=} -\frac{i}{2}G^{-1} + \frac{i}{2}G_0^{-1} + \frac{\delta\Gamma_2[\varphi,G]}{\delta G} \\ \Rightarrow G^{-1} &= G_0^{-1} - iR - \Sigma[G]\,. \end{aligned} \tag{2.26}$$

Here it was introduced

$$\Sigma[G] := 2i\frac{\delta\Gamma_2[\varphi,G]}{\delta G}\,. \tag{2.27}$$

From 1 PI it is known that the full propagator is a geometrical sum of one-particle-irreducible contributions $\Sigma^{(1\,\text{PI})}$ (A.21) and thus indeed $\Sigma = \Sigma^{(1\,\text{PI})}$. This has the important implication, that Γ_2 must be 2-particle-irreducible, that is cutting any two lines (propagators) in any diagrammatic contribution to Γ_2 leads to a (still) connected diagram. This is, because its derivative $\propto \Sigma^{(1\,\text{PI})}$ is 1-particle-irreducible (cutting a single line does not disconnect any contribution).

While the contributions to Γ up to one-loop are given explicitly by equation (2.23), Γ_2 must be obtained by diagrammatic expansion. The observation, that only 2-particle-irreducible diagrams have to be taken into account, drastically reduces the number of contributions. Further we recognize, that in equation (2.26) $\Sigma[G]$ depends on the full propagator. The 2 PI formalism gives a self-consistent treatment of propagators. In fact this is equivalent to an infinite resummation of diagrams and is crucial for avoiding secular terms and IR-divergencies near phase-transitions.

For later reference we establish the following rules to determine Γ_2: Take all closed[3] two-particle-irreducible diagrams with propagator-lines corresponding to the full propagator G.

Also for the field expectation-value φ an equation can be obtained from the stationarity condition (2.16),

$$\frac{\delta\Gamma_2[\varphi,G]}{\delta\varphi} = -\frac{\delta S[\varphi]}{\delta\varphi} - \frac{i}{2}\frac{\delta\,\mathrm{Tr}(G_0^{-1}(\varphi)G)}{\delta\varphi} - J - \frac{1}{2}R\cdot J\,. \tag{2.28}$$

This will later be used to obtain equations also for the macroscopic fields additionally to equation (2.26) for the propagators G.

[3]Partition functions and thus effective actions have no external field-insertions.

2.6 Dynamic Equations

Equations (2.26) and (2.28) already determine G and φ. The free inverse propagator G_0^{-1} contains a term $\propto \partial_t$ (or $i\partial_t^2$ in relativistic models), thus these are actually differential equations in t. By setting J and R to zero for all $t > 0$ (there are no physical external fields present) these remarkably form a closed set of equations, as will become apparent at the end of this section. Note that the absorption of the initial conditions into the values of J, R at $t = 0$ (see 2.2.2) now corresponds to choosing the initial conditions of the set of differential equations to meet the physical initial conditions. However the time-derivative acts on the *time-ordered* propagator G (which is typically not continuous at $t = 0$), and the theory is defined on a closed time-contour ζ, both requiring a careful treatment. In this section these equations are transformed to a set of "normal" differential equations. This is done very similar as in the (relativistic) case covered by [Berges, 2005].

2.6.1 Statistical and Spectral Function

The time-ordered propagator $G(t, t')$, typically is not continuous at $t = 0$, therefore it is often simpler to introduce a decomposition in a spectral part ρ and a statistical part F (for details see appendix C.2)

$$G(t, t') =: F(t, t') - \frac{i}{2} \operatorname{sign}_\zeta(t - t')\rho(t, t') \,, \tag{2.29}$$

where both F and ρ are regular functions (also at $t = 0$). In fact, this is equivalent (cf. appendix, equation (C.17)) to

$$\rho^\alpha_\beta(x, t; y, t') := i \left\langle [\phi^\alpha(x, t), \phi^\dagger_\beta(y, t')] \right\rangle \,, \tag{2.30}$$

$$F^\alpha_\beta(x, t; y, t') := \frac{1}{2} \left\langle \{\phi^\alpha(x, t), \phi^\dagger_\beta(y, t')\} \right\rangle - \frac{1}{2}\{\varphi^\alpha, \varphi^\dagger_\beta\} \,, \tag{2.31}$$

where ρ is the spectral and F the statistical function. The self-energy is decomposed in a local part $\Sigma^{(0)}$ and a non-local part $\bar{\Sigma}$

$$\Sigma(x, t; y, t') = -i\delta(x - y)\delta(t - t')\Sigma^{(0)}(x, t) + \bar{\Sigma}(x, t; y, t') \,, \tag{2.32}$$

and then, similarly to the propagator

$$\bar{\Sigma}(x,t;y,t') = \Sigma^{\mathrm{F}}(t,t') - \frac{i}{2}\,\mathrm{sign}_\zeta(t-t')\Sigma^\rho(t,t')\,. \tag{2.33}$$

2.6.2 Dynamical Equations

In this subsection the problem of the time-derivative term in G_0^{-1} acting on the time-ordered propagator (non-analytic at $t=0$) is treated. From the relation of G to G_0 and Σ given by equation (2.26) we get, by multiplying with G from the right

$$\left(G_0^{-1} - iR - \Sigma\right)\cdot G = \mathbb{1}\,, \tag{2.34}$$

or making the matrix-notation and convolutions explicit ($\vec{x} := (x, t_x)$):

$$\int \mathrm{d}\vec{y}\left[(G_0^{-1})^\alpha_\beta(\vec{x},\vec{y}) - iR^\alpha_\beta(\vec{x},\vec{y}) - \Sigma^\alpha_\beta(\vec{x},\vec{y})\right] G^\beta_\gamma(\vec{y},\vec{z}) = \delta(\vec{x}-\vec{z})\delta^\alpha_\gamma\,. \tag{2.35}$$

Further using the statistical / spectral decomposition (2.29) and $t > 0 \Rightarrow J, R = 0$ we get

$$\begin{aligned}\int \mathrm{d}\vec{y}&\Big[(G_0^{-1})^\alpha_\beta(\vec{x},\vec{y}) - \Sigma^\alpha_\beta(\vec{x},\vec{y})\Big] \\ &\times\Big[F^\beta_\gamma(\vec{y},\vec{z}) - \frac{i}{2}\,\mathrm{sign}_\zeta(t_y - t_z)\rho^\beta_\gamma(\vec{y},\vec{z})\Big] = \delta(\vec{x}-\vec{z})\delta^\alpha_\gamma\,.\end{aligned} \tag{2.36}$$

The "dangerous" part is the time-derivative term of G_0^{-1} acting on the sign_ζ-function. Therefore we want to study the commutator

$$\int \mathrm{d}\vec{y}\,\Big[(G_0^{-1})^\alpha_\beta(\vec{x},\vec{y})\ \ ,\ \ -\frac{i}{2}\,\mathrm{sign}_\zeta(t_y - t_z)\Big]\rho^\beta_\gamma(\vec{y},\vec{z})\,. \tag{2.37}$$

Furthermore typically $G_0^{-1}(\vec{x},\vec{y}) \propto \delta(\vec{x}-\vec{y})$ and in the non-relativistic case the sign of $i\partial_t$ for ϕ^* components is inverted (see (2.2), $V_t := \mathrm{diag}(1,-1,1,-1)$),

$$(G_0^{-1})^\alpha_\beta(\vec{x},\vec{y}) =: \delta(\vec{x}-\vec{y})\Big(V_{t\beta}^\alpha\partial_{t_x} + iM^\alpha_\beta(\vec{x})\Big)\,, \tag{2.38}$$

defining a generalized mass-term $iM^\alpha_\beta(\vec{x})$. The only term not commuting with the $\mathrm{sign}_\zeta(t_y - t_z)$ is the one with the time-derivative. Thus, consider first

$$\begin{aligned} V^\alpha_{t\beta}\Big[\partial_{t_y}, \mathrm{sign}_\zeta(t_y - t_z)\Big]\rho^\beta_\gamma(\vec{y},\vec{z}) \\ &= V^\alpha_{t\beta}\partial_{t_y}\Big(\mathrm{sign}_\zeta(t_y - t_z)\rho^\beta_\gamma(\vec{y},\vec{z})\Big) - \mathrm{sign}_\zeta(t_y - t_z)\partial_{t_y}\rho^\beta_\gamma(\vec{y},\vec{z}) \\ &= \Big(V^\alpha_{t\beta}\partial_{t_y}\,\mathrm{sign}_\zeta(t_y - t_z)\Big)\rho^\beta_\gamma(\vec{y},\vec{z})\,. \end{aligned} \tag{2.39}$$

Now use

$$\partial_{t_y}\,\mathrm{sign}_\zeta(t_y - t_z) = 2\delta(t_y - t_z) \tag{2.40}$$

and the equal-time commutator (cf. equation (2.30))

$$\delta(t_y - t_z)\rho^\beta_\gamma(\vec{y},\vec{z}) = i\delta(\vec{y} - \vec{z})V_t{}^\beta_\gamma \tag{2.41}$$

to write equation (2.39) (using $V_t{}^2 = \mathbb{1}_4$) as

$$V^\alpha_{t\beta}\Big[\partial_{t_y}, \mathrm{sign}_\zeta(t_y - t_z)\Big]\rho^\beta_\gamma(\vec{y},\vec{z}) = 2i\delta(\vec{y} - \vec{z})\delta^\alpha_\gamma\,. \tag{2.42}$$

Returning to the starting point (2.37)

$$\begin{aligned} &\int \mathrm{d}\vec{y}\,\Big[(G_0^{-1})^\alpha_\beta(\vec{x},\vec{y}), -\frac{i}{2}\,\mathrm{sign}_\zeta(t_y - t_z)\Big]\rho^\beta_\gamma(\vec{y},\vec{z}) \\ \overset{(2.38)}{=} &\int \mathrm{d}\vec{y}\,\Big[\delta(\vec{x} - \vec{y})\Big(V^\alpha_{t\beta}\partial_{t_x} + iM^\alpha_\beta(\vec{x})\Big), -\frac{i}{2}\,\mathrm{sign}_\zeta(t_y - t_z)\Big]\rho^\beta_\gamma(\vec{y},\vec{z}) \\ = &\int \mathrm{d}\vec{y}\,\delta(\vec{x} - \vec{y})V^\alpha_{t\beta}\Big[\partial_{t_x}, -\frac{i}{2}\,\mathrm{sign}_\zeta(t_y - t_z)\Big]\rho^\beta_\gamma(\vec{y},\vec{z}) \\ \overset{(2.42)}{=} &\int \mathrm{d}\vec{y}\,\delta(\vec{x} - \vec{y}) \times (-\frac{i}{2})2i\delta(\vec{y} - \vec{z})\delta^\alpha_\gamma \\ &= \delta(\vec{x} - \vec{z})\delta^\alpha_\gamma\,, \end{aligned} \tag{2.43}$$

which is equivalent to the right hand side of the evolution-equation (2.36), or put differently: Pulling the sign-function through the inverse propagator G_0^{-1} in the

evolution-equation is equivalent to setting the r. h. s. to zero[4]

$$\begin{aligned} &\int \mathrm{d}\vec{y}\left[(G_0^{-1})^\alpha_\beta(\vec{x},\vec{y}) - \Sigma^\alpha_\beta(\vec{x},\vec{y})\right] F^\beta_\gamma(\vec{y},\vec{z}) \\ -\frac{i}{2}&\int \mathrm{d}\vec{y}\,\mathrm{sign}_\zeta(t_y - t_z)\left[(G_0^{-1})^\alpha_\beta(\vec{x},\vec{y}) - \Sigma^\alpha_\beta(\vec{x},\vec{y})\right]\rho^\beta_\gamma(\vec{y},\vec{z}) = 0\,. \end{aligned} \tag{2.44}$$

In this form the time-derivative term of G_0^{-1} does not act on the time-ordered propagator (or the sign_ζ-function equivalently) anymore.

2.6.3 Eliminating the Dependence on the Time-Contour ζ

In this subsection the formulation of the theory on the closed time-contour ζ is resolved into standard integrals over time. Integrating expressions which contain a $\mathrm{sign}_\zeta(t-t')$ term over the closed time contour ζ leads to a number of simplifications by noting that for any function $f(t)$ regular in t (details of the derivation are given in appendix C.1):

$$\int_\zeta f(t)\,\mathrm{d}t = 0 \qquad \text{(cf. C.1)}$$

$$\int_\zeta f(t)\,\mathrm{sign}_\zeta(t-t_1)\,\mathrm{d}t = -2\int_0^{t_1} f(t)\,\mathrm{d}t \qquad \text{(cf. C.3)}$$

$$\int_\zeta f(t)\,\mathrm{sign}_\zeta(t-t_1)\,\mathrm{sign}_\zeta(t-t_2)\,\mathrm{d}t = 2\,\mathrm{sign}_\zeta(t_1-t_2)\int_{t_1}^{t_2} f(t)\,\mathrm{d}t \qquad \text{(cf. C.10)}$$

Inserting the decomposition of Σ (2.32,2.33) and the form of G_0^{-1} (2.38) into equation (2.44) yields:

$$\begin{aligned} 0 = &\int \mathrm{d}\vec{y}\left[\delta(\vec{x}-\vec{y})\Big(V^\alpha_{t\beta}\partial_{t_x} + iM^\alpha_\beta(\vec{x})\Big)\right. \\ &\left. + i\delta(\vec{x}-\vec{y})(\Sigma^{(0)})^\alpha_\beta(\vec{x}) - (\Sigma^{\mathrm{F}})^\alpha_\beta(\vec{x},\vec{y}) + \frac{i}{2}\,\mathrm{sign}_\zeta(t_x-t_y)(\Sigma^\rho)^\alpha_\beta(\vec{x},\vec{y})\right] F^\beta_\gamma(\vec{y},\vec{z}) \\ -\frac{i}{2}&\int \mathrm{d}\vec{y}\,\mathrm{sign}_\zeta(t_y-t_z)\left[\delta(\vec{x}-\vec{y})\Big(V^\alpha_{t\beta}\partial_{t_x} + iM^\alpha_\beta(\vec{x})\Big)\right. \\ &\left. + i\delta(\vec{x}-\vec{y})(\Sigma^{(0)})^\alpha_\beta(\vec{x}) - (\Sigma^{\mathrm{F}})^\alpha_\beta(\vec{x},\vec{y}) + \frac{i}{2}\,\mathrm{sign}_\zeta(t_x-t_y)(\Sigma^\rho)^\alpha_\beta(\vec{x},\vec{y})\right]\rho^\beta_\gamma(\vec{y},\vec{z}) \end{aligned}$$

[4] Actually the same result also holds for relativistic theories [Berges, 2005].

Performing integrals over δ-functions

$$
\begin{aligned}
&= \Big[V_{t\beta}^{\alpha}\partial_{t_x} + iM_{\beta}^{\alpha}(\vec{x}) + i(\Sigma^{(0)})_{\beta}^{\alpha}(\vec{x})\Big]F_{\gamma}^{\beta}(\vec{x},\vec{z}) \\
&\quad + \int \mathrm{d}\vec{y}\,\Big[-(\Sigma^{\mathrm{F}})_{\beta}^{\alpha}(\vec{x},\vec{y}) + \frac{i}{2}\,\mathrm{sign}_{\zeta}(t_x - t_y)(\Sigma^{\rho})_{\beta}^{\alpha}(\vec{x},\vec{y})\Big]F_{\gamma}^{\beta}(\vec{y},\vec{z}) \\
&-\frac{i}{2}\,\mathrm{sign}_{\zeta}(t_x - t_z)\Big[V_{t\beta}^{\alpha}\partial_{t_x} + iM_{\beta}^{\alpha}(\vec{x}) + i(\Sigma^{(0)})_{\beta}^{\alpha}(\vec{x})\Big]\rho_{\gamma}^{\beta}(\vec{x},\vec{z}) \\
&\quad - \frac{i}{2}\int \mathrm{d}\vec{y}\,\mathrm{sign}_{\zeta}(t_y - t_z)\Big[-(\Sigma^{\mathrm{F}})_{\beta}^{\alpha}(\vec{x},\vec{y}) + \frac{i}{2}\,\mathrm{sign}_{\zeta}(t_x - t_y)(\Sigma^{\rho})_{\beta}^{\alpha}(\vec{x},\vec{y})\Big]\rho_{\gamma}^{\beta}(\vec{y},\vec{z})
\end{aligned}
$$

using the integration identities (cf. C.1 – cf. C.10) and $\mathrm{sign}_{\zeta}(t_x - t_y) = -\,\mathrm{sign}_{\zeta}(t_y - t_x)$:

$$
\begin{aligned}
&= \Big[V_{t\beta}^{\alpha}\partial_{t_x} + iM_{\beta}^{\alpha}(\vec{x}) + i(\Sigma^{(0)})_{\beta}^{\alpha}(\vec{x})\Big]F_{\gamma}^{\beta}(\vec{x},\vec{z}) \\
&\quad + 2\int_0^{t_x} \mathrm{d}t_y \int \mathrm{d}y\,\frac{i}{2}(\Sigma^{\rho})_{\beta}^{\alpha}(\vec{x},\vec{y})F_{\gamma}^{\beta}(\vec{y},\vec{z}) \\
&-\frac{i}{2}\,\mathrm{sign}_{\zeta}(t_x - t_z)\Big[V_{t\beta}^{\alpha}\partial_{t_x} + iM_{\beta}^{\alpha}(\vec{x}) + i(\Sigma^{(0)})_{\beta}^{\alpha}(\vec{x})\Big]\rho_{\gamma}^{\beta}(\vec{x},\vec{z}) \\
&\quad - \frac{i}{2}\int_0^{t_z} \mathrm{d}t_y \int \mathrm{d}y\,2(\Sigma^{\mathrm{F}})_{\beta}^{\alpha}(\vec{x},\vec{y})\rho_{\gamma}^{\beta}(\vec{y},\vec{z}) \\
&\quad - \frac{1}{2}\,\mathrm{sign}_{\zeta}(t_x - t_z)\int_{t_x}^{t_z} \mathrm{d}t_y \int dy(\Sigma^{\rho})_{\beta}^{\alpha}(\vec{x},\vec{y})\rho_{\gamma}^{\beta}(\vec{y},\vec{z})
\end{aligned}
$$

where the integrals over time-contours have all become "standard" integrals. Now, using the decomposition already applied to G (2.29) and $\bar{\Sigma}$ (2.33) on the entire evolution equation yields two equations:

$$
\begin{aligned}
iV_{t\beta}^{\alpha}\partial_{t_x}F_{\gamma}^{\alpha}(\vec{x},\vec{z}) &= \Big[M_{\beta}^{\alpha}(\vec{x}) + (\Sigma^{(0)})_{\beta}^{\alpha}(\vec{x})\Big]F_{\gamma}^{\beta}(\vec{x},\vec{z}) \\
&\quad + \int_0^{t_x} \mathrm{d}t_y \int \mathrm{d}y(\Sigma^{\rho})_{\beta}^{\alpha}(\vec{x},\vec{y})F_{\gamma}^{\beta}(\vec{y},\vec{z}) \\
&\quad - \int_0^{t_z} \mathrm{d}t_y \int \mathrm{d}y(\Sigma^{\mathrm{F}})_{\beta}^{\alpha}(\vec{x},\vec{y})\rho_{\gamma}^{\beta}(\vec{y},\vec{z})
\end{aligned}
\tag{2.45}
$$

from the part regular at $t_x = t_z$ and from the prefactor of $\mathrm{sign}_{\zeta}(t_x - t_z)$:

$$
\begin{aligned}
iV_{t\beta}^{\alpha}\partial_{t_x}\rho_{\gamma}^{\alpha}(\vec{x},\vec{z}) &= \Big[M_{\beta}^{\alpha}(\vec{x}) + (\Sigma^{(0)})_{\beta}^{\alpha}(\vec{x})\Big]\rho_{\gamma}^{\beta}(\vec{x},\vec{z}) \\
&\quad + \int_{t_x}^{t_z} \mathrm{d}t_y \int \mathrm{d}y(\Sigma^{\rho})_{\beta}^{\alpha}(\vec{x},\vec{y})\rho_{\gamma}^{\beta}(\vec{y},\vec{z})
\end{aligned}
\tag{2.46}
$$

Thereby the "stationary condition" (2.26) has been transformed from an operator-equation into a set of coupled differential equations, and then the integrations over the closed time-contour ζ have been transformed into "normal" integrals implementing the "memory" of the system on earlier times. In this form the equations can be treated with standard techniques.

The "memory-integrals" appear, because, although starting from a Gaussian initial state, non-Gaussian correlations will build up. Thus "restarting" the algorithm at some at $t_0' > 0$, in the sense of discarding all information on times smaller than t_0', is not possible as a Gaussian initial state would be required.

2.7 Non-Perturbative $1/\mathcal{N}$-Expansion

The large $\mathcal{N}$ expansion provides consistent approximations for sufficiently symmetric models including $\mathcal{N}$ field components, even if the absence of a small coupling or large fluctuations in the proximity of a phase-transition preclude application of standard perturbation theory. The role of the small expansion-parameter is played by the inverse number of field components $1/\mathcal{N}$. As is shown also explicitly in the appendix B.2, especially equation (B.25), an expansion in loops / number of vertices leads to unphysical effects for the two-component Bose-gas (see also chapter 3) investigated in this thesis.

2.7.1 General Idea

The expansion is based on two observations: Traces over field-index space like $\mathrm{Tr}(G) \propto \mathcal{N}$ scale proportional to the number of (real) field components, if the model is symmetric in these. For the two-component Bose-gas e. g. traces over the 4×4-matrix F (3.36) scale like $\mathcal{N} = 4$. And to have β-functions (for the coupling-constant g in the Hamiltonian (3.6)) independent of $\mathcal{N}$ a scaling of the bare coupling $g \propto N^{-1}$ is necessary.
Thus the order in $1/\mathcal{N}$ is given by the ratio of vertices to traces (or closed lines in a diagrammatic picture). For an example see next subsection 2.7.2.

2.7.2 Contributions to Low Orders

As figure 2.1 illustrates, for the generic two-loop diagram (2.1c) there are two different ways to trace over the indices, once $\propto \mathrm{Tr}(G)^2$ and once $\propto \mathrm{Tr}(G^2)$, which leads to

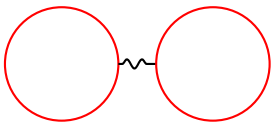

(a) Leading Order Part

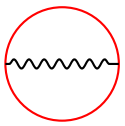

(b) Next-to-Leading Order Part

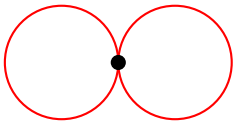

(c) Generic Two-Loop

Figure 2.1: *Distinction of the $^1/_{\mathcal{N}}$-Order of Diagrams:* The red solid lines are (full) propagators G, black curly lines denote the point-interactions. Interactions are drawn such that it is apparent where index-contractions are to be performed. At two-loops in general (2.1c) there are two contributions, one at leading order (2.1a) (there is one vertex vs. two traces / closed lines, so this scales as $\propto \mathcal{N}^1$) and one at next-to-leading order (2.1b) (there is one vertex vs. one trace / closed line, so this scales as $\propto \mathcal{N}^0$).

different scaling with $^1/_{\mathcal{N}}$. The leading order diagram (2.1a) is actually the only LO contribution for the system considered here (chapter 3).

The leading order of this expansion is known not to thermalize. This is because it does not incorporate scattering between different momentum-modes, thereby conserving the number of particles n_k at momentum k individually. Clearly no thermal (Bose-Einstein) momentum-distribution can be reached by these dynamics.

3 The Two-Component Bose-Gas

The System under investigation throughout the rest of this work is the "Two Component Bose Gas", described by a non-relativistic field-theory comprising two bosonic scalar fields, denoted here by $\phi_\uparrow$ and $\phi_\downarrow$. This system is studied in a quasi-one-dimensional setup. The system is assumed to be homogeneous in space and the initial conditions to be described by a Gaussian density-operator, such that the 2 PI-formalism is applicable.

3.1 The System

Here the formal definition of the system and parameters used is given. Further it is rewritten in a dimensionless formulation in terms of symmetrized fields.

3.1.1 Hamiltonian

The Hamiltonian is given as, e. g., in [Nicklas et al., 2015] by the sum

$$H = H_0 + H_{\mathrm{cpl}} + H_{\mathrm{int}} \tag{3.1}$$

of a "free" part (with the index i running over $\{\uparrow, \downarrow\}$ here)

$$H_0 = \int dx \phi_i^\dagger(x) \left(-\frac{\hbar^2}{2m}\partial_x^2 + V(x) \right) \phi_i(x)\,, \tag{3.2}$$

where $V = 0$ in the following, a part accounting for the coupling to the electromagnetic-field (radio-driving) with Rabi-coupling Ω and detuning δ

$$H_{\mathrm{cpl}} = \frac{\hbar}{2} \int dx \left[\Omega \left(\phi_\uparrow^\dagger(x)\phi_\downarrow(x) + \mathrm{h.\,c.} \right) + \delta \left(\phi_\uparrow^\dagger(x)\phi_\uparrow(x) - \phi_\downarrow^\dagger(x)\phi_\downarrow(x) \right) \right]\,, \tag{3.3}$$

where $\delta = 0$ will be assumed for simplicity in the following and a quartic point-interaction term which here is assumed to take the specific form

$$H_{\text{int}} = \frac{g}{2}\int dx \left[(\phi_\uparrow^\dagger(x)\phi_\uparrow(x))^2 + (\phi_\downarrow^\dagger(x)\phi_\downarrow(x))^2 + 2\alpha\phi_\uparrow^\dagger(x)\phi_\uparrow(x)\phi_\downarrow^\dagger(x)\phi_\downarrow(x)\right]. \quad (3.4)$$

Hence, for $\alpha > 1$ (in the experimental setup in [Nicklas et al., 2015]: $\alpha \approx 1.23$), the scattering between the different species is enhanced as compared to scattering of particles of the same type. Clearly any $\alpha \neq 1$ is explicitly braking the $O(2)$-symmetry of the model.

3.1.2 (Anti-)Symmetrization of Field-Basis

We introduce (anti-)symmetrized fields[1]

$$\phi_\pm := \frac{1}{\sqrt{2}}(\phi_\uparrow \pm \phi_\downarrow)\,, \quad (3.5)$$

in order to obtain a diagonal "mass", i. e. replacing the Rabi-coupling Ω by an effective detuning (as of now, units are used where $\hbar = 1$). The Hamiltonian reads then

$$\begin{aligned} H = \int dx \Bigg[& \phi_+^\dagger \left(-\frac{\partial_x^2}{2m} + \frac{\Omega}{2}\right)\phi_+ + \phi_-^\dagger \left(-\frac{\partial_x^2}{2m} - \frac{\Omega}{2}\right)\phi_- \\ & + \frac{g}{2}\left(\frac{\alpha+1}{2}\left[\phi_+^\dagger\phi_+ + \phi_-^\dagger\phi_-\right]^2 - \frac{\alpha-1}{2}\left[\phi_+^\dagger\phi_- + \phi_-^\dagger\phi_+\right]^2\right)\Bigg]. \end{aligned} \quad (3.6)$$

In this basis, also the deviation from the $O(2)$-symmetric model becomes manifest. For $\alpha \to 1$ the symmetric model is approached as $\frac{1}{2}(\alpha+1) \to 1$, while $\frac{1}{2}(\alpha-1) \to 0$. Using a more compact matrix-notation as introduced in section 2.1 this reads

$$H = \frac{1}{2}\int dx \Bigg[-\phi_\alpha^\dagger \frac{\partial_x^2}{2m}\phi^\alpha + \frac{\Omega}{2}\phi_\alpha^\dagger\, \vec{\sigma}_z{}^\alpha_\beta\, \phi^\beta + \frac{g^+}{4}\left[\phi_\alpha^\dagger\, \vec{\sigma}_0{}^\alpha_\beta\, \phi^\beta\right]^2 - \frac{g^-}{4}\left[\phi_\alpha^\dagger\, \vec{\sigma}_x{}^\alpha_\beta\, \phi^\beta\right]^2\Bigg] \quad (3.7)$$

where $g^\pm := \frac{1}{2}(\alpha \pm 1)g$ and with $\mathbb{1}_2$ the 2×2 identity-matrix

$$\vec{\sigma}_0 := \begin{pmatrix} \mathbb{1}_2 & 0 \\ 0 & \mathbb{1}_2 \end{pmatrix} \qquad \vec{\sigma}_x := \begin{pmatrix} 0 & \mathbb{1}_2 \\ \mathbb{1}_2 & 0 \end{pmatrix} \qquad \vec{\sigma}_z := \begin{pmatrix} \mathbb{1}_2 & 0 \\ 0 & -\mathbb{1}_2 \end{pmatrix}. \quad (3.8)$$

[1] We stick to the sign conventions of [Nicklas et al., 2015], while [Karl, 2016], defines H_{cpl} (3.3) with an overall minus sign, thereby exchanging the roles of $\phi_\pm$ (see also 3.6).

3.1.3 Dimensionless Formulation

Define (cf. [Nicklas et al., 2015])

$$\Omega_{\mathrm{c}} := \bar{\rho}(\alpha - 1)g \qquad \text{(mean-field critical point, 3.2.1)}, \tag{3.9}$$

$$\tilde{g} := \frac{\alpha + 1}{\alpha - 1} \approx 9.7 \qquad \text{(assuming } \alpha \approx 1.23\text{)}, \tag{3.10}$$

$$\epsilon := \frac{\Omega - \Omega_{\mathrm{c}}}{\Omega_{\mathrm{c}}} \qquad \text{(dimless distance to critical point)}, \tag{3.11}$$

$$\tilde{y} := y\sqrt{2m\Omega_{\mathrm{c}}} \qquad \to \partial_{\tilde{y}} = \frac{1}{\sqrt{2m\Omega_{\mathrm{c}}}}\partial_y\,, \tag{3.12}$$

$$\tilde{\phi} := \bar{\rho}^{-\frac{1}{2}}\phi \qquad \text{(normalizing densities to 1)}, \tag{3.13}$$

$$\tilde{H} := H\bar{\rho}^{-1}\sqrt{\frac{2m}{\Omega_{\mathrm{c}}}} \qquad \text{(dimless Hamiltonian)}, \tag{3.14}$$

where $\bar{\rho}$ is the total density. It is assumed that $\bar{\rho}$ is conserved and homogeneous in space, both of which are well-satisfied for the experiment [Nicklas et al., 2015]. Then the Hamiltonian can be rewritten as

$$\begin{aligned}\tilde{H} = \int d\tilde{x}\Bigg[&\tilde{\phi}_+^\dagger\left(-\partial_{\tilde{x}}^2 + \frac{\epsilon+1}{2}\right)\tilde{\phi}_+ + \tilde{\phi}_-^\dagger\left(-\partial_{\tilde{x}}^2 - \frac{\epsilon+1}{2}\right)\tilde{\phi}_- \\ &+\frac{1}{8}\left(\tilde{g}\left[\tilde{\phi}_+^\dagger\tilde{\phi}_+ + \tilde{\phi}_-^\dagger\tilde{\phi}_-\right]^2 - \left[\tilde{\phi}_+^\dagger\tilde{\phi}_- + \tilde{\phi}_-^\dagger\tilde{\phi}_+\right]^2\right)\Bigg],\end{aligned} \tag{3.15}$$

dropping the tildes (exept on $\tilde{g}$) as of now and using matrix notation (3.8) this reads

$$\begin{aligned}H = \frac{1}{2}\int d\tilde{x}\Bigg[&-\phi_\alpha^\dagger\partial_{\tilde{x}}^2\phi^\alpha + \frac{\epsilon+1}{2}\phi_\alpha^\dagger\,\vec{\sigma}_z{}_\beta^{\,\alpha}\,\phi^\beta + \frac{\tilde{g}}{8}(\phi_\alpha^\dagger\,\vec{\sigma}_0{}_\beta^{\,\alpha}\,\phi^\beta)(\phi_\delta^\dagger\,\vec{\sigma}_0{}_\gamma^{\,\delta}\,\phi^\gamma) \\ &-\frac{1}{8}(\phi_\alpha^\dagger\,\vec{\sigma}_x{}_\beta^{\,\alpha}\,\phi^\beta)(\phi_\delta^\dagger\,\vec{\sigma}_x{}_\gamma^{\,\delta}\,\phi^\gamma)\Bigg].\end{aligned} \tag{3.16}$$

3.2 Qualitative Understanding

This section is meant to provide a qualitative understanding of the far-from-equilibrium i. e. quench setting and expected dynamics, especially in the quasi-spin-$\frac{1}{2}$ system formed by the relative degrees of freedom. For this qualitative treatment, it useful to separate "central" and "relative" degrees of freedom [Karl, 2016; Nicklas et al., 2015]. To this end suppose that mode-occupations are large in comparison to

the respective commutators and the fields

$$\phi_\uparrow = |\phi_\uparrow| e^{-i\theta_\uparrow} \qquad \text{and} \qquad \phi_\downarrow = |\phi_\downarrow| e^{-i\theta_\downarrow} \tag{3.17}$$

can be treated classically. Then the relative d. o. f. are defined to be

$$\theta := \theta_\uparrow - \theta_\downarrow \qquad \text{and} \qquad s := |\phi_\uparrow| - |\phi_\downarrow| \tag{3.18}$$

while the corresponding central d. o. f. are given by

$$\bar{\theta} := \theta_\uparrow + \theta_\downarrow \qquad \text{and} \qquad n := |\phi_\uparrow| + |\phi_\downarrow| \,. \tag{3.19}$$

These central ones are the (local) total particle density n, and an unobservable absolute phase $\bar{\theta}$ both of which should vary slowly and are assumed to be constant for this qualitative approach here.

3.2.1 Mean-Field Groundstate

The mean-field ground-state (in terms of fundamental fields ϕ) of this system was discussed extensively by [Tommasini et al., 2003]. Here we consider a brief description in terms of local quasi-spins[2] instead, which describe the relative degrees of freedom by (note that $\vec{\sigma}_x$ and $\vec{\sigma}_z$ (3.8) are exchanged for the symmetrized fields $\phi_\pm$):

$$J_x(\vec{x}) := \frac{1}{2\bar{\rho}} \langle \begin{pmatrix} \phi_\uparrow^\dagger(\vec{x}) & \phi_\downarrow^\dagger(\vec{x}) \end{pmatrix} \vec{\sigma}_x \begin{pmatrix} \phi_\uparrow(\vec{x}) \\ \phi_\downarrow(\vec{x}) \end{pmatrix} \rangle = \frac{1}{2} \langle \begin{pmatrix} \phi_+^\dagger(\vec{x}) & \phi_-^\dagger(\vec{x}) \end{pmatrix} \vec{\sigma}_z \begin{pmatrix} \phi_+(\vec{x}) \\ \phi_-(\vec{x}) \end{pmatrix} \rangle \tag{3.20}$$

$$J_z(\vec{x}) := \frac{1}{2\bar{\rho}} \langle \begin{pmatrix} \phi_\uparrow^\dagger(\vec{x}) & \phi_\downarrow^\dagger(\vec{x}) \end{pmatrix} \vec{\sigma}_y \begin{pmatrix} \phi_\uparrow(\vec{x}) \\ \phi_\downarrow(\vec{x}) \end{pmatrix} \rangle = \frac{1}{2} \langle \begin{pmatrix} \phi_+^\dagger(\vec{x}) & \phi_-^\dagger(\vec{x}) \end{pmatrix} \vec{\sigma}_y \begin{pmatrix} \phi_+(\vec{x}) \\ \phi_-(\vec{x}) \end{pmatrix} \rangle \tag{3.21}$$

$$J_z(\vec{x}) := \frac{1}{2\bar{\rho}} \langle \begin{pmatrix} \phi_\uparrow^\dagger(\vec{x}) & \phi_\downarrow^\dagger(\vec{x}) \end{pmatrix} \vec{\sigma}_z \begin{pmatrix} \phi_\uparrow(\vec{x}) \\ \phi_\downarrow(\vec{x}) \end{pmatrix} \rangle = \frac{1}{2} \langle \begin{pmatrix} \phi_+^\dagger(\vec{x}) & \phi_-^\dagger(\vec{x}) \end{pmatrix} \vec{\sigma}_x \begin{pmatrix} \phi_+(\vec{x}) \\ \phi_-(\vec{x}) \end{pmatrix} \rangle \tag{3.22}$$

[2]These are quasi-spins in the sense of having the degrees of freedom of a spin-$\frac{1}{2}$ system. Of cause they do not *transform* as Lorentz-spinors, however.
The prefactor of $\frac{1}{2}$ arises from the combined index notation with $\frac{1}{2}(\phi_i^* \phi_j + \phi_j \phi_i^*)$ etc. terms.

Then the Hamiltonian (3.16) classically becomes

$$H = \int \mathrm{d}x \left[\frac{\epsilon+1}{2} J_x(\vec{x}) + \frac{\tilde{g}}{4} - \frac{1}{4} J_z(\vec{x})^2 \right]. \tag{3.23}$$

Here, it is assumed, that "anomalous" propagators $\propto \phi\phi$ or $\propto \phi^\dagger\phi^\dagger$ do not contribute and that the ground-state has zero momentum (in Fourier-space $H \propto k^2 \phi^\dagger_\alpha \phi^\alpha$ monotonically increasing in $|k|$). Then the ∂_x^2 term can been dropped for finding the ground-state and $J_a(\vec{x}) = J_a$ independent of x is assumed. Total number conservation $\bar{\rho} = \text{const}$ restricts the system to the Bloch-sphere $|\vec{J}| = 1$ and thus – since in this approximation the ground-state always has $J_y = 0$ (a state in J_z direction would always have lower energy) – one can insert $J_z^2 = 1 - J_x^2$ to find, constrained by $-1 \leq J_x \leq 1$

$$\frac{E}{V} \sim (\epsilon+1) J_x + \frac{1}{2} J_x^2 \qquad \text{minimal at} \quad \begin{cases} J_x = -1 & : \epsilon > 0 \\ J_x = -\epsilon - 1 & : -2 < \epsilon < 0 \\ J_x = 1 & : \epsilon < -2 \end{cases}. \tag{3.24}$$

Where $\epsilon = -2 \Leftrightarrow \Omega = -\Omega_\mathrm{c}$ describes the same physics as $\epsilon = 0$, but with $\phi_\pm$ exchanged, as can easily be seen from the Hamiltonian (3.16). This corresponds to

$$J_z = \sqrt{1 - J_x^2} = \begin{cases} 0 & : \epsilon > 0 \\ \sqrt{2|\epsilon|} & : \epsilon \lesssim 0 \end{cases}, \tag{3.25}$$

demonstrating a mean-field phase-transition at $\epsilon = 0$ with mean-field scaling

$$J_z \propto |\epsilon|^{\frac{1}{2}}, \tag{3.26}$$

of the order-parameter.

3.2.2 Phase Transition vs. Crossover

Classically, in (quasi) one-dimensional systems introducing a phase boundary in an ordered system costs *microscopic* energy, while causing a *macroscopic* increase in entropy – from the macroscopic number of possible positions to place the boundary – hence lowering, in the thermodynamic limit, the free energy $F = E - TS$ for any temperature $T \neq 0$. This implies that classically there are no ordered phases in 1D

at finite temperatures. At zero temperature quantum phase transitions can occur, when the ground-state of the system changes.

For a quantum system the situation is more subtle, because the thermal quantum-theory in one dimension maps to a two-dimensional classical theory, as explained at length e. g. by Sachdev [2011]. The second dimension is imaginary-time with extension $\sim {}^{1}/_{T}$, where T is the temperature of the system. However, for $T \neq 0$, in the IR – at energies well below T – excitations have wavelengths much larger then this additional dimension, and the system appears 1D again.

Far-from-equilibrium scenarios always include occupation of non-ground-states, thus non-zero effective temperatures, such that a crossover would be expected instead of a phase-transition. This applies to the setting investigated here.

3.3 Quench Protocol

The system is studied after a sudden quench of Ω from $\Omega_\mathrm{i} \sim \infty$ to some final value Ω_f. That is, it is assumed that the initial state is the ground-state of the Hamiltonian (3.16) for $\Omega = \Omega_\mathrm{i}$ whereas time-evolution is governed by the same Hamiltonian but with $\Omega = \Omega_\mathrm{f}$. The key concept of such quenches is, that the ground-state of the pre-quench Hamiltonian is far-from-equilibrium for the post-quench Hamiltonian. At the same time, by choosing $\Omega \gtrsim \Omega_\mathrm{c}$ dynamics close to criticality, or close to a crossover, can be observed. For example power-law scaling of the correlation length with the distance to the quantum critical point has been observed by Nicklas et al. [2015]. This seems to contradict the result of the discussion at 3.2.2, that a no phase-transition, but rather a crossover is expected. But the difference of both may become visible only close enough to the critical point. The numerical results in [Karl, 2016] suggest, that such deviations occur just outside the experimental range of $\epsilon \gtrsim 0.1$.

In the following, when it is referred to Ω or $\epsilon = \Omega_\mathrm{c}^{-1}(\Omega - \Omega_\mathrm{c})$ this is to be understood as a shorthand $\Omega = \Omega_\mathrm{f}$ if not stated otherwise.

3.4 The 2 PI Treatment

The system is assumed to be Bose-condensed, while the emergent quasi-spin dynamics occurs on length-scales larger than the system-size in two of three spatial dimensions, rendering the system effectively one-dimensional. Nevertheless, the condensate has

to be taken into account. A "macroscopic field" zero-mode $\varphi := \langle\phi\rangle := \langle\phi(x)\rangle$ is used to mimic this condensed background. Further, small deviations of this background-field to the $\Omega_\mathrm{i} = \infty$ ground-state are also included, as described in the following section 3.4.1.

In the present chapter, this setup will be analyzed using 2 PI methods as described in sections 2.5 and 2.6 to leading order in a $1/\mathcal{N}$-expansion (section 2.7). The hereby obtained evolution-equations will then also shed light on the behavior of energy-gap and correlation-length close to the critical point.

3.4.1 Initial State of the Zero-Mode

Let $n^\mathrm{c}_\uparrow$, $n^\mathrm{c}_\downarrow$ the number of condensed particles in the respective modes, $\varphi_\uparrow = \sqrt{n^\mathrm{c}_\uparrow} e^{-i\theta_\uparrow}$ and $\varphi_\downarrow = \sqrt{n^\mathrm{c}_\downarrow} e^{-i\theta_\downarrow}$. The "perfect" ($\Omega_\mathrm{i} = \infty$) mean-field ground-state (see 3.2.1) assumed as initial state by the quench-protocol in section 3.3, would have

$$n^\mathrm{c}_\uparrow = n^\mathrm{c}_\downarrow = \frac{n^\mathrm{c}}{2} \qquad \text{and} \qquad \theta_\uparrow - \theta_\downarrow = \pi\,, \tag{3.27}$$

where $n^\mathrm{c} = n^\mathrm{c}_\uparrow + n^\mathrm{c}_\downarrow$. But any of the two conditions may differ slightly for finite Ω_i

$$\theta_\uparrow - \theta_\downarrow \to \pi + \delta\theta \qquad \text{and} \qquad n^\mathrm{c}_\uparrow - n^\mathrm{c}_\downarrow \to \delta s\,. \tag{3.28}$$

Technically, also a variation in the total number of condensed particles n^c – which is otherwise assumed to be conserved throughout this thesis, as justified later, see equation (4.48) – and the (unphysical[3]) "central" phase $\bar\theta = \theta_\uparrow + \theta_\downarrow$ can be taken into account for completeness,

$$n^\mathrm{c} \to n^\mathrm{c} + \delta n^\mathrm{c} \qquad \text{and} \qquad \bar\theta \to \delta\bar\theta\,, \tag{3.29}$$

[3] "Unphysical" in the sense of *not* uniquely defined within the entire ensemble, because not observable. (see also section 3.4.2)

where the arbitrary $\bar{\theta} = 0$ has been set to zero. Then (recall that the $\pm$ fields are normalized (3.13) so that $\bar{\rho} = 1$, i. e. $\varphi_\pm := (2n^{\mathrm{c}})^{-1/2}(\varphi_\uparrow \pm \varphi_\downarrow)$) one finds

$$\begin{aligned}
\varphi_+ &= \frac{1}{\sqrt{2n^{\mathrm{c}}}} \left(\sqrt{\frac{n^{\mathrm{c}} + \delta n^{\mathrm{c}} + \delta s}{2}} e^{-i(\delta\bar{\theta}+\delta\theta)} + \sqrt{\frac{n^{\mathrm{c}} + \delta n^{\mathrm{c}} - \delta s}{2}} e^{-i(\pi+\delta\bar{\theta}-\delta\theta)} \right) \\
&= \frac{1}{\sqrt{2n^{\mathrm{c}}}} \left(\sqrt{\frac{n^{\mathrm{c}}}{2}} + \frac{\delta n^{\mathrm{c}} + \delta s}{2\sqrt{2n^{\mathrm{c}}}} \right) (1 - i\delta\bar{\theta} - i\delta\theta) \\
&+ \frac{1}{\sqrt{2n^{\mathrm{c}}}} \left(\sqrt{\frac{n^{\mathrm{c}}}{2}} + \frac{\delta n^{\mathrm{c}} - \delta s}{2\sqrt{2n^{\mathrm{c}}}} \right) (-1 + i\delta\bar{\theta} - i\delta\theta) + \mathcal{O}\left(\delta^2\right) \\
&= \frac{1}{2} \left(\frac{\delta s}{n^{\mathrm{c}}} - i\delta\theta \right) + \mathcal{O}\left(\delta^2\right) .
\end{aligned} \tag{3.30}$$

That means that small deviations to the infinite Ω_{i} initial state in the relative phase translate into a imaginary part of φ_+ while those in the relative density of the condensate induce a real part

$$\Re(\varphi_+) = \frac{1}{2}\frac{\delta s}{n^{\mathrm{c}}} \qquad \text{while} \qquad \Im(\varphi_+) = -\frac{1}{2}\delta\theta\,. \tag{3.31}$$

However, it is still natural to assume that the perturbation $\varphi_+ = \mathcal{O}(\delta)$ is very small in comparison to φ_-,

$$|\varphi_+^0| \ll |\varphi_-^0| \lesssim \bar{\rho} = 1\,. \tag{3.32}$$

For the central degrees of freedom, one has to modify equation (3.30) by replacing the plus-sign in between the terms by a minus-sign so as to

$$\begin{aligned}
\varphi_- &= \frac{1}{\sqrt{2n^{\mathrm{c}}}} \left(\sqrt{\frac{n^{\mathrm{c}}}{2}} + \frac{\delta n^{\mathrm{c}} + \delta s}{2\sqrt{2n^{\mathrm{c}}}} \right) (1 - i\delta\bar{\theta} - i\delta\theta) \\
&- \frac{1}{\sqrt{2n^{\mathrm{c}}}} \left(\sqrt{\frac{n^{\mathrm{c}}}{2}} + \frac{\delta n^{\mathrm{c}} - \delta s}{2\sqrt{2n^{\mathrm{c}}}} \right) (-1 + i\delta\bar{\theta} - i\delta\theta) + \mathcal{O}\left(\delta^2\right) \\
&= 1 + \frac{1}{2} \left(\frac{\delta n^{\mathrm{c}}}{n^{\mathrm{c}}} - i\delta\bar{\theta} \right) + \mathcal{O}\left(\delta^2\right) .
\end{aligned} \tag{3.33}$$

This shows that the φ_--mode is given by a mostly static norm ($\delta n^{\mathrm{c}} \approx 0$) and the unphysical "central" phase ($\bar{\theta} = \theta_\uparrow + \theta_\downarrow$), while φ_+ is sensitive to the "spin" degrees of freedom $\delta s = n^{\mathrm{c}}\delta J_z^{\mathrm{c}}$ and $\delta\theta = \delta J_y^{\mathrm{c}}$ (with J_y^{c}, J_z^{c} being the condensate parts of J_y, J_z).

3.4.2 The Ensemble

Typically the zero-mode wave-function implements a number of *macroscopic* observables, and therefore requires a restriction of the ensemble (cf. e. g. [Hohenberg and Martin, 1965]). It is important to recognize, that only the relative phase of the fields $\varphi_\uparrow$, $\varphi_\downarrow$, corresponding to the imaginary part of φ_+ (cf. the previous section 3.4.1), is observable. The sum of the two phases, corresponding to the phase of φ_-, is merely an "unphysical" gauge-degree of freedom. Still $|\varphi_-|$ is physical, although mostly static (see equation (3.33) and discussion thereof), while the arbitrary phase of φ_- should average out in the ensemble,

$$|\varphi_-| = \text{const} \approx 1 \qquad \text{but} \qquad \varphi_- = 0 \quad \text{(ensemble average)}\,. \tag{3.34}$$

Or expressed slightly more rigorous

$$(\varphi_-^*)^m(\varphi_-)^n = \delta_{mn}|\varphi_-|^{m+n}\,. \tag{3.35}$$

The φ_+-mode is physical (well-defined as *macroscopic* observable of the ensemble).

3.4.3 Definitions of Local Densities

The important observables (besides the field expectations values as described in the previous section 3.4.2) are constructed form local densities. First, consider the propagator G_β^α with "statistical" part (2.31)

$$\begin{aligned} F_\beta^\alpha(\vec{x},\vec{y}) &= \frac{1}{2}\left\langle \phi^\alpha(\vec{x})\otimes\phi_\beta^\dagger(\vec{y}) + \phi^\beta(\vec{x})\otimes\phi_\alpha^\dagger(\vec{y})\right\rangle_c \\ &= \begin{pmatrix} f_{++}(\vec{x},\vec{y}) & h_{++}(\vec{x},\vec{y}) & f_{+-}(\vec{x},\vec{y}) & h_{+-}(\vec{x},\vec{y}) \\ h_{++}^*(\vec{x},\vec{y}) & f_{++}^*(\vec{x},\vec{y}) & h_{+-}^*(\vec{x},\vec{y}) & f_{+-}^*(\vec{x},\vec{y}) \\ f_{-+}(\vec{x},\vec{y}) & h_{-+}(\vec{x},\vec{y}) & f_{--}(\vec{x},\vec{y}) & h_{--}(\vec{x},\vec{y}) \\ h_{-+}^*(\vec{x},\vec{y}) & f_{-+}^*(\vec{x},\vec{y}) & h_{--}^*(\vec{x},\vec{y}) & f_{--}^*(\vec{x},\vec{y}) \end{pmatrix}, \end{aligned} \tag{3.36}$$

where $\langle\ldots\rangle_c$ denotes a cummulant / connected part. The f are "normal" parts of the form $\langle\phi^\dagger\phi + \phi\phi^\dagger\rangle_c$, while h are "anomalous" $\langle\phi\phi + \phi\phi\rangle_c$ correlators. The Kronecker product (or equivalently the outer product, i. e., a $n\times 1$ times $1\times n$ matrix product) means

$$(\phi\otimes\phi^\dagger)_\beta^\alpha := \phi^\alpha\phi_\beta^\dagger\,. \tag{3.37}$$

Explicitly, this implies for the components

$$\begin{aligned} f^*_{++}(\vec{x},\vec{y}) &= \langle \phi_+(\vec{x})\phi^\dagger_+(\vec{y}) + \phi^\dagger_+(\vec{y})\phi_+(\vec{x})\rangle^*_c \\ &= \langle \phi_+(\vec{y})\phi^\dagger_+(\vec{x}) + \phi^\dagger_+(\vec{x})\phi_+(\vec{y})\rangle_c = f_{++}(\vec{y},\vec{x})\,, \end{aligned} \tag{3.38}$$

and analogously for f_{--}, while for the "off-diagonal" terms

$$\begin{aligned} f^*_{+-}(\vec{x},\vec{y}) &= \langle \phi_+(\vec{x})\phi^\dagger_-(\vec{y}) + \phi^\dagger_-(\vec{y})\phi_+(\vec{x})\rangle^*_c \\ &= \langle \phi_-(\vec{y})\phi^\dagger_+(\vec{x}) + \phi^\dagger_+(\vec{x})\phi_-(\vec{y})\rangle_c = f_{-+}(\vec{y},\vec{x})\,. \end{aligned} \tag{3.39}$$

Focusing on local densities, as those will appear in the leading order local self-energy $\Sigma^{(0)}$,

$$N_{ij}(\vec{x}) := f_{ij}(\vec{x},\vec{x}) \qquad \text{and} \qquad M_{ij}(\vec{x}) := h_{ij}(\vec{x},\vec{x})\,, \tag{3.40}$$

and the shorthand notations for the spatially homogeneous system

$$N_{ij}(t) := N_{ij}(x,t) \qquad \text{and} \qquad M_{ij}(t) := M_{ij}(x,t)\,, \tag{3.41}$$

can be defined. Clearly from the definition of F specifically equations (3.38, 3.39)

$$N_{++}(t), N_{--}(t) \in \mathbb{R} \qquad \text{while} \qquad N_{+-}(t) = N^*_{-+}(t)\,. \tag{3.42}$$

Further of great importance will be

$$N(t) := N_{++}(t) + N_{--}(t) \qquad \text{and} \qquad S_x(t) := N_{++}(t) - N_{--}(t)\,, \tag{3.43}$$

which are physically the connected / cummulant parts of the (conserved) local density

$$\begin{aligned} \bar{\rho} :=& \frac{1}{2}\langle \phi^\dagger_+(\vec{x})\phi_+(\vec{x}) + \phi_+(\vec{x})\phi^\dagger_+(\vec{x})\rangle + \frac{1}{2}\langle \phi^\dagger_-(\vec{x})\phi_-(\vec{x}) + \phi_-(\vec{x})\phi^\dagger_-(\vec{x})\rangle \\ =& |\varphi_+(t)|^2 + |\varphi_-(t)|^2 + N(t) \end{aligned} \tag{3.44}$$

and of the pseudo-spin in x-direction (the population imbalance in (anti-)symmetric field-components) previously defined for discussing the mean-field limit (3.20)

$$\begin{aligned} \bar{\rho}\,\langle J_x\rangle :=& \frac{1}{2}\langle \phi^\dagger_+(\vec{x})\phi_+(\vec{x}) + \phi_+(\vec{x})\phi^\dagger_+(\vec{x})\rangle - \frac{1}{2}\langle \phi^\dagger_-(\vec{x})\phi_-(\vec{x}) + \phi_-(\vec{x})\phi^\dagger_-(\vec{x})\rangle \\ =& |\varphi_+(t)|^2 - |\varphi_-(t)|^2 + S_x(t)\,, \end{aligned} \tag{3.45}$$

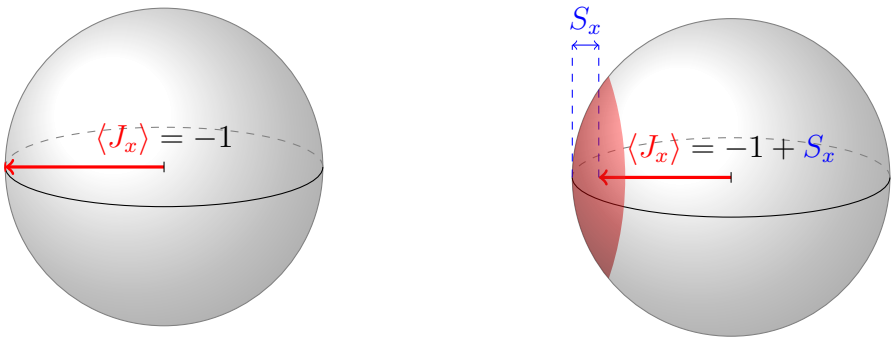

Figure 3.1: *Relevance of S_x to Capture Growth in the Variances of the Spins in y- and z-direction:* In the initial state, the pseudo-spin points straight to the left. If the variance in y- and z-direction is negligible this means $\langle J_x \rangle = -1$ (left image). For increasing variance in y- and z-direction, pictured by the colored region (right image) the average $\langle J_x \rangle \neq -1$, even if still $\langle J_y \rangle = \langle J_z \rangle = 0$ is maintained.

where the macroscopic field (zero-mode)

$$\varphi_\pm(t) := \langle \phi_\pm(t) \rangle := \langle \phi_\pm(t, x) \rangle \qquad \text{(spatially constant)} \tag{3.46}$$

has been used.

Because of the macroscopic field mimicking the condensate-mode, $N(t)$ describes the density of those particles *not* condensed and is henceforth referred to as a condensate-"depletion". The significance of S_x lies in the way it can capture increasing variances of J_y and J_z without the requirement of calculating four-point functions like $\langle J_z^2 \rangle$. (This is indeed a *four*-point function in the fundamental fields ϕ.) This is illustrated in figure 3.1.

3.4.4 Inverse Free Propagator

The inverse free propagator $i(G_0^{-1})^\alpha_\beta(\vec{x}, \vec{y}) = \frac{\delta^2 S}{\delta\phi^\dagger_\alpha(\vec{x})\delta\phi^\beta(\vec{y})}$ can be read of from the Hamiltonian (3.16), using

$$S = \int_\zeta dt \int dx \frac{i}{2} \overbrace{\left(\phi^*_+ \partial_t \phi_+ + \phi^*_- \partial_t \phi_- - \text{h. c.}\right)}^{= V_t{}^\alpha_\beta \phi^\dagger_\alpha \partial_t \phi^\beta} - \int_\zeta dt H(t)\,, \tag{3.47}$$

and employing $V_t = \mathrm{diag}(1,-1,1,-1)$ (as defined before around (2.38))

$$\begin{aligned}(G_0^{-1})^\alpha_\beta = \delta(\vec{x}-\vec{y})\Bigg[& V_{t\beta}^\alpha \partial_{t_x} - i\delta^\alpha_\beta \partial_x^2 + i\frac{\epsilon+1}{2}\,\vec{\sigma}_z{}^\alpha_\beta \\ & + \frac{i\tilde{g}}{4}\left(2\big[\,\vec{\sigma}_0{}^\alpha_\gamma\,\varphi^\gamma\big]\big[\varphi^\dagger_\delta\,\vec{\sigma}_0{}^\delta_\beta\,\big] + \big[\varphi^\dagger_\gamma\,\vec{\sigma}_0{}^\gamma_\delta\,\varphi^\delta\big]\big[\,\vec{\sigma}_0{}^\alpha_\beta\,\big]\right) \\ & - \frac{i}{4}\left(2\big[\,\vec{\sigma}_x{}^\alpha_\gamma\,\varphi^\gamma\big]\big[\varphi^\dagger_\delta\,\vec{\sigma}_x{}^\delta_\beta\,\big] + \big[\varphi^\dagger_\gamma\,\vec{\sigma}_x{}^\gamma_\delta\,\varphi^\delta\big]\big[\,\vec{\sigma}_x{}^\alpha_\beta\,\big]\right)\Bigg].\end{aligned} \tag{3.48}$$

Further, splitting of the time-derivative to assume the form (2.38)

$$\begin{aligned}M^\alpha_\beta(\vec{x}) = & -\delta^\alpha_\beta\partial_x^2 + \frac{\epsilon+1}{2}\,\vec{\sigma}_z{}^\alpha_\beta \\ & + \frac{\tilde{g}}{4}\left(2\big[\,\vec{\sigma}_0{}^\alpha_\gamma\,\varphi^\gamma\big]\big[\varphi^\dagger_\delta\,\vec{\sigma}_0{}^\delta_\beta\,\big] + \big[\varphi^\dagger_\gamma\,\vec{\sigma}_0{}^\gamma_\delta\,\varphi^\delta\big]\big[\,\vec{\sigma}_0{}^\alpha_\beta\,\big]\right) \\ & - \frac{1}{4}\left(2\big[\,\vec{\sigma}_x{}^\alpha_\gamma\,\varphi^\gamma\big]\big[\varphi^\dagger_\delta\,\vec{\sigma}_x{}^\delta_\beta\,\big] + \big[\varphi^\dagger_\gamma\,\vec{\sigma}_x{}^\gamma_\delta\,\varphi^\delta\big]\big[\,\vec{\sigma}_x{}^\alpha_\beta\,\big]\right).\end{aligned} \tag{3.49}$$

3.4.5 Applicability of the $1/N$-Expansion

The model under investigation becomes $O(2)$-symmetric when setting $\alpha = 1$ and $\Omega = 0$ (i. e. $\epsilon = -1$). In this case a non-perturbative $1/N$-expansion as described beforehand in section section 2.7 can be applied.

If the limit of large $\mathcal{N}$ is understood as the limit of almost classical statistics – in the sense that two particles scattering are almost always of different "species", thus distinguishable – then an expansion in $1/\mathcal{N}$ would be applicable, also for parameters as used here, if there is a similar number of excitations in the different fields. This also fits to the underlying idea of symmetry under exchange of species. Although the zero-mode is mostly in the lighter mode $|\varphi_-| \gg |\varphi_+|$ the fluctuations of both are similar as long as the connected part of the spin in x-direction $S_x = F_{++} - F_{--}$ is small compared to the total fluctuations / condensate-depletion $N = F_{++} + F_{--} \approx N_0$. This will be reviewed using the final results at 5.3.2.

4 Derivation of the Evolution Equations

In this chapter the 2 PI formalism is used to derive a set of differential equations describing the system and quench-setup presented in chapter 3.

4.1 Two Particle Irreducible Contributions

Here the diagrammatic contributions and the resulting expressions for Γ_2 and the self-energy Σ are given. Therefor the leading order in $1/\mathcal{N}$ – in the inverse number of field-components, see section 2.7 – is considered. An expansion in loops (Hartree–Fock) is *not* used here as it is expected to break down near second-order phase-transitions in general (cf. section 2.3) and is found to induce unphysical features for this system in particular (appendix B.2). As noted in the derivation of the 2 PI framework, see 2.5.2 only two-particle-irreducible closed diagrams contribution to Γ_2. To leading order this is only the "double-bubble" diagram (figure 4.1a). It implies the following beyond one-loop correction $\Gamma_2[\varphi, G] = \Gamma_2[G]$,

$$\Gamma_2^{\mathrm{db}}[G] = -\frac{i}{2} \times \frac{1}{8} \int dx \int_\zeta dt \Big[\tilde{g} \operatorname{Tr}\big(G(x,x;t,t)\, \vec{\sigma}_0 \big)^2 - \operatorname{Tr}\big(G(x,x;t,t)\, \vec{\sigma}_x \big)^2 \Big] . \tag{4.1}$$

This implies a local self-energy, independent of ρ, of the form

$$\Sigma^{(0)}(x,t) = \frac{\tilde{g}}{4} \operatorname{Tr}\big(F(x,x;t,t)\, \vec{\sigma}_0 \big)\, \vec{\sigma}_0 - \frac{1}{4} \operatorname{Tr}\big(F(x,x;t,t)\, \vec{\sigma}_x \big)\, \vec{\sigma}_x \ , \tag{4.2}$$

while the non-local part $\bar{\Sigma} = 0$ vanishes in this order. With a local self-energy only, the dynamic equations (2.45, 2.46) read (again $V_t = \operatorname{diag}(1,-1,1,-1)$ (3.48))

$$iV_t \partial_{t_x} F(\vec{x},\vec{y}) = \big(M[\varphi(\vec{x})] + \Sigma^{(0)}[F(\vec{x},\vec{x})] \big) F(\vec{x},\vec{y}) \,, \tag{4.3}$$

$$iV_t \partial_{t_x} \rho(\vec{x},\vec{y}) = \big(M[\varphi(\vec{x})] + \Sigma^{(0)}[F(\vec{x},\vec{x})] \big) \rho(\vec{x},\vec{y}) \,. \tag{4.4}$$

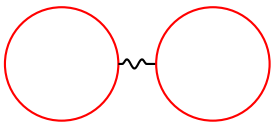

(a) The "Double-Bubble" Diagram: This is the only leading order contribution to the 2 PI effective action Γ_2.

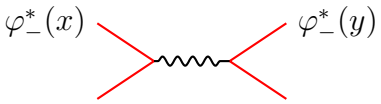

(b) Due to contributions like this, the effective anomalous propagators $M \neq 0$ in general.

Figure 4.1: *Examples of Relevant Diagrams:* The red solid lines are (full) propagators G, black curly lines denote the point-interactions. (see 2.7.2).

Important simplifications to this order as compared to the general case are: There are no memory-integrals appearing, equal-time two-point functions depend on equal-time two-point functions only and the equations of F and ρ decouple. Throughout this thesis the focus is on equal-time functions, where ρ is trivially given by an equal-time commutator (cf. equation (2.30)). Treated in the following are the (matrix-)equation for *local* and *equal-time* F given by (4.3) after setting $\vec{y} = \vec{x}$. The implications of these equations will be discussed in the next sections.

4.2 Macroscopic Fields

In this section we present technical details for the derivation of the equations which govern the time-evolution of the macroscopic field φ. Major findings will be a frame in which $\varphi_- = \text{const}$ and the time-evolution for φ_+ (4.20) (in this frame called $\tilde{\varphi}_+$)

$$i\partial_t \tilde{\varphi}_+ = \frac{1}{2}\big[2\epsilon + 1 + N + (\tilde{g}+1)S_x\big]\tilde{\varphi}_+ - \frac{1}{2}\big[1 - N + \tilde{g}\tilde{M}_{++} - \tilde{M}_{--}\big]\tilde{\varphi}^*_+ \,.$$

This result will be stated again the beginning of chapter 5, where physical implications are discussed.

Evolution equations for the macroscopic fields are deduced from the second stationary condition (2.28) where Γ_2, given by (4.1), is independent of φ to this order. Using the explicit form of the free inverse propagator G_0^{-1} (3.48) one gets

$$\begin{aligned} iV_t\partial_t\varphi = {} & \frac{\epsilon+1}{2}\,\vec{\sigma}_z\,\varphi + \frac{\tilde{g}}{4}\big(\varphi^\dagger\,\vec{\sigma}_0\,\varphi\big)\,\vec{\sigma}_0\,\varphi - \frac{1}{4}\big(\varphi^\dagger\,\vec{\sigma}_x\,\varphi\big)\,\vec{\sigma}_x\,\varphi \\ & + \frac{\tilde{g}}{4}\Big(2\,\vec{\sigma}_0\,F\,\vec{\sigma}_0\,\varphi + \mathrm{Tr}\,\big(\,\vec{\sigma}_0\,F\big)\,\vec{\sigma}_0\,\varphi\Big) \\ & - \frac{1}{4}\Big(2\,\vec{\sigma}_x\,F\,\vec{\sigma}_x\,\varphi + \mathrm{Tr}\,\big(\,\vec{\sigma}_x\,F\big)\,\vec{\sigma}_x\,\varphi\Big)\,, \end{aligned} \tag{4.5}$$

where the term $\propto \partial_x^2\varphi$ has been dropped because φ, mimicking the coherent zero-mode, is assumed to be spatially constant. If not stated otherwise, $F = F(\vec{x},\vec{x})$ denotes local densities throughout this section. The time-dependence of F, N, M and φ is also not written explicitly for the sake of readability. While $V_t = \mathrm{diag}(1,-1,1,-1)$ (3.48), the $\vec{\sigma}$ are the matrices defined at before in equation (3.8). One finds for the individual terms of (4.5),

$$\varphi^\dagger\ \vec{\sigma}_0\ \varphi = \varphi^\dagger \mathbb{1}_4 \varphi = \varphi_+^*\varphi_+ + \varphi_+\varphi_+^* + \varphi_-^*\varphi_- + \varphi_-\varphi_-^* = 2\big[|\varphi_+|^2 + |\varphi_-|^2\big]\,, \quad (4.6)$$

which describes coupling to the total condensate-density $n^{\mathrm{c}} = |\varphi_+|^2 + |\varphi_-|^2$. The term

$$\varphi^\dagger\ \vec{\sigma}_x\ \varphi = \varphi^\dagger \begin{pmatrix} 0 & \mathbb{1}_2 \\ \mathbb{1}_2 & 0 \end{pmatrix} \varphi = 2\big[\varphi_+^*\varphi_- + \varphi_-^*\varphi_+\big]\,. \quad (4.7)$$

couples the two field-components to each other. Furthermore by the form of F as given in equation (3.36) we have

$$\mathrm{Tr}\,\big(\ \vec{\sigma}_0\ F\big) = \mathrm{Tr}\, F = 2N\,, \quad (4.8)$$

describing coupling to the total non-condensed density, that is to the depletion. Using a "symbolic" notation for F apparent from the definition in (3.36)

$$\begin{aligned} \mathrm{Tr}\,\big(\ \vec{\sigma}_x\ F\big) &= \mathrm{Tr}\left[\begin{pmatrix} 0 & \mathbb{1}_2 \\ \mathbb{1}_2 & 0 \end{pmatrix}\begin{pmatrix} F_{++} & F_{+-} \\ F_{-+} & F_{--} \end{pmatrix}\right] = \mathrm{Tr}\begin{pmatrix} F_{-+} & F_{--} \\ F_{++} & F_{+-} \end{pmatrix} \\ &= N_{+-} + N_{+-}^* + N_{-+} + N_{-+}^* \overset{(3.42)}{=} 2\big[N_{+-} + N_{-+}\big]\,, \end{aligned} \quad (4.9)$$

shows coupling to off-diagonal terms N_{+-}, which are related to $\langle J_y\rangle$ and $\langle J_z\rangle$. Now combining (4.6 – 4.9) in equation (4.5) and using $\bar{\rho} \overset{(3.44)}{:=} |\varphi_+|^2 + |\varphi_-|^2 + N$ the result reads

$$\begin{aligned} &iV_t\partial_t\varphi \quad (4.10)\\ &= \frac{1}{2}\Big\{ \overbrace{(\epsilon+1)\ \vec{\sigma}_z + \tilde{g}\bar{\rho}}^{=:\mathcal{A}\ \text{(diagonal part)}} - \overbrace{\big[\varphi_+^*\varphi_- + \varphi_-^*\varphi_+ + N_{+-} + N_{-+}\big]\ \vec{\sigma}_x}^{=:\mathcal{B}} + \overbrace{\tilde{g}F - \vec{\sigma}_x\ F\ \vec{\sigma}_x}^{=:\mathcal{C}} \Big\}\varphi\,. \end{aligned}$$

In the symmetric phase the "off-diagonal" terms (spins in y- / z-direction) vanish, as

can be seen from the ground-state treatment in subsection 3.2.1

$$N_{+-} = 0 \qquad \text{and} \qquad M_{+-} = 0\,. \tag{4.11}$$

The term $\mathcal{C}$ simplifies, using the form of F as given in equation (3.36), to

$$\mathcal{C} = \begin{pmatrix} \tilde{g}N_{++} - N_{--} & \tilde{g}M_{++} - M_{--} & 0 & 0 \\ \tilde{g}M^*_{++} - M^*_{--} & \tilde{g}N^*_{++} - N^*_{--} & 0 & 0 \\ 0 & 0 & \tilde{g}N_{--} - N_{++} & \tilde{g}M_{--} - M_{++} \\ 0 & 0 & \tilde{g}M^*_{--} - M^*_{++} & \tilde{g}N^*_{--} - N^*_{++} \end{pmatrix}, \tag{4.12}$$

and by inspection of the term $\mathcal{B}$, a linear expansion around $|\varphi_+| = 0$ (3.32) yields

$$\mathcal{B}\varphi = \left[\varphi^*_+\varphi_- + \varphi^*_-\varphi_+\right] \begin{pmatrix} \varphi_- \\ \varphi^*_- \\ \varphi_+ \\ \varphi^*_+ \end{pmatrix} = \begin{pmatrix} \varphi^2_-\varphi^*_+ + |\varphi_-|^2\varphi_+ \\ (\varphi^*_-)^2\varphi_+ + |\varphi_-|^2\varphi^*_+ \\ 0 \\ 0 \end{pmatrix} + \mathcal{O}\left(|\varphi_+|^2\right). \tag{4.13}$$

Thereby in the symmetric regime the "central" degrees of freedom (φ_-) decouple from the "relative" degrees of freedom (φ_+), because clearly the diagonal part $\mathcal{A}$ does not couple them either. Dropping the V_t on the left hand side of equation (4.10) changes the sign of the equation for φ^*_- such that:

$$i\partial_t \begin{pmatrix} \varphi_- \\ \varphi^*_- \end{pmatrix} = \frac{1}{2} \begin{pmatrix} -(\epsilon+1) + \tilde{g}\bar{\rho} + \tilde{g}N_{--} - N_{++} & \tilde{g}M_{--} - M_{++} \\ -\tilde{g}M^*_{--} + M^*_{++} & (\epsilon+1) - \tilde{g}\bar{\rho} - \tilde{g}N^*_{--} + N^*_{++} \end{pmatrix} \begin{pmatrix} \varphi_- \\ \varphi^*_- \end{pmatrix} \tag{4.14}$$

Neglecting anomalous terms for the central degrees of freedom (φ_-) – which is equivalent to approximate conservation of the norm $|\varphi_-|$ which will be found to be consistent to $\mathcal{O}\left(|\varphi_+|^2\right)$ a posteriori (cf. equation (4.48)) – and going to a rotating frame with[1]

$$\tilde{\varphi}_\pm = e^{-i\mu t}\varphi_\pm \quad , \quad \tilde{\varphi}^*_\pm = e^{i\mu t}\varphi^*_\pm \quad \text{and} \quad \tilde{M}_{\pm\pm} = e^{-2i\mu t}M_{\pm\pm} \tag{4.15}$$

[1] Although clearly $\tilde{\varphi}^2_\pm = e^{-2i\mu t}\varphi^2_\pm$, technically it is not obvious, that this holds for the connected parts of $\langle\phi_\pm\phi_\pm\rangle_c = M_{\pm\pm}$ as well, however this will be checked later, cf. (4.30).

gives, according to equation (4.14) the evolution of $\tilde{\varphi}_-$ in time as

$$\begin{aligned} i\partial_t\tilde{\varphi}_- &= i\partial_t\big(e^{-i\mu t}\varphi\big) \\ &= (\mu + t\partial_t\mu)e^{-i\mu t}\varphi_- + e^{-i\mu t}\big[-(\epsilon+1) + \tilde{g}\bar{\rho} + \tilde{g}N_{--} - N_{++}\big]\varphi_- \\ &= \big[\mu + t\partial_t\mu - (\epsilon+1) + \tilde{g}\bar{\rho} + \tilde{g}N_{--} - N_{++}\big]\tilde{\varphi}_- \,. \end{aligned} \tag{4.16}$$

Now choose μ such that $\tilde{\varphi}_-$ is constant for $\partial_t\mu \approx 0$,

$$\mu := \epsilon + 1 - \tilde{g}\bar{\rho} - \tilde{g}N_{--} + N_{++} = \epsilon + 1 - \tilde{g}\bar{\rho} - \frac{\tilde{g}-1}{2}N + \frac{\tilde{g}+1}{2}S_x \,. \tag{4.17}$$

That $\partial_t\mu \approx 0$ is the case if S_x and N are static or vary slowly in time compared to μ. This proves to be consistent later on, because either (for "large" ϵ)[2] $S_x \ll 1$ is negligible (5.40, 5.51) or (for "small" ϵ) it varies with frequencies on the order of $\sqrt{\Delta_{\epsilon^2}} \approx 10^{-2}$ (5.43) while $\mu \approx \tilde{g}\bar{\rho} \approx 10^1$ (4.17). At the same time, $N = N_0$ is constant (to $\mathcal{O}\left(|\varphi_+|^2\right)$), see (4.48).

In this rotating frame the relative degrees of freedom (φ_+) follow the equation (4.10) with values for $\mathcal{B}$ and $\mathcal{C}$ from (4.12 – 4.13) and an explicit expression for the diagonal part $\mathcal{A}$. This equation then reads

$$i\partial_t \begin{pmatrix} \tilde{\varphi}_+ \\ \tilde{\varphi}_+^* \end{pmatrix} = \begin{pmatrix} \epsilon + 1 - \frac{1}{2}|\tilde{\varphi}_-|^2 + \frac{\tilde{g}+1}{2}S_x & \frac{1}{2}\big[(\tilde{\varphi}_-)^2 + \tilde{g}\tilde{M}_{++} - \tilde{M}_{--}\big] \\ -\frac{1}{2}\big[(\tilde{\varphi}_-)^2 + \tilde{g}\tilde{M}^*_{++} - \tilde{M}^*_{--}\big] & -(\epsilon+1) + \frac{1}{2}|\tilde{\varphi}_-|^2 - \frac{\tilde{g}+1}{2}S_x \end{pmatrix} \begin{pmatrix} \tilde{\varphi}_+ \\ \tilde{\varphi}_+^* \end{pmatrix}. \tag{4.18}$$

Now, the dimensionless formulation of the theory (3.13) was chosen such that

$$1 = \bar{\rho} = |\varphi_+|^2 + |\varphi_-|^2 + N \,. \tag{4.19}$$

Furthermore choosing the phase of the constant $\tilde{\varphi}_-$ such that $\tilde{\varphi}_- \in \mathbb{R}_+$ the equation of motion for $\tilde{\varphi}_+$ (4.18) finally reads

$$i\partial_t\tilde{\varphi}_+ = \frac{1}{2}\big[2\epsilon + 1 + N + (\tilde{g}+1)S_x\big]\tilde{\varphi}_+ - \frac{1}{2}\big[1 - N + \tilde{g}\tilde{M}_{++} - \tilde{M}_{--}\big]\tilde{\varphi}_+^* \,. \tag{4.20}$$

[2]Large ϵ means $(\epsilon + \Delta_\epsilon)^2 \gg \Delta_{\epsilon^2}$, see final results and discussion around equation (5.43).

4.3 Densities

In this section we present technical details on the derivation of the time-evolution of the condensate depletion N and the connected part S_x of the spin in x-direction, which is of special interest (see discussion of figure 3.1 at the end of subsection 3.4.3). The important results are (4.44 – 4.46)

$$\begin{aligned}\partial_t N &= \partial_t\big(N_{++} + N_{--}\big) = m_- \Im(\varphi_+^2)\,,\\ \partial_t S_x &= \partial_t\big(N_{++} - N_{--}\big) = m_+ \Im(\varphi_+^2)\,,\\ m_\pm &= \tilde{g} M_{++} \pm M_{--} = \mathrm{const}_\pm\,.\end{aligned}$$

These results will be stated again at the beginning of chapter 5.

Returning now to two-point functions, we are in particular interested in the central-time evolution of equal-time densities, while the dynamic equation (4.3) describes changes with respect to the first time-coordinate only. Therefore observe

$$\begin{aligned} iV_t\partial_{t_y} F(\vec{x},\vec{y})|_{\vec{y}=\vec{x}} &\overset{(3.36)}{=} \big[-iV_t\partial_{t_y} F(\vec{y},\vec{x})|_{\vec{y}=\vec{x}}\big]^\dagger \\ &\overset{(4.3)}{=} -\big[\big(M+\Sigma^{(0)}\big)F(\vec{y},\vec{y})\big]^\dagger_{\vec{y}=\vec{x}} \\ &\overset{(3.36)}{=} -F(\vec{x},\vec{x})\big(M+\Sigma^{(0)}\big)\,, \end{aligned} \tag{4.21}$$

where in the last step, it was used that both M and $\Sigma^{(0)}$ are Hermitian. Combining this with the "original" equation (4.3) yields a commutator

$$\begin{aligned} iV_t\partial_{t_x} F(\vec{x},\vec{x}) &= (iV_t\partial_{t_x} + iV_t\partial_{t_y})F(\vec{x},\vec{y})|_{\vec{y}=\vec{x}} \\ &= \Big[M+\Sigma^{(0)}, F(\vec{x},\vec{x})\Big]\,. \end{aligned} \tag{4.22}$$

Using the specific form of $\Sigma^{(0)}$ given in (4.2) and the inverse bare propagator G_0^{-1} (3.48), or rather M (3.49) yields – after dropping terms of M which are $\propto \mathbb{1}_4$ as they

clearly vanish in the commutator[3]

$$
\begin{aligned}
iV_t\partial_{t_x}F(\vec{x},\vec{x}) = \Big[\;& \frac{\epsilon+1}{2}\,\vec{\sigma}_z \\
&+ \frac{\tilde{g}}{4}\Big(2\,\vec{\sigma}_0\,\varphi\otimes\varphi^\dagger\,\vec{\sigma}_0 + \mathrm{Tr}\,\big(\,\vec{\sigma}_0\,\varphi\otimes\varphi^\dagger\big)\,\vec{\sigma}_0\,\Big) \\
&- \frac{1}{4}\Big(2\,\vec{\sigma}_x\,\varphi\otimes\varphi^\dagger\,\vec{\sigma}_x + \mathrm{Tr}\,\big(\,\vec{\sigma}_x\,\varphi\otimes\varphi^\dagger\big)\,\vec{\sigma}_x\,\Big) \\
&+ \frac{\tilde{g}}{4}\,\mathrm{Tr}\,\big(F(\vec{x},\vec{x})\,\vec{\sigma}_0\,\big)\,\vec{\sigma}_0 - \frac{1}{4}\,\mathrm{Tr}\,\big(F(\vec{x},\vec{x})\,\vec{\sigma}_x\,\big)\,\vec{\sigma}_x \quad , \quad F(\vec{x},\vec{x})\Big]\,.
\end{aligned}
\tag{4.23}
$$

Again the Kronecker product (or equivalently the outer product i. e. a $n\times 1$ times $1\times n$ matrix product) has been used,

$$
(\varphi\otimes\varphi^\dagger)^\alpha_\beta := \varphi^\alpha\varphi^\dagger_\beta\,. \tag{4.24}
$$

For the remainder of this section, time-dependencies will not be written explicitly and if not stated otherwise, all $F = F(\vec{x},\vec{x})$ are local.

4.3.1 General Simplifications

Assuming again a symmetric phase with vanishing "off-diagonal" terms $N_{+-} = M_{+-} = 0$ as before (4.11), F becomes block-diagonal of the form

$$
F = \begin{pmatrix} F_{++} & 0 \\ 0 & F_{--} \end{pmatrix} \quad \text{where} \quad F_{\pm\pm} := \begin{pmatrix} N_{\pm\pm} & M_{\pm\pm} \\ M^*_{\pm\pm} & N_{\pm\pm} \end{pmatrix}\,. \tag{4.25}
$$

Going again to a rotating frame is equivalent to shifting the time-derivative, i. e. modifying the dynamic equation for $\tilde{F}$ to become

$$
iV_t\partial_{t_x}\tilde{F}(\vec{x},\vec{y})|_{\vec{y}=\vec{x}} = iV_t(\partial_{t_x}+\mu)F(\vec{x},\vec{y})|_{\vec{y}=\vec{x}}\,, \tag{4.26}
$$

and thus in central time

$$
i\partial_{t_x}\tilde{F}(\vec{x},\vec{x}) = i\partial_{t_x}F(\vec{x},\vec{x}) + \mu[V_t, F(\vec{x},\vec{x})]\,, \tag{4.27}
$$

[3]Special care has to be taken for the spatial derivative ∂_x^2, but carefully repeating the above derivation confirms the result. Alternatively it can be seen, that after a Fourier-transformation, $k^2 = (-k)^2$ can be canceled against each other.

which for the different blocks of F reads

$$\left[\begin{pmatrix}1 & 0\\ 0 & -1\end{pmatrix}, \begin{pmatrix}N_{\pm\pm} & M_{\pm\pm}\\ M^*_{\pm\pm} & N_{\pm\pm}\end{pmatrix}\right] = \begin{pmatrix}0 & 2M_{\pm\pm}\\ -2M^*_{\pm\pm} & 0\end{pmatrix}. \tag{4.28}$$

Thus the full blocks become:

$$\tilde{F}_{\pm\pm} := \begin{pmatrix}N_{\pm\pm} & \tilde{M}_{\pm\pm}\\ \tilde{M}^*_{\pm\pm} & N_{\pm\pm}\end{pmatrix} \tag{4.29}$$

where consistently with the previous equation (4.15)

$$\tilde{M}_{\pm\pm} = e^{-2i\mu t} M_{\pm\pm} \qquad \text{and} \qquad \tilde{M}^*_{\pm\pm} = e^{2i\mu t} M^*_{\pm\pm} \tag{4.30}$$

Working in the ensemble as specified in section 3.4.2, the phase of $\tilde{\varphi}_-$ is undetermined, and while $|\tilde{\varphi}_-|^2 = 1 - N - |\tilde{\varphi}_+|^2$, any appearances of $\tilde{\varphi}_-$ or $\tilde{\varphi}^*_-$ alone effectively average out within the ensemble (3.35) and thereby the matrix $\tilde{\varphi} \otimes \tilde{\varphi}^\dagger$ takes the block-diagonal form

$$\tilde{\varphi} \otimes \tilde{\varphi}^\dagger \overset{(3.35)}{=} \begin{pmatrix}\tilde{\varphi}_+ \otimes \tilde{\varphi}^\dagger_+ & 0\\ 0 & |\tilde{\varphi}_-|^2 \times \mathbb{1}_2\end{pmatrix}. \tag{4.31}$$

From now on, dropping the tildes again, all expressions will refer the quantities in the rotating frame. For the observables of interest, which are constructed from the "normal" two-point functions, i. e. from $N_{\pm\pm}$ and absolute values $|\varphi_\pm|$, the expressions in rotating and "normal" frame coincide.

4.3.2 Individual Terms

Now analyzing equation (4.23) term by term using these simplifications one finds

$$[\vec{\sigma}_z\,, F] = \left[\begin{pmatrix}\mathbb{1} & 0\\ 0 & -\mathbb{1}\end{pmatrix}, \begin{pmatrix}F_{++} & 0\\ 0 & F_{--}\end{pmatrix}\right] = 0\,, \tag{4.32}$$

canceling any explicit ϵ-dependence. By using the form of $\varphi \otimes \varphi^\dagger$ given in equation (4.31),

$$\begin{aligned}
&\big[\, \vec{\sigma}_0 \, \varphi \otimes \varphi^\dagger \, \vec{\sigma}_0 \, , F\big] = \big[\varphi \otimes \varphi^\dagger, F\big] \\
&= V_t \begin{pmatrix} \big[M^*_{++}\varphi_+^2 - M_{++}(\varphi_+^*)^2\big] \times \mathbb{1}_2 & 0 \\ 0 & 0 \end{pmatrix} ,
\end{aligned} \tag{4.33}$$

F_{++} is found to couple to the macroscopic field φ_+ via anomalous terms M_{++}. The term proportional to the identity matrix must vanish

$$\big[\, \mathrm{Tr}\,\big(\, \vec{\sigma}_0 \, \varphi \otimes \varphi^\dagger\big) \, \vec{\sigma}_0 \, , F\big] = \mathrm{Tr}\,\big(\, \vec{\sigma}_0 \, \varphi \otimes \varphi^\dagger\big) \big[\mathbb{1}_4, F\big] = 0\,. \tag{4.34}$$

Similarly, for the terms from coupling to the macroscopic field by the second vertex,

$$\big[\, \vec{\sigma}_x \, \varphi \otimes \varphi^\dagger \, \vec{\sigma}_x \, , F\big] = V_t \begin{pmatrix} 0 & 0 \\ 0 & \big[M^*_{--}\varphi_+^2 - M_{--}(\varphi_+^*)^2\big] \times \mathbb{1}_2 \end{pmatrix} , \tag{4.35}$$

$$\big[\, \mathrm{Tr}\,\big(\, \vec{\sigma}_x \, \varphi \otimes \varphi^\dagger\big) \, \vec{\sigma}_x \, , F\big] = 0 \qquad (\text{the trace is already zero})\,, \tag{4.36}$$

F_{--} is found to couple to the macroscopic field φ_+ via anomalous terms M_{--}. Furthermore the terms introduced by the double-bubble diagram, describing the the coupling of densities to themselves, vanish either because they involve commutators with the identity-matrix,

$$\big[\, \mathrm{Tr}\,\big(F(\vec{x},\vec{x}) \, \vec{\sigma}_0 \,\big) \, \vec{\sigma}_0 \, , F\big] = \mathrm{Tr}\,\big(F(\vec{x},\vec{x})\big) \big[\mathbb{1}_4, F\big] = 0\,, \tag{4.37}$$

or because they are proportional to $\langle J_y \rangle$, $\langle J_z \rangle$ which vanish in the symmetric phase

$$\begin{aligned}
\big[\, \mathrm{Tr}\,\big(F(\vec{x},\vec{x}) \, \vec{\sigma}_x \,\big) \, \vec{\sigma}_x \, , F\big] &= 2(N_{+-} + N_{-+}) \begin{pmatrix} 0 & F_{--} - F_{++} \\ F_{++} - F_{--} & 0 \end{pmatrix} \\
&= 0 \qquad (N_{+-} = 0 \text{ in the symmetric phase})\,.
\end{aligned} \tag{4.38}$$

As none of these terms has (non-zero) entries on the off-diagonal blocks, the N_{+-} and M_{+-} terms remain zero, i. e. the symmetric phase is stable, consistent with the approximation used.

4.3.3 Evolution of N and S_x

In this subsection we use the non-vanishing fragments (4.33, 4.35) collected throughout the last subsection in equation (4.23). On the one hand, we obtain for the upper left block F_{++}

$$i\partial_t F_{++} = \frac{\tilde{g}}{2}\big[M^*_{++}\varphi_+^2 - M_{++}(\varphi_+^*)^2\big] \times \mathbb{1}_2\,, \tag{4.39}$$

or put differently (still in the rotating frame, but tildes on $M_{\pm\pm}$ have been dropped after 4.3.1),

$$i\partial_t N_{++} = \frac{\tilde{g}}{2}\big[M^*_{++}\varphi_+^2 - M_{++}(\varphi_+^*)^2\big]\,, \tag{4.40}$$

$$i\partial_t M_{++} = 0\,. \tag{4.41}$$

On the other hand, for the lower right block F_{--} we get

$$i\partial_t N_{--} = -\frac{1}{2}\big[M^*_{--}\varphi_+^2 - M_{--}(\varphi_+^*)^2\big]\,, \tag{4.42}$$

$$i\partial_t M_{--} = 0\,. \tag{4.43}$$

Assuming $M_{\pm\pm} \in \mathbb{R}$ (reviewed later at 4.4.1) allows to simplify these to

$$\partial_t N = \partial_t\big(N_{++} + N_{--}\big) = m_-\Im(\varphi_+^2)\,, \tag{4.44}$$

$$\partial_t S_x = \partial_t\big(N_{++} - N_{--}\big) = m_+\Im(\varphi_+^2)\,. \tag{4.45}$$

The anomalous contributions have been packed into

$$m_\pm = \tilde{g}M_{++} \pm M_{--}\,. \tag{4.46}$$

This shows, that both N and S_x couple to the macroscopic field φ_+ via the constant anomalous correlators. The time-evolution of φ_+ (4.20) being dependent on S_x and N in return couples the equations in a non-trivial way. Before investigating this set of equations further in chapter 5, we want to understand the initial conditions for which the system shell be solved. This will allow for a number of simplifications.

4.4 Choice of Initial Values

In this section the initial conditions for solving the set of equations obtained beforehand in this chapter are discussed. The initial values are chosen such as to reproduce the dynamics directly after a fast quench from $\Omega_\mathrm{i} \approx \infty$ to $\Omega_\mathrm{f} \gtrsim \Omega_\mathrm{c}$ (section 3.3). This means that zero-mode / macroscopic field values are initially given by the ground-state values for $\Omega_\mathrm{i} \to \infty$ (subsection 3.2.1). Slight deviations from this ground-state are included, as for realistic quenches $\Omega_\mathrm{i} < \infty$. This has already been discussed in section section 3.4.1 before fixing the physical ensemble. The major results where

$$\varphi_+ \approx \frac{1}{2}\left(\frac{\delta s}{n^\mathrm{c}} - i\delta\theta\right), \qquad \text{(cf. 3.30)}$$

$$|\varphi_+^0| \ll |\varphi_-^0| \lesssim 1\,. \qquad \text{(cf. 3.32)}$$

Deviations to $\Omega_\mathrm{i} = \infty$ are assumed in the population imbalance $\delta s := n_\uparrow - n_\downarrow$ of particle-species and in their relative phase $\delta\theta = \theta_\uparrow - \theta_\downarrow - \pi$. The central mode φ_- does not appear in the obtained set of equations for φ_+ (4.20), N (4.44) and S_x (4.45) and is not discussed further.

4.4.1 Anomalous Terms

For the derivation of the mean-field ground-state (subsection 3.2.1) anomalous terms $M_{\pm\pm}$ where neglected. So they have to be fixed otherwise. From the equations (4.41, 4.43) just derived it is apparent that the they are constant and determined by the initial state. Estimating from the relevant diagrams (figure 4.1b) while neglecting φ_+^2 terms (cf. equation (3.32)) yields

$$M_{++} \propto (\varphi_-^*)^2 \qquad \text{and} \qquad M_{--} \propto \tilde{g}(\varphi_-^*)^2 \qquad \Rightarrow \qquad m_- \approx 0\,, \qquad (4.47)$$

which means physically that the condensate-depletion is time-independent to this order, see equation (4.44). It is hence given by its initial value N_0

$$N(t) = N_0\,. \qquad (4.48)$$

In principle, the anomalous terms $M_{\pm\pm}$ and thus also m_+ could be complex numbers. However, a numeric approximation of the evolution equations including also an imaginary part for m_+, shows that already small values of $\Im(m_+)$ lead to unphysical

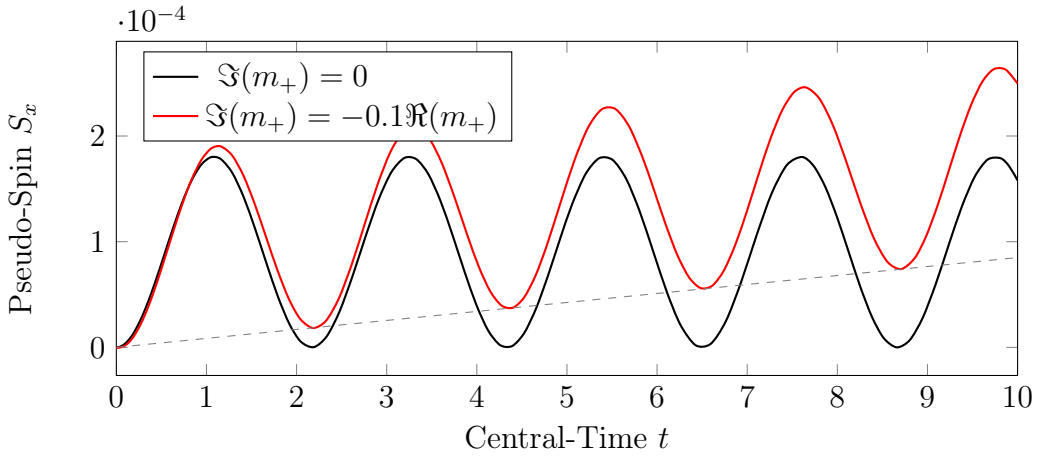

Figure 4.2: Exemplary numerical time-evolution of S_x with a real value of m_+ (black) and with a small imaginary part (red). The non-zero imaginary part leads to a slow drift, linear in time (the gray dashed line is linear in time, as guide to the eye). Both plots use $\epsilon = 1$, $|\varphi_+| \approx 10^{-2}$, $n_0 = 0.05$.

drifts, linear in time, of the oscillations of S_x. An example illustrating this behavior is shown in figure 4.2. The direction of this drift (up or down) depends on the sign of $\Im(m_+)$. To be consistent with Bogolibov-theory in the appropriate limit (large ϵ, small N_0; see section 5.1), where this drift is not observed, it is assumed in the following that

$$m_+ \in \mathbb{R}\,. \tag{4.49}$$

This allows to simplify the evolution equations derived in this chapter.

4.4.2 Initial Value of Densities

The simple mean-field treatment of the ground-state (subsection 3.2.1) does not encompass connected two-point functions, notably N and S_x, either. The initial condensate depletion N_0 is a property of the really three-dimensional system, not of the quasi one-dimensional dynamics investigated here and hence not fixed by the quench-protocol. It is considered as an experimental parameter in the further treatment. For the comparison to numerical simulations in chapter 6 it can be deduced from the numerical setup.

Initially, in the $\Omega_\mathrm{i} \approx \infty$ ground state, $\langle J_x \rangle = -1$. Since we have

$$-1 = \langle J_x \rangle \,|_{t=0} \approx -1 + S_x^0 \tag{4.50}$$

the connected part S_x^0 is initially set to zero

$$S_x^0 = 0\,. \tag{4.51}$$

This fixes most of the initial conditions. It remains to understand possible values of φ_+^0, which is only expressed in terms of the also unknown deviations δs and $\delta\theta$ (see beginning of this section), and of m_+, which has only been argued to be real so far. Both will be revisited using results for the limit comparable to Bogoliubov-theory (see subsection 5.1.5).

5 Solution of the Evolution Equations

In this chapter, physical implications are inferred from equations and initial conditions derived in the previous chapter 4. We obtained the following set of equations (4.20, 4.44, 4.45, 4.41, 4.43)

$$i\partial_t\varphi_+ = \frac{1}{2}\big[2\epsilon + 1 + N + (\tilde{g}+1)S_x\big]\varphi_+ - \frac{1}{2}\big[1 - N + m_-\big]\varphi_+^*\,, \tag{5.1}$$

$$\partial_t N = m_-\Im(\varphi_+^2) \approx 0\,, \tag{5.2}$$

$$\partial_t S_x = m_+\Im(\varphi_+^2)\,, \tag{5.3}$$

$$i\partial_t M_{\pm\pm} = 0\,, \tag{5.4}$$

$$m_\pm = \tilde{g}M_{++} \pm M_{--} \qquad \text{with} \qquad m_- \overset{(4.47)}{\approx} 0\,,$$

where $m_+ \in \mathbb{R}$ (see 4.4.1) has been assumed, and $m_- \approx 0$ implies $N(t) \approx N_0$ (4.48).

5.1 Bogoliubov Limit

A simple Bogoliubov-treatment of effective quasi-spin fields is valid for values of ϵ far away from the instability at $\epsilon = 0$, when fluctuations are moderate and the depletion $N_0 \approx 0$ is negligible. Assume now, for this limit of large ϵ, that then $S_x \ll 1$, to be checked for consistency in hindsight, cf. equation (5.14). The equation (5.1) for φ_+ then becomes

$$i\partial_t\varphi_+ = \frac{1}{2}\big[2\epsilon + 1 + N_0\big]\varphi_+ - \frac{1}{2}\big[1 - N_0\big]\varphi_+^*\,, \tag{5.5}$$

or separating real and imaginary part

$$-\partial_t\Im(\varphi_+) = \frac{1}{2}\big[2\epsilon + 1 + N_0\big]\Re(\varphi_+) - \frac{1}{2}\big[1 - N_0\big]\Re(\varphi_+)\,, \qquad (\Re \text{ of } 5.5)$$

$$\partial_t\Re(\varphi_+) = \frac{1}{2}\big[2\epsilon + 1 + N_0\big]\Im(\varphi_+) + \frac{1}{2}\big[1 - N_0\big]\Im(\varphi_+)\,. \qquad (\Im \text{ of } 5.5)$$

Inserting one in the other after differentiation of both sides one has

$$\partial_t^2 \Re(\varphi_+) = -\Big(\frac{1}{2}\big[2\epsilon{+}1{+}N_0\big]+\frac{1}{2}\big[1{-}N_0\big]\Big)\Big(\frac{1}{2}\big[2\epsilon{+}1{+}N_0\big]-\frac{1}{2}\big[1{-}N_0\big]\Big)\Re(\varphi_+)\,, \quad (5.6)$$

which is a simple harmonic oscillator with angular frequency

$$\omega_+^2 = \big(\epsilon+1\big)\big(\epsilon+N_0\big)\,. \quad (5.7)$$

Analogously for the imaginary part $\Im(\varphi_+)$. However, real and imaginary part are still "coupled" by initial conditions: $\varphi_+^0 := \varphi_+(T=0)$ can be chosen arbitrarily while first time-derivatives $\partial_t\Re(\varphi_+)$ etc. are fixed here via equation (5.5), or rather its real and imaginary parts: $\partial_t\Re(\varphi_+)|_{t=0} \propto \Im(\varphi_+^0)$ and vice versa. Thus

$$\Re(\varphi_+(t)) = \Re(\varphi_+^0)\cos(\omega_+ t) + (\epsilon+1)\Im(\varphi_+^0)\frac{\sin(\omega_+ t)}{\omega_+}\,, \quad (5.8)$$

$$\Im(\varphi_+(t)) = \Im(\varphi_+^0)\cos(\omega_+ t) - (\epsilon+N_0)\Re(\varphi_+^0)\frac{\sin(\omega_+ t)}{\omega_+}\,, \quad (5.9)$$

such that $\Im(\varphi_+^2) = 2\Re(\varphi_+)\Im(\varphi_+)$ as appearing in the equation for S_x (5.3) becomes

$$\begin{aligned}\Im(\varphi_+^2) = {}& 2\Re(\varphi_+^0)\Im(\varphi_+^0)\Big[\cos^2(\omega_+ t) - (\epsilon+1)(\epsilon+N_0)\frac{\sin^2(\omega_+ t)}{\omega_+^2}\Big] \\ & + 2\Big[(\epsilon+1)\Im(\varphi_+^0)^2 - (\epsilon+N_0)\Re(\varphi_+^0)^2\Big]\frac{\sin(\omega_+ t)}{\omega_+}\cos(\omega_+ t)\,.\end{aligned} \quad (5.10)$$

5.1.1 Unstable Direction

Consider for a moment fluctuations in the relative phase of the zero-mode only leading by equation (3.31) to $\Re(\varphi_+^0) = 0$, $\Im(\varphi_+^0)^2 = |\varphi_+^0|^2$ then,

$$\Im(\varphi_+^2) = 2(\epsilon+1)|\varphi_+^0|^2\frac{\sin(\omega_+ t)}{\omega_+}\cos(\omega_+ t)\,. \quad (5.11)$$

Furthermore inserting this into the evolution for S_x (5.3) yields after integration

$$\begin{aligned} S_x(t) &= S_x^0 + m_+ \int_0^t \mathrm{d}t'\, 2(\epsilon+1)|\varphi_+^0|^2 \frac{\sin(\omega_+ t')}{\omega_+} \cos(\omega_+ t') \\ &= S_x^0 + 2m_+(\epsilon+1)|\varphi_+^0|^2 \frac{\sin^2(\omega_+ t)}{2\omega_+^2} \\ &= S_x^0 + m_+|\varphi_+^0|^2 \frac{\sin^2(\sqrt{(\epsilon+1)(\epsilon+N_0)}t)}{\epsilon+N_0}\,. \end{aligned} \tag{5.12}$$

For $N_0 \to 0$ this is the same form as is known from Bogoliubov-Theory for $\langle J_z^2 \rangle$ [Nicklas et al., 2015]

$$\langle J_z^2 \rangle\,|_{k=0} = \frac{1}{4\pi\tilde{\rho}} \frac{\sin^2(\sqrt{\epsilon(\epsilon+1)}t)}{\epsilon} \qquad \text{(Bogoliubov)}\,, \tag{5.13}$$

with $\tilde{\rho} \approx 210$ some dimensionless line density. The N_0 (condensate-depletion) dependency is not expected to be captured by Bogoliubov theory, where $N_0 = 0$ is assumed explicitly. A connection of both observables (S_x and $\langle J_z^2 \rangle$) will be given shortly at (5.1.3). For large ϵ and $S_x^0 = 0$ (equation (4.51)) this also implies

$$\text{large} \quad \epsilon \qquad \Rightarrow \qquad S_x \ll 1\,, \tag{5.14}$$

justifying the initial assumption of this section, at least for this special choice $\Re(\varphi_+^0) = 0$ and $\Im(\varphi_+^0)^2 = |\varphi_+^0|^2$. It is easy to see however (see also the other case for φ_+^0 considered below) that this is always true.

Since this choice of the initial phase of φ_+ scales like $1/\epsilon$, becoming large for small values of ϵ, it is termed a "unstable direction" here. These results are compared to numerical approximations of the full equations (5.1 – 5.3) in figure 5.1 and found to describe the dynamics well for $\epsilon \gtrsim 1$ as expected.

5.1.2 Stable Direction

Considering deviations of the zero-mode wave-function in the balance of relative densities $\delta s = n_\uparrow - n_\downarrow$ instead leads to $\Im(\varphi_+^0) = 0$, $\Re(\varphi_+^0)^2 = |\varphi_+^0|^2$ (3.31) such that

$$\Im(\varphi_+^2) = -2(\epsilon+N_0)|\varphi_+^0|^2 \frac{\sin(\omega_+ t)}{\omega_+} \cos(\omega_+ t)\,, \tag{5.15}$$

and performing the integration as before

$$S_x(t) = S_x^0 - m_+|\varphi_+^0|^2 \frac{\sin^2(\sqrt{(\epsilon+1)(\epsilon+N_0)}t)}{\epsilon+1}\,. \tag{5.16}$$

This behaves in the limit of $N_0 \to 0$ like the Bogoliubov result for $\langle J_y^2\rangle$ [Nicklas et al., 2015]

$$\langle J_y^2\rangle\,|_{k=0} = \frac{1}{4\pi\tilde{\rho}} \frac{\sin^2(\sqrt{\epsilon(\epsilon+1)}t)}{\epsilon+1} \qquad \text{(Bogoliubov)}\,, \tag{5.17}$$

but oscillates "outside" the Bloch-sphere (for $S_x^0 = 0$), which contradicts particle-number conservation: If $S_x < 0$, it holds both $n_+ - n_- = \langle J_x\rangle = -1 + S_x < -1$, but at the same time $|n_+ - n_-| \leq n_+ + n_- = \bar{\rho} = 1$. Since the 2 PI-equations themselves conserve the particle number (see e. g. [Branschädel and Gasenzer, 2008]), this is a inconsistency of the approximation used. The coupling of φ_- to φ_+ is only calculated to $\mathcal{O}\left(|\varphi_+|^2\right)$, cf. equation (4.13), and thus particle-number conservation is expected to hold only to this order as well. This problem does not occur in the "unstable direction" (previous subsection 5.1.1), which will be the relevant one in the further treatment (see subsection 5.1.5). This choice of the initial phase of φ_+ is termed a "stable direction" here, as the result scales like $1/\epsilon+1$ and does not become large for small values of ϵ.

5.1.3 Bloch Sphere Picture

From a naïve Bloch-Sphere picture the local densities are related to Euler-angles ($\theta_{\text{Euler}} \approx 0$ and $\pi + \phi'_{\text{Euler}} := \phi_{\text{Euler}} \approx \pi$) by

$$-1 + S_x \approx \langle J_x\rangle = \cos(\theta_{\text{Euler}})\cos(\phi_{\text{Euler}}) \approx -1 + \frac{1}{2}\theta_{\text{Euler}}^2 + \frac{1}{2}(\phi'_{\text{Euler}})^2\,, \tag{5.18}$$

$$\langle J_z^2\rangle = \sin^2(\theta_{\text{Euler}}) \approx \theta_{\text{Euler}}^2\,, \tag{5.19}$$

$$\langle J_y^2\rangle = \sin^2(\phi_{\text{Euler}}) \approx (\phi'_{\text{Euler}})^2\,. \tag{5.20}$$

Thus in this simple ansatz it is found that

$$S_x \approx \frac{1}{2}\big(\,\langle J_y^2\rangle + \langle J_z^2\rangle\,\big) \tag{5.21}$$

This explains, in part, the similarity of the results for S_x found above (5.12, 5.16) to the known Bogoliubov results for J_z (5.13) or J_y (5.17) depending on the choice of the initial φ_+^0.

5.1.4 Diagrammatic Picture

Here the result from the previous subsection is verified by a "diagrammatic expansion" of $\langle J_z^2 \rangle$ taking into account the Gaussian / disconnected contributions only. By the index structure of $\langle J_z^2 \rangle$ or rather $J_z = \Re(\phi_+^\dagger \phi_- + \phi_- \phi_+^\dagger)$, in the symmetric phase ($\langle \phi_+^\dagger \phi_- \rangle = 0$) there are four orderings to combine one "+" and one "−" on the "left" with one of both one the right (neglecting anomalous terms) leading to four non-vanishing disconnected diagrams and

$$\begin{aligned} \langle J_z^2 \rangle &= 4 \big[\langle \phi_+^\dagger \phi_+ + \phi_+ \phi_+^\dagger \rangle \langle \phi_-^\dagger \phi_- + \phi_- \phi_-^\dagger \rangle \big] \overset{(3.44,3.45)}{=} \bar{\rho}^2 - \langle J_x \rangle^2 \\ &\approx 1^2 - (-1 + S_x)^2 = 2S_x - S_x^2 \end{aligned} \tag{5.22}$$

where $\langle J_x \rangle \approx -1 + S_x$ has been used (as in the previous subsection). Neglecting $\langle J_y^2 \rangle$ in the Bloch-sphere picture would have given the same result

$$\langle J_z^2 \rangle = \sin^2(\arccos(S_x - 1)) = 1 - \cos^2(\arccos(S_x - 1)) = 2S_x - S_x^2 \,. \tag{5.23}$$

So this can be seen as a generalization of equation (5.21) valid also for larger values of S_x corresponding to smaller values of ϵ.

5.1.5 Implications for Further Treatment

We want to use the results for the Bogoliubov limit to improve our understanding of initial-values and parameters before proceeding towards the full equations. The previous discussion of initial conditions (section 4.4) left open how to choose φ_+ and m_+. These are revisited now.

Depending on the choice of the initial phase of φ_+, an unstable direction (subsection 5.1.1) for $\varphi_+ \in i\mathbb{R}$ and a stable direction (subsection 5.1.2) for $\varphi_+ \in \mathbb{R}$ have been observed, scaling with $1/\epsilon$ and $1/\epsilon + 1$ respectively. Any "classical" average over initial phases of φ_+ is dominated by the unstable one for values of ϵ small enough. We are interested especially in the region of very small ϵ, so subsequent results are derived

for the dominant case. Therefore as of now assume

$$\varphi_+^0 \in i\mathbb{R}\,. \tag{5.24}$$

Furthermore, from the relation $\langle J_z^2 \rangle \approx 2S_x$ equation (5.22) for $S_x \ll 1$ (5.14) together with the limit for S_x in equation (5.12) and the Bogoliubov result from Nicklas et al. [2015] for $\langle J_z^2 \rangle$ given in equation (5.13) one finds by comparison of the prefactors

$$m_+|\varphi_+^0|^2 \approx \chi^0 \qquad \text{with} \qquad \chi^0 := \frac{1}{8\pi\tilde{\rho}} \approx 1.9 \times 10^{-4}\,, \tag{5.25}$$

where $\tilde{\rho}$ is a dimensionless line-density given in the experiment [Nicklas et al., 2015] by $\tilde{\rho} \approx 210$. This fixes the product $m_+|\varphi_+^0|^2$, but the individual factors wont play any role in the final results, so from a pragmatic perspective this is sufficient.

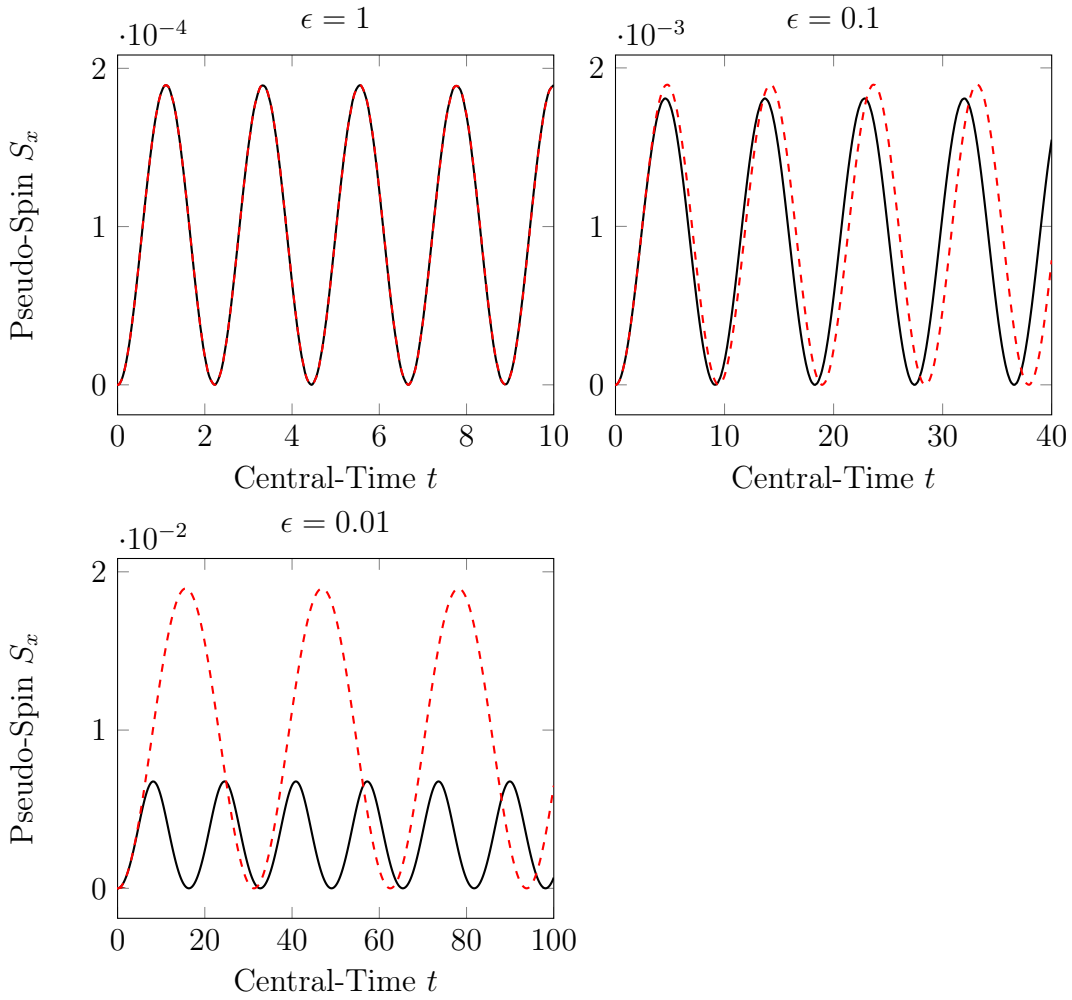

Figure 5.1: Numerical time-evolution of S_x (black) compared to analytic results for mean-field limit (red dashed). As expected both agree well for "large" ϵ, but differ both in frequency and amplitude for smaller values of ϵ. Parameters are: $N_0 = 0$ and $\chi = \chi^0 = (8\pi\tilde{\rho})^{-1}$

5.2 Beyond Bogoliubov

In this section the evolution equations (5.1 – 5.3) are investigated without further approximation, thus leading to results which go beyond usual Bogoliubov theory and show qualitatively new behavior.

5.2.1 Conserved Quantities

A direct solution of equations (5.1 – 5.3) is hard to find analytically. However, identifying conserved quantities can simplify that system of equations. Initial conditions are assumed, as described in section 4.4 and revisited in subsection 5.1.5, to be $m_- = 0$ and thus $N(t) = N_0$ (4.48), $m_+ \in \mathbb{R}$ (4.49), $S_x^0 = 0$ (4.51), $\varphi_+ \in i\mathbb{R}$ (5.24) and $m_+|\varphi_+^0|^2 \approx \chi^0$ (5.25).

The Bloch-Sphere radius $R^2 = \langle J_x\rangle^2 + \langle J_y\rangle^2 + \langle J_z\rangle^2$ cannot be conserved anymore as $J_y = J_z = 0$, but J_x has non-trivial dynamics. However the "generalized norm"

$$\chi = m_+|\varphi_+|^2 - S_x(1 - N_0)\,, \tag{5.26}$$

can easily be checked to be conserved under the evolution-equations (5.1 – 5.3). By $S_x^0 = 0$ this is (initially) estimated by the χ^0 defined before in equation (5.25)

$$\chi = \chi|_{t=0} = m_+|\varphi_+^0|^2 \approx \chi^0\,. \tag{5.27}$$

Using this information, one of the remaining equations can be eliminated. Since we are interested in S_x, it seems suitable to eliminate $|\varphi_+|$. Defining a phase $\theta_+(t)$ via $\tilde{\varphi}_+ = |\tilde{\varphi}_+|e^{-i\theta_+}$ the new set of equations reads (cf. appendix C.3, equation (C.23))

$$\partial_t\theta_+ = \frac{1}{2}\big[2\epsilon + 1 + N + (\tilde{g}+1)S_x\big] - \frac{1}{2}\big[1 - N\big]\cos(2\theta_+)\,, \tag{5.28}$$

$$\partial_t S_x = m_+|\tilde{\varphi}_+|^2\sin(2\theta_+)\,. \tag{5.29}$$

Furthermore, it can be seen, that under these equations

$$E = \chi\cos^2(\theta_+) - (\epsilon+1)S_x - \frac{\tilde{g}+1}{4}S_x^2 + (1-N_0)\cos^2(\theta_+)S_x\,, \tag{5.30}$$

which resembles an energy[1] is conserved as well. One could thereby reduce the

[1] E contains, schematically, terms $\propto \phi^2$ ($\cos^2(\theta_+)$), $\propto N_{\pm\pm}$ (S_x), $\propto N_{\pm\pm}^2$ (S_x^2) and $\propto \phi^2 N_{\pm\pm}$ ($\cos^2(\theta_+)Sx$), which are the terms that would be expected for an energy. However the actual

system to a single equation, however in the next subsection E is exploited otherwise. Using the initial values $S_x^0 = 0$ and $\varphi_+ \in i\mathbb{R} \Rightarrow \cos(\theta_+)|_{t=0} = 0$ this has takes on the value

$$E = E^0 = 0\,. \tag{5.31}$$

5.2.2 Energy Gap

In this thesis φ_+ describes, by construction, the zero-momentum mode and its angular frequency ω_+ is thus the gap of the full dispersion $\omega_+(k)$ of the relative degrees of freedom

$$\omega_+ = \Delta_+^{\text{gap}} := \omega_+(k=0)\,. \tag{5.32}$$

Under the assumption that close to the phase-transition / crossover only a single dominating energy-scale exists (in the IR), this energy-gap of the macroscopic fields is an interesting quantity not only by its own right, but also to compare to different results for energy-gaps or correlation-lengths, e. g. from numerics. Generalizing the uncorrected energy-gap from the mean-field limit (5.7), including "quasi-static" corrections[2] due to S_x terms in (5.1), the corrected gap ω_+ reads

$$\begin{aligned}\omega_+^2 &= \frac{1}{4}\big[2\epsilon + 1 + N_0 + (\tilde{g}+1)S_x\big]^2 - \frac{1}{4}\big[1 - N_0\big]^2 \\ &= (\epsilon + N_0)(\epsilon + 1) + \left(2\epsilon + 1 + N_0 + \frac{\tilde{g}+1}{2}S_x\right)\frac{\tilde{g}+1}{2}S_x\,.\end{aligned} \tag{5.33}$$

Hence "typical values" of ω_+ correspond to typical values of S_x. A numerical approximation suggests: S_x is periodic with minima at 0, but non-trivial maxima (see e. g. figure 5.1). Therefore the maxima of S_x are investigated further. The full time-dependence of S_x is complicated, but equation (5.30) can be solved for S_x,

$$E(\theta_+, S_x) = \text{const} \qquad \overset{(5.30)}{\Rightarrow} \qquad S_x(\theta_+)\,, \tag{5.34}$$

and numerical approximation robustly shows a phase θ_+ which is surjective on $[0, 2\pi]$ (see figure 5.2). Thereby

energy can well be a linear combination $a\chi + bE$.

[2] By "quasi-static" corrections, we mean, the new ω_+ is defined as before, but now including the dependence on S_x and thus on time t. The defining equation is no harmonic oscillator equation anymore.

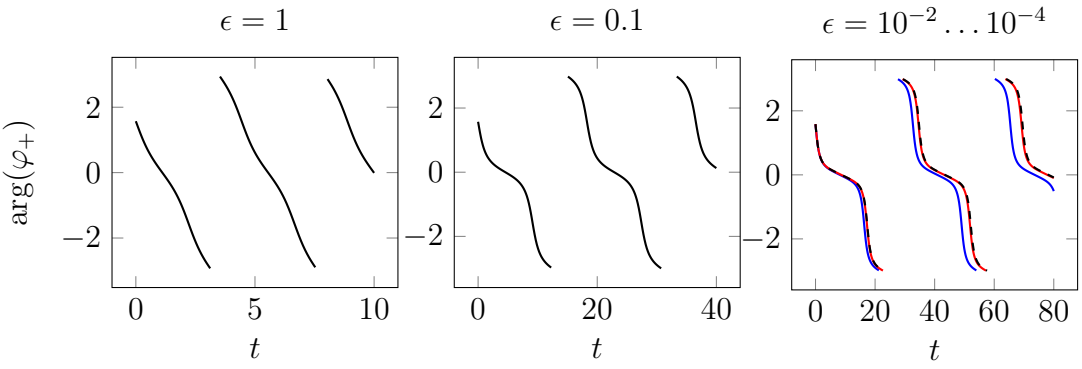

Figure 5.2: Phases $-\theta_+ = \arg(\varphi_+)$, from numerical solution of (5.1 – 5.3), for different values of ϵ demonstrate stable surjective (on $[0, 2\pi]$) angles. Timescales are different (as denoted). In the third plot $\epsilon = 10^{-2}$ (blue), $\epsilon = 10^{-3}$ (red) and $\epsilon = 10^{-4}$ (black, dashed) are shown, they are strongly affected by the non-zero $\chi = \chi^0$, and thus very similar.

$$\max_{T\in[0,\infty)} \big(S_x(T)\big) \qquad = \qquad \max_{\theta_+\in[0,2\pi]} \big(S_x(\theta_+)\big)\,, \tag{5.35}$$

where the r. h. s. can be calculated analytically from (5.34). Explicitly one finds

$$\begin{aligned} S_x(\theta_+) = -\frac{2}{\tilde{g}+1}\Big[&\epsilon + N_0 + (1-N_0)\sin^2(\theta_+) \\ &\pm \sqrt{(\epsilon + N_0 + (1-N_0)\sin^2(\theta_+))^2 + (\tilde{g}+1)(\chi\cos^2(\theta_+) - E)}\Big]\,. \end{aligned} \tag{5.36}$$

Finding the maximum with respect to $\theta_+ \in [0, 2\pi]$ is also equivalent to finding the maximum with respect to

$$x := \sin^2(\theta_+) \in [0, 1]\,, \tag{5.37}$$

that is – additionally using $E = 0$ (5.31) for the initial conditions used – the maximum, under the constraint that $0 \le x \le 1$, of

$$\begin{aligned} S_x(x) = -\frac{2}{\tilde{g}+1}\Big[&\epsilon + N_0 + (1-N_0)x \\ &\pm \sqrt{\big(\epsilon + N_0 + (1-N_0)x\big)^2 + (\tilde{g}+1)(1-x)\chi}\Big]\,. \end{aligned} \tag{5.38}$$

We focus on the solution with the minus sign, the other one is always negative, thus violating total particle number conservation, see discussion at the end of 5.1.2).

Derivation with respect to x shows

$$\begin{aligned}\frac{\tilde{g}+1}{2}\frac{d}{dx}S_x(x) &= \frac{1}{2}\Big[\big(\epsilon+N_0+(1-N_0)x\big)^2+(\tilde{g}+1)(1-x)\chi\Big]^{-\frac{1}{2}}\\ &\quad\times\Big[2\big(\epsilon+N_0+(1-N_0)x\big)(1-N_0)-(\tilde{g}+1)\chi\Big]-(1-N_0)\\ &\overset{\chi\geq 0}{<}\frac{1}{2}\Big[\big(\epsilon+N_0+(1-N_0)x\big)^2\Big]^{-\frac{1}{2}}\\ &\quad\times 2\big(\epsilon+N_0+(1-N_0)x\big)(1-N_0)-(1-N_0)\\ &= 0 \qquad \Rightarrow S_x(x) \text{ is monotonically decreasing.}\end{aligned} \tag{5.39}$$

Thus the maximum is always at minimal x, or including the constraints, at $x=0$. Inserting this maximum into the expression for $S_x(x)$ (5.38) yields

$$\frac{\tilde{g}+1}{2}\hat{S}_x = \sqrt{\big(\epsilon+N_0\big)^2+(\tilde{g}+1)\chi}-(\epsilon+N_0)\,, \tag{5.40}$$

and putting this into the energy-gap (5.33) we obtain

$$\begin{aligned}\hat{\omega}_+^2 &= (\epsilon+N_0)(\epsilon+1)+\left(\epsilon+1+\sqrt{\big(\epsilon+N_0\big)^2+(\tilde{g}+1)\chi}\right)\\ &\qquad\times\left[\sqrt{\big(\epsilon+N_0\big)^2+(\tilde{g}+1)\chi}-(\epsilon+N_0)\right]\\ &= (1-N_0)\sqrt{\big(\epsilon+N_0\big)^2+(\tilde{g}+1)\chi}+\big(\epsilon+N_0\big)^2+(\tilde{g}+1)\chi\,.\end{aligned} \tag{5.41}$$

Note that consistently

$$\frac{\epsilon}{(\tilde{g}+1)\chi}\to\infty \qquad \Rightarrow \qquad \frac{\hat{S}_x}{\epsilon}\to 0 \quad\text{and}\quad \hat{\omega}_+^2\to(\epsilon+N_0)(\epsilon+1)\,, \tag{5.42}$$

as found before in the "large epsilon" limit (here: large as compared to $(\tilde{g}+1)\chi$; cf. (5.7)). Using

$$\tilde{\epsilon}^2 := (\epsilon+\Delta_\epsilon)^2+\Delta_{\epsilon^2}\,, \tag{5.43}$$

$$\Delta_\epsilon := N_0\,, \tag{5.44}$$

$$\Delta_{\epsilon^2} := (\tilde{g}+1)\chi\,, \tag{5.45}$$

this takes again the effective mean-field form ($\tilde{\epsilon}$ is the positive sqare-root of $\tilde{\epsilon}^2$)

$$\hat{\omega}_+^2 = \tilde{\epsilon}\big(\tilde{\epsilon}-N_0+1\big)\,. \tag{5.46}$$

The appearance of an effective $\tilde{\epsilon}$ has two major consequences. On the one hand the condensate depletion, which is explicitly neglected in a Bogoliubov treatment, moves the critical point away from the mean-field position

$$\epsilon_{\text{critical}} = 0 \qquad \overset{(5.44)}{\rightarrow} \qquad \epsilon_{\text{critical}} = -\Delta_\epsilon \,. \tag{5.47}$$

By construction of the equations used to derive this result, it is valid in the symmetric phase only. From the observed structure the symmetric phase is assumed to correspond to $\epsilon + \Delta_\epsilon > 0$.

On the other hand the combination of both anomalous Bose correlators ($m_+ \neq 0$) and deviations in the zero-mode from the initial state for $\Omega_\text{i} = \infty$ – for realistic quenches $\Omega_\text{i} < \infty$ – leading to $\varphi_+ \neq 0$, implies a $\chi \neq 0$ and thus a "quadratic" shift through $\Delta_{\epsilon^2} \neq 0$. This affects the gap similar to an effective "mass", i. e. maintaining a final (non-zero) value for quenches arbitrary close to the critical point

$$\tilde{\epsilon}^2 \geq \Delta_{\epsilon^2} \qquad \text{for all values of } \epsilon \text{ in the symmetric phase.} \tag{5.48}$$

Thereby, also the typical correlation-length $\xi \sim \hat{\omega}_+^{-1}$ remains regular. This is similar to the behavior expected at a cross-over, rather then near a phase-transition. It fits the expectation that real phase-transitions in 1D occur only at zero temperature, while post-quench dynamics are naturally far from their ground-state.

The only difference (besides $\epsilon \to \tilde{\epsilon}$) to the form $\omega_+^2 = \epsilon\big(\epsilon + 1\big)$ in the Bogoliubov-theory [Nicklas et al., 2015] is the additional $N_0 = \Delta_\epsilon$ in the second factor. This term can be understood from studying the roots of $\hat{\omega}_+^2$: In the mean-field limit these are found at $\epsilon = 0$ – now "shifted" to $\tilde{\epsilon} = 0$, which is effectively "masked" by a non-zero Δ_{ϵ^2} and shifted by Δ_ϵ – as well as at $\epsilon = -1$, corresponding to $\Omega = 0$ (i. e. a vanishing mixing term), where

$$\epsilon + 1 \to \tilde{\epsilon} + 1 - \Delta_\epsilon \overset{\Delta_{\epsilon^2} \ll 1}{\approx} \epsilon + 1 \tag{5.49}$$

shows that the zero-point at $\Omega = 0$ is effectively untouched, as is expected, since it corresponds to a change of symmetry of the Hamiltonian.

5.3 Consistency Checks

Before discussing the relation of the results obtained here to existing numerical results, a quick check of general plausibility and known pitfalls is done for completeness.

5.3.1 Unphysical Gaps

It is known [Griffin, 1996; Hohenberg and Martin, 1965], that considering self-consistent treatments of Bose gases can lead to unphysical energy-gaps. These are found in $O(\mathcal{N})$-models however, while the gap found here is in relative degrees of freedom, which appear in the symmetric phase due to the model *not* being fully $O(\mathcal{N})$-symmetric. Further the gap in the system under investigation here is certainly not expected to vanish for $\epsilon \neq 0$, and also at the quantum critical point, in one spatial dimension a non-vanishing gap is expected at non-zero temperature or far-from-equilibrium (see 3.2.2). This is probably also related to the subtleties in treating a *quasi* one-dimensional system, where a condensate from the underlying three-dimensional system appears, while in general there is no Bose-Einstein condensation in one dimension. Additionally the $1/\mathcal{N}$-leading order approximation discussed here becomes exact in the limit $\mathcal{N} \to \infty$, so the results are unlikely to be artifacts of the low expansion order only.
The observed gap is presumed to be physical from these arguments.

5.3.2 Consistency of $1/\mathcal{N}$ as Expansion Parameter

From equation (5.40) it can be seen that

$$\frac{\tilde{g}+1}{2}\frac{d}{d\epsilon}\hat{S}_x = \frac{\epsilon + N_0}{\sqrt{\left(\epsilon+N_0\right)^2 + (\tilde{g}+1)\chi}} - 1 < 0\,, \tag{5.50}$$

i. e. $\hat{S}_x$ is monotonically decreasing with ϵ in the symmetric phase ($\epsilon + \Delta_\epsilon > 0$) and it holds that

$$\hat{S}_x \leq \hat{S}_x|_{\epsilon+\Delta_\epsilon=0} \overset{(5.40)}{=} \sqrt{\frac{4\chi}{\tilde{g}+1}}\,. \tag{5.51}$$

Returning to the very start of this thesis, specifically to the discussion of the applicability of a $1/\mathcal{N}$ approximation in section 2.7, this shows that the expansion is

meaningful[3] in the entire symmetric phase, if

$$10^{-2} \overset{(5.25)}{\approx} \sqrt{\frac{4\chi}{\tilde{g}+1}} \ll N_0. \tag{5.52}$$

More generically the condition $\hat{S}_x \ll N_0$ can be checked for arbitrary ϵ from equation (5.40). Note that the results in section 5.1 describe the Bogoliubov-limit of $N_0 = 0$, but still yields useful results. This may be due to the order of limits, taking $\epsilon \to \infty$ first implies $\hat{S}_x \to 0$ and thus $\hat{S}_x \ll N_0$ for any N_0, also in the limit $N_0 \to 0$.

5.3.3 Requirement of a Condensate

The treatment as considered here relies on the existence of a condensed zero-mode. This is physically plausible for the *quasi* one-dimensional system, but from a general perspective the Hamiltonian (3.16) could also be implemented differently, with the expectation of a cross-over for 1D remaining. Thinking of applications in the spirit of quantum simulators, this raises the question if IR-effective properties are affected by the Bose-broken symmetry.

In principle from the results without macroscopic field show in the appendix B.1, although there is no real dynamics in the symmetric phase at leading order, it is already evident that a non-trivial J_x would suffice modify the properties of the instability at $\Omega = \Omega_c$. Going to next-to-leading order would therefore most likely change the critical behavior as well. This is however not analytically feasible, since both infinite resumamtions in Γ_2 and memory integrals would be involved [e. g. Branschädel and Gasenzer, 2008].

Both Bogoliubov-theory and the numeric treatment by Karl [2016] assume a mostly condensed system and describe experimental data from Nicklas et al. [2015] well, within the experimental range $\epsilon \gtrsim 0.1$. It is therefore reasonable to assume that the results obtained in this thesis are applicable to this experimental setup.

[3] I. e. $1/\mathcal{N}$ is well-defined, this is no statement on the "smallness" of $1/\mathcal{N}$ however.

6 Comparison to Existing Numerical Data

Here the above findings are compared to numerical data from [Karl, 2016, p. 124], obtained from "truncated Wigner" [Blakie et al., 2008] simulations. This data is also consistent, in the experimental range ($\epsilon \gtrsim 0.1$), to experimental results from [Nicklas et al., 2015]. Good agreement is found after adjusting only an overall multiplier and one additional parameter (χ). The comparison indicates that the treatment carried out in chapters 4 and 5 is applicable to the system and captures important features beyond the scope of usual Bogoliubov treatments.

6.1 Definition of a Correlation Length

The quantity under investigation in these references, is a correlation-length obtained form the falloff of correlators of the form $\langle J_z(x) J_z(y)\rangle$. Neither are four-point functions easily accessible from the treatment presented here, nor are there any comparable spatial dependencies for the spatially homogeneous $\langle J_a\rangle$ used. In principle the dynamic equation (4.22) could be (trivially) generalized to non-local densities of the form $F(x, y)$, but these would have no interpretation in terms of spins $J(x) \sim F(x, x)$ and also not induce any new dynamics.

To overcome this difficulties, a typical correlation-length is defined from the inverse energy-gap $\hat{\omega}_+$, with the understanding that this definition is *not* identical to the ones in the references given above, *but* if only a single scale exists near the (quantum) critical point, it should be comparable to those results up to a constant dimensionless factor / amplitude. This is expected to hold only for small enough values of ϵ.

$$\xi := \frac{c_\mathrm{s}}{\hat{\omega}_+} = \frac{\sqrt{2\epsilon + 1}}{\hat{\omega}_+} \approx \sqrt{\frac{2(\tilde{\epsilon} - \Delta_\epsilon) + 1}{\tilde{\epsilon}(\tilde{\epsilon} - \Delta_\epsilon + 1)}} \tag{6.1}$$

Here $c_\mathrm{s} = \sqrt{2\epsilon + 1}$ is the mean-field speed of sound. For $\epsilon \ll 1$ this simplifies by $c_\mathrm{s} \approx 1$ and $\tilde{\epsilon} - \Delta_\epsilon + 1 \approx 1$ to

$$\epsilon \ll 1 \qquad \Rightarrow \qquad \xi \approx \tilde{\epsilon}^{-\frac{1}{2}} \,. \tag{6.2}$$

6.2 The Numerical Treatment

The data by Karl [2016] was obtained from numerical "truncated Wigner" [Blakie et al., 2008] simulations. The correlation length there is found to oscillate in time, with a decreasing amplitude. Typical scales are set by the values of the maxima, which are plotted in figure 6.1. Numbers subsequently are taken from [Karl, 2016, table (B.2)]. Most of the 10^6 atoms per species are assumed to be in the zero-mode. Non-condensed is only the "noise" $n_k = 1/2$ in the $L = 2^{14}$ momentum-modes per species, to represent the vacuum partition of independent harmonic oscillators. Equal partition of momentum modes independent of k translates into a spatially local density of both species equivalently, i. e. in the notation used in this thesis, where the non-condensed part of the total density N is normalized and constant:

$$N_0 \approx \frac{1}{2} \times 2^{14}/10^6 \approx 0.8\,\% \,. \tag{6.3}$$

From the estimate on the range of applicability of the $1/\mathcal{N}$-expansion given before by equation (5.52), applied for this value of N_0, care has to taken for small values of ϵ, if $\chi = \chi^0$ is assumed. However, with the smaller χ found from the fits, arbitrary ϵ should be valid in the analytic treatment.

6.3 Results and Discussion

Figure (6.1) shows both numerical results [Karl, 2016] (colored circles) and analytical curves (colored lines) according to equation (6.1). For the analytic results shown, N_0 is chosen according to equation (6.3), while χ and an overall amplitude (accounting for the different definitions of correlation lengths) are fitted to the numerical data points. Points are weighted with the inverse error-square, where weights have been cut off at some reasonably large value, such that the fits are not dominated by only two or three points.

For large ϵ both $\epsilon + 1$ and c_s induce an additional qualitative ϵ-dependence, and "far" from criticality there is no reason to believe that only a single relevant energy scale exists. No match of the numerical results and the differently defined correlation length is expected here. However the gap was seen to approach the mean-field form in this limit before (section 5.1). Since also the numerical results agree with Bogoliubov results in this limit, the deviation for large ϵ is assumed to be only due to this difference in definition.

For this reason, for all parameter-fits carried out, the 5 points with largest ϵ-values have been taken out, leaving another 35 points for the fit. The interesting dynamics are expected for smaller ϵ, and we will focus on those in the following. In this regime, the results found for ξ fit the numerical data well, with only two fitted parameters, one of which is simply the overall amplitude to account for the different definitions used here and in the numerical reference.

It is interesting, that the values of χ required to fit the numerical data are very small for the first maxima, as compared to the estimate χ^0 obtained far away from criticality (equation (5.25)), but increases afterwards. It is easy to see from the numbers given in figure 6.1, that especially the first three maxima show a near-quadratic rise of χ, and also the fourth one is not far off compared to fit-errors.

This rise of χ in time could be a remnant of the slightly different initial states considered here and for the numerics. Initially (5.26) $\chi|_{t=0} = m_+|\varphi_+^0|^2$ (for $S_x^0 = 0$) is only non-zero, because a quench from an initial value $\Omega_\mathrm{i} < \infty$ and therefore nonzero φ_+^0 is assumed. This is physically plausible for any real (experimental) system, but not the same as assumed for the numerical treatment ($\Omega_\mathrm{i} = \infty$). However, while in the leading order approximation employed here, χ is conserved, it could (and probably does) evolve over time when higher orders are included.

This also means, that in the numerical setup, although $\chi|_{t=0} = 0$, it could be "switched on" dynamically. After a sudden quench for a smooth $\chi(t)$ it would be expected that $\partial_t\chi|_{t=0} = 0$ as well. Then the quadratic rise of χ in maxima or time equivalently, as seen in the fit data, appears to be a natural first order expectation.

For applications to an experimental setup, a finite quench (starting at $\Omega_\mathrm{i} \neq \infty$) must be considered, and an initial value for $\chi|_{t=0} \neq 0$ is expected. If this value is of similar order of magnitude as χ^0 (5.25) – which was the estimate obtained form comparison of prefactors in the Bogoliubov-limit – it may be much larger then the change over time seen in the fit parameters (at figure 6.1) over multiple maxima / oscillations. Then the analytic result would possibly require only the condensate-depletion as input to predict the behavior of the correlation-length for moderately early times.

Overall, the approximation discussed in this work seems to describe relevant physics when it comes to understanding what actually causes the shift of the critical point $\Delta_\epsilon = N_0$ and also the effective mass $\Delta_{\epsilon^2} = (\tilde{g} + 1)\chi$, but fails to describe their time-evolution. Especially the dynamics of χ could to be non-trivial.

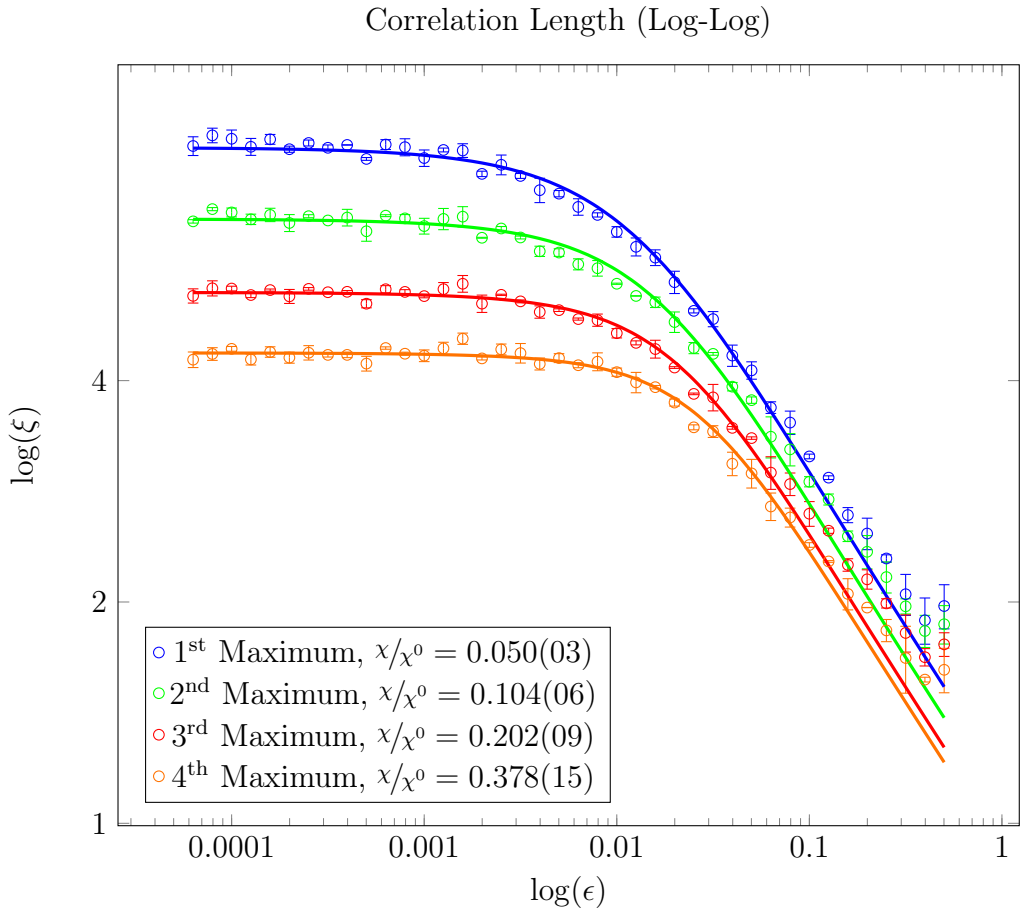

Figure 6.1: The dimensionless correlation-length ξ as a function of the distance ϵ to the mean-field critical point. Colored circles show numerical (truncated Wigner) results by Karl [2016]. Solid lines show curves according to equation (6.1) with $N_0 \approx 0.8\,\%$ (6.3) fixed, while χ and an overall amplitude are fitted, with results given relative to $\chi^0 \approx \frac{1}{8\pi\tilde{\rho}} \approx 2 \times 10^{-4}$ which was the estimate from the Bogoliubov-limit (5.25).

7 Conclusion

A self-consistent (2 PI) treatment to leading-order in $1/\mathcal{N}$ (inverse number of field-components) of the two-component Bose-gas in the symmetric phase has been derived. We showed that, for large values of the dimensionless distance to the mean-field quantum-critical point, ϵ, and small condensate-depletion N_0, known results from Bogoliubov-theory (at $k \to 0$) can be recovered. Other than in Bogoliubov-theory a non-vanishing condensate-depletion N_0 could be included and was found to cause a linear shift of the critical point away from the mean-field value $\Omega = \Omega_c$ ($\epsilon = 0$). As the system is treated in presence of a condensed mode, i. e. for non-vanishing macroscopic fields $\varphi(k = 0)$, also "anomalous" correlators ($M_{\pm\pm}$) were taken into account. These have been found to be constant in time for the considered LO-approximation, thus they are determined by the initial state of the system. After inclusion of small modifications in the initial condensate-wave-function, to account for finiteness of realistic quenches ($\Omega_\mathrm{i} \neq \infty$), a "mass-like" shift of ϵ^2, regularizing the correlation length at the phase-transition / cross-over has been encountered. If the parameter χ, quantifying these modifications, together with anomalous Bose correlators, is left open, correlation lengths determined by Karl [2016] numerically in truncated Wigner approximation can be reproduced well. Due to a subtle difference in initial states, an initial rise of χ, as observed from fitting to numerical data, seems plausible. The treatment presented here is able to describe the leading corrections to both the position of the critical point and the "effective mass" precluding divergences at the crossover. It provides a qualitative and quantitative understanding of these corrections, but it does *not* describe their time-evolution.

In future work, the results found here could be tested further, by calculating in numerical simulations values of the "fundamental" parameters m_+ and $|\varphi_+^0|^2$, to then determine $\chi = m_+|\varphi_+^0|^2$ from those and check for consistency with numerical results of the correlation-length again. On similar lines, estimates for S_x could be determined directly in the numerical treatment and compared to the results for S_x found here. To capture the actual spatial dependence better than a usual Bogoliubov-treatment, and avoid the construction of a typical correlation-length from the inverse energy

gap, would probably require a next-to-leading order treatment, which is numerically, but not analytically feasible.

A General 1 PI Identities

In this part of the appendix, a number of well-known "textbook" identities for the 1 PI-Effective-Action are reviewed. The contents are based on [Weinberg, 1996]. For a motivation of the use of effective actions in general, see chapter 2 in the main-text.

A.1 Definition

The (moment) generating functional $Z[J]$ for a theory with action S (such that the Hamiltonian H is Weyl-ordered) can be defined in the path-integral formalism via

$$Z[J] = \int \mathcal{D}\phi \, e^{i(S[\phi]+J^\dagger\cdot\phi)}. \tag{A.1}$$

And the respective scalar-product (with sum over repeated indices implicit):

$$J^\dagger \cdot \phi := \int_\zeta \mathrm{d}t \int \mathrm{d}x \, J^\dagger_\alpha \phi^\alpha \tag{A.2}$$

Here ζ denotes a closed time-contour (see main text, section 2.2). Further one is usually interested in connected diagrams (cumulants) which can, by a subtle rearrangement of summands, be established as being generated by $W[J]$ where

$$e^{iW[J]} = Z[J]. \tag{A.3}$$

Finally we define the field expectation value

$$\varphi^\alpha_J := \frac{\langle \phi^\alpha \rangle_J}{\langle 1 \rangle_J} = \frac{1}{Z[J]} \frac{\delta Z[J]}{\delta (i J^\dagger_\alpha)} = \frac{\delta W[J]}{\delta J^\dagger_\alpha} \tag{A.4}$$

and – assuming this relation is invertible with inverse J_φ – the quantum effective action $\Gamma[\varphi]$ as the Legendre-transform of W:

$$\Gamma[\varphi] = W[J_\varphi] - J^\dagger_\varphi \cdot \varphi \tag{A.5}$$

This is a functional of φ only, and generates the "1 PI" correlation-functions. That is, the correlation functions whose Feynman-diagrams cannot be disconnected by cutting a single line. Γ is termed an "effective action" since (as a property of the Legendre-transformation):

$$\frac{\delta\Gamma[\varphi]}{\delta\varphi^\alpha} = -J^\dagger_{\varphi,\alpha} \tag{A.6}$$

Resembling, for $J = 0$, the classical e. o. m. at the stationary point of the (classical) action. Not surprisingly it hold that $S = \Gamma$ at 0-loop order or generally:

$$\Gamma[\varphi] = S[\varphi] + K[\varphi] = S[\varphi] + \mathcal{O}(\text{1-loop}) \tag{A.7}$$

A.2 Background-Field Method

By definition of W

$$e^{iW[J]} = \int \mathcal{D}\phi\, e^{i(S[\phi]+J^\dagger\cdot\phi)}. \tag{A.8}$$

together with the inverse Legendre-transform $W[J] = \Gamma[\varphi_J] + J^\dagger \cdot \varphi_J$ we have

$$e^{i(\Gamma[\varphi_J]+J^\dagger\cdot\varphi_J)} = \int \mathcal{D}\phi\, e^{i(S[\phi]+J^\dagger\cdot\phi)}. \tag{A.9}$$

Replacing $\varphi_J \to \varphi$ (J is arbitrary, set $J^\dagger = J^\dagger_\varphi = \frac{\delta\Gamma[\varphi]}{\delta\varphi}$ on both sides) and using equation (A.6) this reads:

$$e^{i\Gamma[\varphi]} = \int \mathcal{D}\phi\, e^{i\left(S[\phi]-\frac{\delta\Gamma[\varphi]}{\delta\varphi}\cdot(\phi-\varphi)\right)}. \tag{A.10}$$

After shifting $\phi = \phi - \varphi$ and assuming the path-integral measure to be translation invariant we finally arrive at:

$$e^{i\Gamma[\varphi]} = \int \mathcal{D}\phi\, e^{i(S[\varphi+\phi]-\frac{\delta\Gamma[\varphi]}{\delta\varphi}\cdot\phi)}. \tag{A.11}$$

A.3 One-Loop Order

Using equation (A.7) on both sides of equation (A.11) yields

$$e^{i(S[\varphi]+K[\varphi])} = \int \mathcal{D}\phi\, e^{i(S[\varphi+\phi]-\frac{\delta S[\varphi]}{\delta\varphi}\dot{\phi}-\frac{\delta K[\varphi]}{\delta\varphi}\cdot\phi)} \tag{A.12}$$

which, together with the expansion

$$S[\varphi+\phi] = S[\varphi] + \frac{\delta S[\varphi]}{\delta\varphi}\cdot\phi + \frac{1}{2}\phi^\dagger\cdot\frac{\delta^2 S[\varphi]}{\delta\varphi^2}\cdot\phi + \mathcal{O}(\text{2-loop}) \tag{A.13}$$

reads (because K is already of 1-loop order)

$$e^{i(S[\varphi]+K[\varphi])} = \int \mathcal{D}\phi\, e^{i(S[\varphi]+\frac{1}{2}\phi^\dagger\cdot\frac{\delta^2 S[\varphi]}{\delta\varphi^2}\cdot\phi+\mathcal{O}(\text{2-loop}))}. \tag{A.14}$$

Thus resulting in the Gaussian integral

$$K[\varphi] = -i\ln\int \mathcal{D}\phi\, e^{\frac{i}{2}\phi^\dagger\cdot\frac{\delta^2 S[\varphi]}{\delta\varphi^2}\cdot\phi} + \mathcal{O}(\text{2-loop}) \tag{A.15}$$

which can be evaluated to (a factor $(2\pi)^n$ is absorbed by the measure)

$$K_{(\text{1-loop})}[\varphi] = -i\ln\left(\det\left(-i\frac{\delta^2 S[\varphi]}{\delta\varphi^2}\right)^{-\frac{1}{2}}\right) = \frac{i}{2}\ln\det\left(G_0^{-1}\right) \tag{A.16}$$

in terms of the free-propagator / Greens-function $i(G_0^{-1})^\beta_\alpha = \frac{\delta^2 S[\varphi]}{\delta\varphi^\alpha\delta\varphi^\dagger_\beta}$. This can be rewritten as

$$\Gamma[\varphi] = S[\varphi] + \frac{i}{2}\operatorname{Tr}\ln\left(G_0^{-1}\right) \tag{A.17}$$

A.4 The Full Propagator

From the stationary condition equation (A.6) we know

$$\frac{\delta^2\Gamma[\varphi]}{\delta\varphi^\dagger_\alpha\delta\varphi^\beta} = -\frac{\delta J^\dagger_{\varphi,\beta}}{\delta\varphi^\dagger_\alpha} \tag{A.18}$$

and by definition of φ we have

$$G_\alpha^\beta := \frac{\delta^2 W[J]}{\delta(iJ^\alpha)\delta(iJ_\beta^\dagger)} = \frac{\delta\varphi_{J,\alpha}^\dagger}{\delta(iJ_\beta^\dagger)} = -i\frac{\delta\varphi_{J,\beta}^\dagger}{\delta J_\beta^\dagger} \tag{A.19}$$

therefore we can write the full propagator G as

$$(G_\alpha^\beta)^{-1} = i\left(\frac{\delta\varphi_{J,\beta}^\dagger}{\delta J_\alpha^\dagger}\right)^{-1} = i\frac{\delta J_\alpha^\dagger}{\delta\varphi_{J,\beta}^\dagger} = -i\frac{\delta^2\Gamma[\varphi]}{\delta\varphi_\beta^\dagger\delta\varphi^\alpha} \tag{A.20}$$

and using the decomposition equation (A.7) this becomes

$$(G^{-1})_\alpha^\beta = -i\frac{\delta^2 S[\varphi]}{\delta\varphi_\beta^\dagger\delta\varphi^\alpha} - i\frac{\delta^2 K[\varphi]}{\delta\varphi_\beta^\dagger\delta\varphi^\alpha} = (G_0^{-1})_\alpha^\beta - (\Sigma^{(1\,\mathrm{PI})})_\alpha^\beta. \tag{A.21}$$

With the mass-renormalization $(\Sigma^{(1\,\mathrm{PI})})_\alpha^\beta = i\frac{\delta^2 K[\varphi]}{\delta\varphi^\alpha\delta\varphi_\beta^\dagger}$. This is tantamount to the observation, that wherever there is a source φ coupled to a contribution to Γ there could also be attached an external line instead. Done twice this results in the one-particle-irreducible contributions to G. The same logic of identifying external-field-insertions with possible starting-points of external lines can be extended to higher order correlators as well.

B Recovering Classical Spin Equations

Treating the system without macroscopic fields reproduces the behavior of classical quasi-spins, which correspond to densities, not single fields in the fundamental ϕ. To leading order in $1/\mathcal{N}$ indeed the classical equations of motion are reproduced. An expansion consistent in loops (Hartree–Fock) on the contrary shows unphysical behavior, attributed here to a not well-suited expansion-parameter.

B.1 Leading Order in $1/\mathcal{N}$

Starting from the evolution equations for the local densities (4.23) in central-time, but neglecting the macroscopic fields $\varphi_\pm$ and the anomalous terms yields

$$\begin{aligned} iV_t\partial_{t_x}F(\vec{x},\vec{x}) = \Big[\quad & \frac{\epsilon+1}{2}\,\vec{\sigma}_z \\ & + \frac{\tilde{g}}{4}\,\mathrm{Tr}\left(F(\vec{x},\vec{x})\,\vec{\sigma}_0\,\right)\vec{\sigma}_0 - \frac{1}{4}\,\mathrm{Tr}\left(F(\vec{x},\vec{x})\,\vec{\sigma}_x\,\right)\vec{\sigma}_x \quad , \quad F(\vec{x},\vec{x})\Big] \end{aligned} \tag{B.1}$$

adapt the total density to $\rho := N = 1$, then including f_{+-} and h_{+-} terms (release the restriction to the symmetric phase) one finds:

$$[\vec{\sigma}_z\,, F] = \left[\begin{pmatrix} \mathbb{1} & 0 \\ 0 & -\mathbb{1} \end{pmatrix}, \begin{pmatrix} F_{++} & F_{+-} \\ F_{-+} & F_{--} \end{pmatrix}\right] = \begin{pmatrix} 0 & 2F_{+-} \\ -2F_{-+} & 0 \end{pmatrix} \tag{B.2}$$

and while $[\vec{\sigma}_0, F] = [\mathbb{1}_4, F] = 0$ still vanishes

$$\left[\,\mathrm{Tr}\left(F(\vec{x},\vec{x})\,\vec{\sigma}_x\,\right)\vec{\sigma}_x\,, F\right] = 2(N_{+-}+N_{-+})\begin{pmatrix} F_{-+}-F_{+-} & F_{--}-F_{++} \\ F_{++}-F_{--} & F_{+-}-F_{-+} \end{pmatrix} \tag{B.3}$$

is no longer zero. Using again a quasi-spin notation as for finding the mean-field ground-state (3.2.1):

$$J_x(\vec{x}) := \frac{1}{2\bar{\rho}} \langle \begin{pmatrix} \phi_\uparrow^\dagger(\vec{x}) & \phi_\downarrow^\dagger(\vec{x}) \end{pmatrix} \vec{\sigma}_x \begin{pmatrix} \phi_\uparrow(\vec{x}) \\ \phi_\downarrow(\vec{x}) \end{pmatrix} \rangle = \frac{1}{2} \langle \begin{pmatrix} \phi_+^\dagger(\vec{x}) & \phi_-^\dagger(\vec{x}) \end{pmatrix} \vec{\sigma}_z \begin{pmatrix} \phi_+(\vec{x}) \\ \phi_-(\vec{x}) \end{pmatrix} \rangle \quad \text{(cf. 3.20)}$$

$$J_z(\vec{x}) := \frac{1}{2\bar{\rho}} \langle \begin{pmatrix} \phi_\uparrow^\dagger(\vec{x}) & \phi_\downarrow^\dagger(\vec{x}) \end{pmatrix} \vec{\sigma}_y \begin{pmatrix} \phi_\uparrow(\vec{x}) \\ \phi_\downarrow(\vec{x}) \end{pmatrix} \rangle = \frac{1}{2} \langle \begin{pmatrix} \phi_+^\dagger(\vec{x}) & \phi_-^\dagger(\vec{x}) \end{pmatrix} \vec{\sigma}_y \begin{pmatrix} \phi_+(\vec{x}) \\ \phi_-(\vec{x}) \end{pmatrix} \rangle \quad \text{(cf. 3.21)}$$

$$J_z(\vec{x}) := \frac{1}{2\bar{\rho}} \langle \begin{pmatrix} \phi_\uparrow^\dagger(\vec{x}) & \phi_\downarrow^\dagger(\vec{x}) \end{pmatrix} \vec{\sigma}_z \begin{pmatrix} \phi_\uparrow(\vec{x}) \\ \phi_\downarrow(\vec{x}) \end{pmatrix} \rangle = \frac{1}{2} \langle \begin{pmatrix} \phi_+^\dagger(\vec{x}) & \phi_-^\dagger(\vec{x}) \end{pmatrix} \vec{\sigma}_x \begin{pmatrix} \phi_+(\vec{x}) \\ \phi_-(\vec{x}) \end{pmatrix} \rangle \quad \text{(cf. 3.22)}$$

or put differently:

$$J_x = \frac{1}{2}\big(F_{++} - F_{--}\big) \tag{B.4}$$

$$J_y = \Im\big(F_{+-}\big) \tag{B.5}$$

$$J_z = \Re\big(F_{+-}\big) \tag{B.6}$$

Inserting this into equation (B.1) gives (using $N_{+-}^* = N_{-+}$)

$$iV_t \partial_{t_x} F(\vec{x}, \vec{x}) = (\epsilon + 1) \begin{pmatrix} 0 & F_{+-} \\ -F_{-+} & 0 \end{pmatrix} - J_z \begin{pmatrix} iJ_y & -J_x \\ J_x & -iJ_y \end{pmatrix} \tag{B.7}$$

Or rewritten fully in terms of quasi-spins:

$$\partial_t J_x = J_y J_z \tag{B.8}$$

$$\partial_t J_y = -(\epsilon + 1 + J_x) J_z \tag{B.9}$$

$$\partial_t J_z = (\epsilon + 1) J_y \tag{B.10}$$

These become unstable for $\epsilon \to 0$ for the ground-state configuration (3.2.1) with $J_x \approx -1$. The same set of equations can be obtained as the classical equations of motion from the mean-field Hamiltonian (3.23). These equations preserve both the

quasi-spin "norm" and mean-field energy:

$$J_x^2 + J_y^2 + J_z^2 = 1 \tag{B.11}$$

$$E_{\mathrm{mf}} := (\epsilon + 1)J_x - \frac{1}{2}J_z^2 \tag{B.12}$$

These conservation laws can be used to determine the the classical trajectories: Three d. o. f. minus two constraints leaves a (maximally) one-dimensional curve. Technically the system could "get stuck" on some section of the curve, never reaching some of the other points, however, if this was the case there would either be points where $\forall a : \partial_t J_a = 0$, but for $\epsilon > 0$ ($\Rightarrow \epsilon + 1 + J_x \neq 0$) these points are trivial with $J_y = J_z = 0$, $J_x = \pm 1$, or the dynamics would have to become arbitrary slow, which is also not the case, as there is no damping-term.

Thus the trajectories lie on the "Bloch-sphere" of radius one, and projected on the x-y-plane they take the form (insert (B.12) into (B.11)):

$$\left(\frac{E_{\mathrm{mf}} + \frac{1}{2}J_z^2}{\epsilon + 1}\right)^2 + J_y^2 + J_z^2 = 1 \tag{B.13}$$

Or put differently:

$$J_y^2 = 1 - J_z^2 - \left(\frac{E_{\mathrm{mf}} + \frac{1}{2}J_z^2}{\epsilon + 1}\right)^2 \tag{B.14}$$

B.2 One-Loop Hartree–Fock

Using all one-loop ($\mathcal{O}\left(()\, g\right)$ in not dimensionless quantities, i. e. first order in the number of vertices) contributions one finds three channels:

$$\begin{aligned}\Gamma_2^{\mathrm{HF}}[G] = -\frac{i}{2} \times \frac{1}{8} \int dx \int_\zeta dt \Big[& \tilde{g}\, \mathrm{Tr}\left(G(x,x;t,t)\, \vec{\sigma}_0\, \right)^2 \\ & + 2\tilde{g}\, \mathrm{Tr}\left(G(x,x;t,t)\, \vec{\sigma}_0\, G(x,x;t,t)\, \vec{\sigma}_0\, \right) \\ & - \mathrm{Tr}\left(G(x,x;t,t)\, \vec{\sigma}_x\, \right)^2 - 2\, \mathrm{Tr}\left(G(x,x;t,t)\, \vec{\sigma}_x\, G(x,x;t,t)\, \vec{\sigma}_x\, \right) \Big]\end{aligned} \tag{B.15}$$

Inducing a local self-energy of the form

$$\begin{aligned}\Sigma^{(0)}(x,t) = \frac{\tilde{g}}{4}\,\mathrm{Tr}\left(F(x,x;t,t)\;\vec{\sigma}_0\;\right)\;\vec{\sigma}_0 + \frac{\tilde{g}}{2}\;\vec{\sigma}_0\;F(x,x;t,t)\;\vec{\sigma}_0 \\ - \frac{1}{4}\,\mathrm{Tr}\left(F(x,x;t,t)\;\vec{\sigma}_x\;\right)\;\vec{\sigma}_x - \frac{1}{2}\;\vec{\sigma}_x\;F(x,x;t,t)\;\vec{\sigma}_x\end{aligned} \tag{B.16}$$

and in the dynamic equation

$$iV_t\partial_{t_x}F(\vec{x},\vec{x}) = \Big[\;\;\frac{\epsilon+1}{2}\;\vec{\sigma}_z + \Sigma^{(0)}\quad,\quad F(\vec{x},\vec{x})\Big] \tag{B.17}$$

The new terms as compared to equation (B.1) are:

$$\frac{\tilde{g}}{2}[\vec{\sigma}_0\;F(x,x;t,t)\;\vec{\sigma}_0\;,F(x,x;t,t)] = \frac{\tilde{g}}{2}[F(x,x;t,t),F(x,x;t,t)] = 0 \tag{B.18}$$

and

$$\begin{aligned}-\frac{1}{2}[\vec{\sigma}_x\;F(x,x;t,t)\;\vec{\sigma}_x\;,F(x,x;t,t)] &= -\frac{1}{2}\left[\begin{pmatrix}F_{--} & F_{-+}\\ F_{+-} & F_{++}\end{pmatrix},\begin{pmatrix}F_{++} & F_{+-}\\ F_{-+} & F_{--}\end{pmatrix}\right] \\ &= \begin{pmatrix}F_{-+}^2 - F_{+-}^2 & \big(F_{+-}+F_{-+}\big)\big(F_{--}-F_{++}\big)\\ \big(F_{+-}+F_{-+}\big)\big(F_{--}-F_{++}\big) & F_{+-}^2 - F_{-+}^2\end{pmatrix}\end{aligned} \tag{B.19}$$

which can be rewritten (still assuming vanishing anomalous terms h) using the form of F (3.36) and

$$F_{+-}+F_{-+} = \begin{pmatrix}N_{+-} & 0\\ 0 & N_{+-}^*\end{pmatrix} + \begin{pmatrix}N_{-+} & 0\\ 0 & N_{-+}^*\end{pmatrix} = (N_{+-}+N_{-+})\mathbb{1}_2 \tag{B.20}$$

where $N_{+-}^* = N_{-+}$ (3.42) was used again. Such that finally

$$[\vec{\sigma}_x\;F(x,x;t,t)\;\vec{\sigma}_x\;,F(x,x;t,t)] \overset{(B.3)}{=} \frac{1}{2}\big[\;\mathrm{Tr}\left(F(\vec{x},\vec{x})\;\vec{\sigma}_x\;\right)\;\vec{\sigma}_x\;,F\big] \tag{B.21}$$

thus the quasi-spin evolution equations (B.8 – B.10) are only slightly modified to

$$\partial_t J_x = 2J_yJ_z \tag{B.22}$$

$$\partial_t J_y = -(\epsilon+1+2J_x)J_z \tag{B.23}$$

$$\partial_t J_z = (\epsilon+1)J_y \tag{B.24}$$

moving, for the fully polarized initial state ($J_x = -1$), the instability to $\epsilon \approx 1$ i. e.

$$\Omega = 2\Omega_c \,. \tag{B.25}$$

This is assumed to be an unphysical shift, as it was neither observed in experiment [Nicklas et al., 2015] nor in numerical simulation [Karl, 2016]. It is attributed to the dimension-full coupling g / the vertex-number not being a good expansion parameter. Therefore throughout the rest of this thesis an $^1/_{\mathcal{N}}$-expansion (see section 2.7) is used instead.

C Mathematical Identities

In this chapter some of the formula appearing in the main text are derived.

C.1 Integration Identities

Integrating expressions which contain a $\mathrm{sign}_\zeta(t-t')$ over a closed time contour ζ leads to a number of simplifications by noting that for any function $f(t)$ regular in t:

$$\int_\zeta f(t)dt = \int_0^{t_{\max}} f(t)dt + \int_{t_{\max}}^0 f(t)dt = 0 \tag{C.1}$$

C.1.1 One "sign" Term

Including one term $\propto \mathrm{sign}_\zeta(t-t_1)$ for $t_1 <_\zeta t_{\max}$ yields

$$\begin{aligned}\int_\zeta f(t)\,\mathrm{sign}_\zeta(t-t_1)dt &= -\int_0^{t_1} f(t)dt + \int_{t_1}^{t_{\max}} f(t)dt + \int_{t_{\max}}^{t_1} f(t)dt + \int_{t_1}^0 f(t)dt \\ &= -2\int_0^{t_1} f(t)dt \end{aligned} \tag{C.2}$$

and also for $t_1 >_\zeta t_{\max}$:

$$\begin{aligned}\int_\zeta f(t)\,\mathrm{sign}_\zeta(t-t_1)dt &= -\int_0^{t_1} f(t)dt - \int_{t_1}^{t_{\max}} f(t)dt - \int_{t_{\max}}^{t_1} f(t)dt + \int_{t_1}^0 f(t)dt \\ &= -2\int_0^{t_1} f(t)dt \end{aligned} \tag{C.3}$$

C.1.2 Second "sign" Term

With two sign terms, there is actually a number of orderings of t_1, t_2 and $t_{\max}$ to be considered.

First we investigate in the two distinct cases $t_{\max} >_\zeta t_2 >_\zeta t_1$ (when $t_2 > t_1 \Leftrightarrow t_2 >_\zeta t_1$)

$$\begin{aligned}\int_\zeta f(t)\,\mathrm{sign}_\zeta(t-t_1)\;\mathrm{sign}_\zeta(t-t_2)dt\Big|_{t_2>t_1} \\ &= \int_0^{t_1} f(t)dt - \int_{t_1}^{t_2} f(t)dt + \int_{t_2}^{t_{\max}} f(t)dt \\ &+ \int_{t_{\max}}^{t_2} f(t)dt + \int_{t_2}^{t_1} f(t)dt + \int_{t_1}^{0} f(t)dt \\ &= -2\int_{t_1}^{t_2} f(t)dt\end{aligned} \tag{C.4}$$

and analogously for $t_{\max} >_\zeta t_1 >_\zeta t_2$ simply replace $\int_{t_1}^{t_2} \to \int_{t_2}^{t_1} = -\int_{t_1}^{t_2}$:

$$\int_\zeta f(t)\,\mathrm{sign}_\zeta(t-t_1)\;\mathrm{sign}_\zeta(t-t_2)dt\Big|_{t_1>t_2} = 2\int_{t_1}^{t_2} f(t)dt \tag{C.5}$$

Thus altogether (when $t_1, t_2 <_\zeta t_{\max}$):

$$\int_\zeta f(t)\,\mathrm{sign}_\zeta(t-t_1)\,\mathrm{sign}_\zeta(t-t_2)dt = 2\,\mathrm{sign}_\zeta(t_1-t_2)\int_{t_1}^{t_2} f(t)dt \tag{C.6}$$

Secondly consider $t_2 >_\zeta t_{\max} >_\zeta t_1$ and $t_2 > t_1$:

$$\begin{aligned}\int_\zeta f(t)\,\mathrm{sign}_\zeta(t-t_1)\,\mathrm{sign}_\zeta(t-t_2)dt \\ &= \int_0^{t_1} f(t)dt - \int_{t_1}^{t_2} f(t)dt - \int_{t_2}^{t_{\max}} f(t)dt \\ &- \int_{t_{\max}}^{t_2} f(t)dt + \int_{t_2}^{t_1} f(t)dt + \int_{t_1}^{0} f(t)dt \\ &= -2\int_{t_1}^{t_2} f(t)dt = 2\,\mathrm{sign}_\zeta(t_1-t_2)\int_{t_1}^{t_2} f(t)dt\end{aligned} \tag{C.7}$$

And for $t_2 >_\zeta t_{\max} >_\zeta t_1$ and $t_2 < t_1$:

$$\begin{aligned}\int_\zeta f(t)\,\mathrm{sign}_\zeta(t-t_1)\,\mathrm{sign}_\zeta(t-t_2)dt \\ &= \int_0^{t_2} f(t)dt + \int_{t_2}^{t_1} f(t)dt - \int_{t_1}^{t_{\max}} f(t)dt \\ &- \int_{t_{\max}}^{t_1} f(t)dt - \int_{t_1}^{t_2} f(t)dt + \int_{t_2}^{0} f(t)dt \\ &= -2\int_{t_1}^{t_2} f(t)dt = 2\,\mathrm{sign}_\zeta(t_1-t_2)\int_{t_1}^{t_2} f(t)dt\end{aligned} \tag{C.8}$$

Exchanging $t_1 \leftrightarrow t_2$ would again change the sign of both the integral and the $\mathrm{sign}_\zeta(t_1 - t_2)$ (cf. discussion around equation (C.5)).

Finally we are left with the case $t_2 >_\zeta t_1 >_\zeta t_{\max}$, where $t_2 >_\zeta t_1 \Leftrightarrow t_2 < t_1$:

$$\begin{aligned}\int_\zeta f(t)\,\mathrm{sign}_\zeta(t-t_1)\,\mathrm{sign}_\zeta(t-t_2)dt \\ &= \int_0^{t_2} f(t)dt + \int_{t_2}^{t_1} f(t)dt + \int_{t_1}^{t_{\max}} f(t)dt \\ &+ \int_{t_{\max}}^{t_1} f(t)dt - \int_{t_1}^{t_2} f(t)dt + \int_{t_2}^{0} f(t)dt \\ &= -2\int_{t_1}^{t_2} f(t)dt = 2\,\mathrm{sign}_\zeta(t_1-t_2)\int_{t_1}^{t_2} f(t)dt\end{aligned} \tag{C.9}$$

And thereby, for arbitrary ordering of t_1, t_2 and $t_{\max}$ it always holds that:

$$\int_\zeta f(t)\,\mathrm{sign}_\zeta(t-t_1)\,\mathrm{sign}_\zeta(t-t_2)dt = 2\,\mathrm{sign}_\zeta(t_1-t_2)\int_{t_1}^{t_2} f(t)dt \tag{C.10}$$

Note that none of the integrals actually depends on the arbitrary $t_{\max}$ as it has to be the case.

C.2 Timeordered Propagator Decomposition

Correlation-functions calculated in a path-integral formalism are naturally time-ordered, and thereby non-analytic when approaching times where two operator-insertions appear at the same time. For two-point functions such as the propagator this happens precisely when both time-arguments are equal.

C.2.1 General Case

This is not meant to be a strict mathematical prove, but rather an illustration of the idea underlying this decomposition. Let $F(t)$ a function which is analytic $\forall t \neq 0$, then $\exists! f(t), g(t)$ analytic $\forall t$:

$$F(t) = f(t) + \text{sign}(t)g(t). \tag{C.11}$$

To this end, define (using the n-th derivatives $F^{(n)}(t)$)

$$f_0^{(n)} := \frac{1}{2}\Big(\lim_{t\searrow 0} F^{(n)}(t) + \lim_{t\nearrow 0} F^{(n)}(t)\Big) \tag{C.12}$$

$$g_0^{(n)} := \frac{1}{2}\Big(\lim_{t\searrow 0} F^{(n)}(t) - \lim_{t\nearrow 0} F^{(n)}(t)\Big). \tag{C.13}$$

Because $\forall t > 0 : F(t)$ is analytic

$$\sum_{n=0}^{\infty} \lim_{t\searrow 0} F^{(n)}(t) = \sum_{n=0}^{\infty} \frac{f_0^{(n)} + g_0^{(n)}}{n!} < \infty \tag{C.14}$$

converges absolutely as well as by $\forall t < 0 : F(t)$ being analytic

$$\sum_{n=0}^{\infty} \lim_{t\nearrow 0} F^{(n)}(t) = \sum_{n=0}^{\infty} \frac{f_0^{(n)} - g_0^{(n)}}{n!} < \infty \tag{C.15}$$

and the functions

$$f(t) := \sum_{n=0}^{\infty} \frac{f_0^{(n)}}{n!} t^n \qquad \text{and} \qquad g(t) := \sum_{n=0}^{\infty} \frac{g_0^{(n)}}{n!} t^n \tag{C.16}$$

must converge / exist at $t = 0$. By analyticity of $F(t)$ away from $t = 0$ they exist at $t \neq 0$ anyway. Any other f' and g' with these properties must have the same series-expansion around zero, so by identity theorem $f' = f$ and $g' = g$, i. e. the decomposition is unique. Note however, that $F(t)$ is a *function* not a distribution and thereby must not contain terms $\propto \delta(t)$ or similar expressions.

C.2.2 The Propagator

We want to see how the time-ordered propagator can be brought to this form and how the components of the decomposition relate to the intuitive definition of spectral

and statistical function via (anti-)commutators.

$$\begin{aligned}
G(t,t') &= \theta(t-t')\,\langle\phi^\dagger(t)\phi(t')\rangle &&+ \theta(t'-t)\,\langle\phi(t')\phi^\dagger(t)\rangle \\
&= \frac{1}{2}\,\langle\{\phi^\dagger(t),\phi(t')\}\rangle + \frac{1}{2}\theta(t-t')\,\langle\phi^\dagger(t)\phi(t')\rangle &&- \frac{1}{2}\theta(t-t')\,\langle\phi(t')\phi^\dagger(t)\rangle \\
&\qquad - \frac{1}{2}\theta(t'-t)\,\langle\phi^\dagger(t)\phi(t')\rangle &&+ \frac{1}{2}\theta(t'-t)\,\langle\phi(t')\phi^\dagger(t)\rangle \\
&= \frac{1}{2}\,\langle\{\phi^\dagger(t),\phi(t')\}\rangle + \frac{1}{2}\,\mathrm{sign}(t-t')\,\langle\phi^\dagger(t)\phi(t')\rangle &&- \frac{1}{2}\,\mathrm{sign}(t-t')\,\langle\phi(t')\phi^\dagger(t)\rangle \\
&= \frac{1}{2}\,\langle\{\phi^\dagger(t),\phi(t')\}\rangle - \frac{i}{2}\,\mathrm{sign}(t-t')i\,\langle[\phi^\dagger(t),\phi(t')]\rangle
\end{aligned} \tag{C.17}$$

Therefore the explicit form assumed for ρ and F in the main text is justified.

In the main-text, the definition

$$G(t,t) := \frac{1}{2}\Big(\lim_{t'\searrow t} G(t,t') + \lim_{t'\nearrow t} G(t,t')\Big) = F(t,t) \tag{C.18}$$

is used, therefore avoiding $\rho(t,t) = i\,\langle[\phi^\dagger,\phi]\rangle = i\delta(x-y)$ terms.

C.3 Absolute / Phase Decomposition

This section contains some short calculations for decomposing an equation for a complex function φ of the form:

$$i\partial_t\varphi = \alpha\varphi + \beta\varphi^* \tag{C.19}$$

with $\alpha,\beta\in\mathbb{R}$ where φ is written as

$$\varphi = |\varphi|e^{-i\theta} \tag{C.20}$$

and thus

$$(i\partial_t|\varphi| + |\varphi|\partial_t\theta)e^{-i\theta} = i\partial_t\varphi = \alpha\varphi + \beta\varphi^* = \alpha|\varphi|e^{-i\theta} + \beta|\varphi|e^{i\theta} \tag{C.21}$$

Dividing both sides by $|\varphi|e^{-i\theta}$ leads to

$$\frac{i\partial_t|\varphi|}{|\varphi|} + \partial_t\theta = \alpha + \beta e^{2i\theta} \tag{C.22}$$

Taking the real part of this equation yields

$$\partial_t \theta = \alpha + \beta \cos(2\theta) \tag{C.23}$$

D Lists

D.1 List of Figures

E Bibliography

J. Berges. Introduction to Nonequilibrium Quantum Field Theory. *AIP Conf.Proc*, 739:3–62, 2005. doi: 10.1063/1.1843591.

J. Berges and J. Cox. Thermalization of quantum fields from time-reversal invariant evolution equations. *Physics Letters B*, 517(3–4):369 – 374, 2001. ISSN 0370-2693. doi: http://dx.doi.org/10.1016/S0370-2693(01)01004-8. URL `http://www.sciencedirect.com/science/article/pii/S0370269301010048`.

J. Berges and D. Mesterházy. Introduction to the nonequilibrium functional renormalization group. *Nuclear Physics B - Proceedings Supplements*, 228:37 – 60, 2012. ISSN 0920-5632. doi: http://dx.doi.org/10.1016/j.nuclphysbps.2012.06.003. URL `http://www.sciencedirect.com/science/article/pii/S0920563212001600`.

J. Berges and J. Serreau. Progress in Nonequilibrium Quantum Field Theory, 2003. URL `https://arxiv.org/abs/hep-ph/0302210`.

J. Berges and J. Serreau. Progress in nonequilibrium quantum field theory II, 2004. URL `https://arxiv.org/abs/hep-ph/0410330`.

J. Berges, Sz. Borsányi, and C. Wetterich. Prethermalization. *Phys. Rev. Lett.*, 93: 142002, Sep 2004. doi: 10.1103/PhysRevLett.93.142002. URL `http://link.aps.org/doi/10.1103/PhysRevLett.93.142002`.

J. Berges, A. Rothkopf, and J. Schmidt. Nonthermal fixed points: Effective weak coupling for strongly correlated systems far from equilibrium. *Phys. Rev. Lett.*, 101:041603, Jul 2008. doi: 10.1103/PhysRevLett.101.041603. URL `http://link.aps.org/doi/10.1103/PhysRevLett.101.041603`.

P.B. Blakie, A.S. Bradley, M.J. Davis, R.J. Ballagh, and C.W. Gardiner. Dynamics and statistical mechanics of ultra-cold bose gases using c-field techniques. *Advances in Physics*, 57(5):363–455, 2008. doi: 10.1080/00018730802564254. URL `http://dx.doi.org/10.1080/00018730802564254`.

I. Bloch, J. Dalibard, and W. Zwerger. Many-body physics with ultracold gases. *Rev. Mod. Phys.*, 80:885–964, Jul 2008. doi: 10.1103/RevModPhys.80.885. URL http://link.aps.org/doi/10.1103/RevModPhys.80.885.

A. Branschädel and T. Gasenzer. 2pi nonequilibrium versus transport equations for an ultracold bose gas. *Journal of Physics B: Atomic, Molecular and Optical Physics*, 41(13):135302, 2008. URL http://stacks.iop.org/0953-4075/41/i=13/a=135302.

A. J. Bray. Theory of phase-ordering kinetics. *Advances in Physics*, 51(2):481–587, 2002. doi: 10.1080/00018730110117433. URL http://dx.doi.org/10.1080/00018730110117433.

M. E. Fisher. The theory of equilibrium critical phenomena. *Rep. Prog. Phys.*, 30 (306):615–730, 1967. doi: 10.1088/0034-4885/30/2/306.

M. E. Fisher. The renormalization group in the theory of critical behavior. *Rev. Mod. Phys.*, 46:597–616, Oct 1974. doi: 10.1103/RevModPhys.46.597. URL http://link.aps.org/doi/10.1103/RevModPhys.46.597.

A. Griffin. Conserving and gapless approximations for an inhomogeneous bose gas at finite temperatures. *Phys. Rev. B*, 53:9341–9347, Apr 1996. doi: 10.1103/PhysRevB.53.9341. URL http://link.aps.org/doi/10.1103/PhysRevB.53.9341.

P. C. Hohenberg and B. I. Halperin. Theory of dynamic critical phenomena. *Rev. Mod. Phys.*, 49:435–479, Jul 1977. doi: 10.1103/RevModPhys.49.435. URL http://link.aps.org/doi/10.1103/RevModPhys.49.435.

P.C. Hohenberg and P.C. Martin. Microscopic theory of superfluid helium. *Annals of Physics*, 34(2):291 – 359, 1965. ISSN 0003-4916. doi: 10.1016/0003-4916(65)90280-0. URL http://www.sciencedirect.com/science/article/pii/0003491665902800.

L. P. Kadanoff, W. Glötze, D. Hamblen, R. Hecht, E. A. S. Lewis, V. V. Palciauskas, M. Rayl, J. Swift, D. Aspnes, and J. Kane. Static phenomena near critical points: Theory and experiment. *Rev. Mod. Phys.*, 39:395–431, Apr 1967. doi: 10.1103/RevModPhys.39.395. URL http://link.aps.org/doi/10.1103/RevModPhys.39.395.

M. Karl. *From quenches to critical dynamics and non-equilibrium steady states*. PhD thesis, Universität Heidelberg, Heidelberg, 2016. URL http://nbn-resolving.de/urn:nbn:de:bsz:16-heidok-217847.

L.V. Keldysh. Diagram technique for nonequilibrium processes. *JETP*, 20:1018, Apr 1965. URL http://www.jetp.ac.ru/cgi-bin/e/index/e/20/4/p1018?a=list.

T. Kinoshita, T. Wenger, and D. S. Weiss. A quantum newton's cradle. *Nature*, 440:900–903, Apr 2006. doi: 10.1038/nature04693. URL http://dx.doi.org/10.1038/nature04693M3.

L. Landau. On the theory of phase transitions. *Ukr. J. Phys.*, 53:25–35, 2008. Special Issue.

T. Langen, T. Gasenzer, and J. Schmiedmayer. Prethermalization and universal dynamics in near-integrable quantum systems. *Journal of Statistical Mechanics: Theory and Experiment*, 2016(6):064009, 2016. doi: 10.1088/1742-5468/2016/06/064009. URL http://stacks.iop.org/1742-5468/2016/i=6/a=064009.

A. Pi neiro Orioli, K. Boguslavski, and J. Berges. Universal self-similar dynamics of relativistic and nonrelativistic field theories near nonthermal fixed points. *Phys. Rev. D*, 92:025041, Jul 2015. doi: 10.1103/PhysRevD.92.025041. URL http://link.aps.org/doi/10.1103/PhysRevD.92.025041.

E. Nicklas, M. Karl, M. Höfer, A. Johnson, W. Muessel, H. Strobel, J. Tomkovič, T. Gasenzer, and M. K. Oberthaler. Observation of scaling in the dynamics of a strongly quenched quantum gas. *Phys. Rev. Lett.*, 115:245301, 2015. doi: 10.1103/PhysRevLett.115.245301.

A.M. Polyakov. Conformal symmetry of critical fluctuations. *JETP Letters*, 12:381–383, Dez 1970. URL http://www.jetpletters.ac.ru/ps/1737/article_26381.shtml.

S. Sachdev. *Quantum phase transitions*. Cambridge University Press, Cambridge, U.K., 2nd ed edition, 2011. ISBN 978-0-521-51468-2. URL http://proquest.tech.safaribooksonline.de/9781139636001.

J. Serreau. Kinetic equilibration in heavy ion collisions: the role of elastic processes. *Nuclear Physics A*, 715:805c – 808c, 2003. ISSN 0375-9474. doi: 10.

1016/S0375-9474(02)01493-8. URL http://www.sciencedirect.com/science/article/pii/S0375947402014938.

H. E. Stanley. Scaling, universality, and renormalization: Three pillars of modern critical phenomena. *Rev. Mod. Phys.*, 71:S358–S366, Mar 1999. doi: 10.1103/RevModPhys.71.S358. URL http://link.aps.org/doi/10.1103/RevModPhys.71.S358.

P. Tommasini, E. J. V. de Passos, A. F. R. de Toledo Piza, M. S. Hussein, and E. Timmermans. Bogoliubov theory for mutually coherent condensates. *Phys. Rev. A*, 67:023606, Feb 2003. doi: 10.1103/PhysRevA.67.023606. URL http://link.aps.org/doi/10.1103/PhysRevA.67.023606.

S. Weinberg. *Modern Applications*, volume 2 of *The Quantum Theory of Fields*, chapter 16. Cambridge Univ. Press, Cambridge, 1996. ISBN 978-0-521-55002-4; 978-0-521-67054-8.

K. G. Wilson and M. E. Fisher. Critical exponents in 3.99 dimensions. *Phys. Rev. Lett.*, 28:240–243, Jan 1972. doi: 10.1103/PhysRevLett.28.240. URL http://link.aps.org/doi/10.1103/PhysRevLett.28.240.

Erklärung:

Ich versichere, dass ich diese Arbeit selbstständig verfasst habe und keine anderen als die angegebenen Quellen und Hilfsmittel benutzt habe.

Heidelberg, den 27. Februar 2017 .....